Recovery of hematite from fluorspar tailings using reverse cationic flotation

By

Thembelihle Portia Lubisi

A Master's Research dissertation submitted in fulfilment of the requirements for the degree of Magister technologiae

in

Chemical Engineering

in the

Faculty of Engineering and the Built Environment

at the

UNIVERSITY OF JOHANNESBURG

SUPERVISOR: Dr Willie Nheta

CO-SUPERVISOR: Prof Freeman Ntuli

22 February 2017

Dedication

This thesis is dedicated to my loving husband. I am grateful for his support throughout the project. I thank him for his continuous understanding and listening to me on my frustration days, my overenthusiastic days and everything in between. I thank my helper for taking care of my children when I came home late and exhausted. I thank my sister for her continuous encouragement, ensuring I don’t quit.

Declaration

I, THEMBELIHLE PORTIA LUBISI hereby declare that this master's research dissertation is wholly my own work and has not been submitted anywhere else for academic credit either by myself or another person. I understand what plagiarism implies and declare that this proposal is my own ideas, words, phrase, arguments, graphics, figures, results and organisation except where reference is explicitly made to other authors' work. I understand further that any unethical academic behaviour, which includes plagiarism, is seen in a serious light by the University of Johannesburg and is punishable by disciplinary action.

Signed……..... Date: 22 February 2017

Acknowledgements

I am grateful and wish to acknowledge the following persons for their contributions towards the successful completion of this research work:

- Doctor W. Nheta of Metallurgy Department (University of JHB)

I thank my project supervisor for giving me an opportunity to embark on a project that is outside my Chemical Engineering field. I am grateful for his continuous encouragement, guidance, good supervisory skills, his timely feedbacks, his open door policy and his interest on my progress. He fast tracked my familiarity with the topic by sharing with me his in depth knowledge of the research area, ensured I got all I needed for the project and pushed me in times when I slacked.

- Prof F. Ntuli of Chemical Engineering (University of JHB)

I thank my co-supervisor for referring me to Dr Nheta. He has also ensured I had all I needed for the success of the project, including arranging office space. I thank his commitment to the project and his interest in my timely completion of the degree.

- Mineral Processing laboratory staff

I would like to thank the staff of mineral processing laboratory for providing me with required PPE during the test work, teaching me how to use laboratory equipment at University of Johannesburg, bearing with my highly staining red sample during lengthy period of experiments and their kindness. I thank Mr Abram for his understanding and his stories made laboratory a good place to visit. I thank Ms Mapilane for the ladies talks we shared, it brightened heavy days.

- Analytical laboratory staff

I would like to thank the lab technician, Mr Edward Malenga for his timely testing of samples. I thank him for the "un-official" brainstorming sessions that he has allowed me to have with him. His support is greatly appreciated - God bless him. I would also like to thank the lab technician, Mrs Nomsa Baloyi for the advices she gave. Her commitment to assisting students and her friendliness was uplifting.

- Project sponsors

I thank CSIR for giving me a scholarship and Department of Higher Education and Training for funding the project. I thank University of JHB for purchasing of consumables and equipment required for timely completion of my project.

- Suppliers

I thank Betachem Company for kindly supplying reagents (Betacol 373, Betachem 30D and Dow 200 frother) and Vergenoeg Mine for kindly supplying me with the sample.

Publications

Papers published and submitted on the contents of this dissertation are as follows:

Status	Title	Published in;
Published	Beneficiation of hematite from fluorspar tailings by reverse flotation	Proceedings of the World Congress on Mechanical, Chemical and Materia Engineering, 2015
Published	Physical, chemical and mineralogical characterization of fluorspar flotation tailings	Proceedings of Materials, Minerals and Energy, 2016
Published	Effect of different binders on mechanical properties of iron flotation concentrates briquettes.	Proceedings of Materials, Minerals and Energy, 2016
Submitted	Optimization of reverse cationic flotation of low grade oxide from fluorspar tails using Taguchi method.	Arabian Journal for Science and Engineering

Abstract

The exploration of fluorspar ore in mining results in large amount of unrecovered valuable products found associated with fluorspar in the ore, representing 60% of the run of mine. Several million tons of valuable minerals are discarded every year into tailings ponds, incurring disposal costs, loss of potential company revenue and environmental pollution. This study was undertaken to identify the valuable mineral in the fluorspar tails with an aim of recovering such minerals, thus contributing to an ongoing treatment of waste minerals.

A representative sample was received from Vergenoeg Mine, South Africa, in 2014. Characterisation of the sample was conducted to determine physical, chemical and mineralogical properties. Particle size distribution analysis using Micratrac Particle Size Analyser showed that the sample was of fine texture, with 80% passing 120µm. Chemical analysis using X-ray fluorescent spectrometer (XRF) showed that the major element was Fe assaying 48.9%Fe. Major gangue minerals were SiO_2 (16.8%) and minor presence of CaO (3.8%) and F (2.25%) while all other components were reported at <1%. The metal distribution showed that iron was concentrating in the finer size range with 33.59%Fe reported in the +150µm and 52.09%Fe in the <38µm size fraction. The mineral phase test using X-ray powder diffraction (XRD) showed that iron was abundantly (>50%) found in the form of hematite while minor presence (3-10%) of iron in a form of goethite and magnetite was observed. The Quantitative evaluation of minerals by scanning electron microscopy (QEMSCAN) results showed that the largest portion of iron oxides (12.04wt%) occurred between the 40-50µm particle size range and the majority of Fe-oxide in the sample occurred between 10-70µm size range. Mineral liberation analysis showed that 81% of the iron oxide is liberated, while 16% and 3% were middling and locked Fe-oxide respectively. The locked particles were found to be in the <20µm size range. From the characterization results the sample was classed as low grade iron oxide and reverse cationic flotation was selected as the best concentration method.

This study used reverse cationic flotation to concentrate the iron, whereby two types of depressants and amine collectors were studied. The objective was to concentrate the low grade iron into quality standards required for blast furnace feed; ≥63%Fe, alumina to silica ratio of ≤1% with alumina <2%. The collectors investigated were the primary mono-amine (Dodecylamine) and tertiary amine (Betacol 373). The investigated depressants were soluble starch and a dextrin (Betachem 30D). The flotation parameters investigated were collector dosage, depressant dosage, pH, solids content, conditioning time, agitation speed, air rate and

effect of de-sliming. The Taguchi design of experiments was used to statistically provide a predictive knowledge of this complex and multi-variable process using few trials since the experiments would be lengthy if all possible combinations were to be considered. A combination of L25, L16 and L9 orthogonal array matrices were used depending on the number of parameters and levels investigated. The analysis of data was done using the Signal to Noise ratio and ANOVA. The SN ration was used to determine optimum conditions and analyse the relative significance of parameters studied. Analysis of data using ANOVA was done to identify and quantify the errors resulting from deviations of a set of results. The ranking of parameters using Signal to Noise ratio indicated that pH is the most significant parameter in achieving higher Fe grade. Depressant dosage and collector dosage were also important control factors in the flotation performance.

Flotation kinetics was conducted, using the optimum condition predicted by Taguchi, to compare the performance of depressants where DDA was used as the collector. The results showed that though both type of depressants were good for iron oxide, soluble starch gave superior results. However due to high cost of soluble starch, Betachem 30D was the preferred depressant. The optimum conditions for the selected Betachem 30D – DDA system used the optimum conditions; pH 10, Betachem 30D dosage of 500g/t, DDA dosage of 500g/t, solids content of 50%, conditioning time of 6 minutes, agitation speed of 1300rpm and air rate of valve ¾ open. Flotation using Betachem 30D – DDA yielded 60.41%Fe, hence removal of slimes was conducted with an aim to reduce possible metal loss as a result of slime coating; reagent consumption and sludge formation.

Notably, the removal of slimes resulted in 13% metal loss. Reduction in collector consumption was observed since the process was able to achieve a 62.62%Fe using 300g/t DDA, when compared to the 60.41%Fe achieved using 500g/t on feed with slimes. The highest 63.84%Fe grade at 75.16% recovery was achieved at 500g/t, when de-slimed feed was used. However, coupling the 24.84% metal loss during flotation and the 13% loss due to action of slime removal, the high metal loss in de-slimed feed made this process not beneficial. Conditioning time of the un-de-slimed feed was then increased from 6 minutes to 15 minutes and flotation conducted on the Betachem 30D – DDA, using the selected optimum conditions. The results showed a 63.79%Fe at 70.78% recovery, which was well in the required concentrate quality. The Al_2O_3 content was at 0.87% and SiO_2 at 3.8%.

The trial of Betachem 30D - Betacol 373 system showed that the optimum conditions for this system were at 3328g/t collector dosage, 500g/t Betachem 30D dosage, pH 10, 35% solids content, ¾ air valve opening, 1300rpm agitation speed and 15 minutes conditioning time. The Betacol 373 results showed a concentrate with 62.04%Fe at 69.07% recovery, where Al_2O_3 content of 0.6% was obtained and SiO_2 at 3.39%.

When comparing the collectors, Betacol 373 and DDA it was concluded that both reagents were good quartz collectors. They were able to concentrate the Fe in fluorspar feed significantly though DDA showed superior results under the investigated conditions. Betacol 373 required higher reagent dosage. It must be mentioned that Betacol 373 cost was much lower than DDA and it is manufactured locally. However, for the objectives within the scope of this project a conclusion was made that Betachem 30D – DDA system performed well, since the required ≥63%Fe was achieved. Since the best results were obtained using a rougher stage only in concentration of Fe in fluorspar tails, it was recommended that a cleaner stage be investigated with an aim to improve Fe assay and lower silica level.

Taguchi method was able to show optimum conditions required to achieve the highest Fe grade in the concentrate using the minimum number of experiments. The repeatability tests were conducted and the one way repeated measures ANOVA proved a null hypothesis which assumed no significant change between repeated experimental results. ANOVA further showed a 95% confidence levels on the results. This laboratory investigation proved it is possible to concentrate the low grade iron oxide, using reverse cationic flotation. Taguchi DOE method is suitable for optimization of reverse cationic flotation.

Keywords: Fluorspar tails, characterisation, reverse cationic flotation, Taguchi design of experiments, signal-noise ratio and ANOVA.

List of abbreviations

Abbreviation	Meaning
DDA	Dodecylamine
SN	Signal to noise ratio
ANOVA	Analysis of variance
SS	Soluble starch
DOE	Design of experiments
XRD	X-ray diffractometer
XRF	X-ray fluorescence
NWA	National Water Act
NEMA	National Environmental Management
OHSA	Occupational Health and Safety Act
Bet 30D	Betachem 30D
Bet 373	Betacol 373
OA	Orthogonal array
SEM	Scanning electron microscopy
EDS	Energy dispersive x-ray spectroscopy
BMA	Bulk modal analysis
PMA	Particle Mineralogical Analysis
QEMSCAN	Quantitative evaluation of minerals by scanning electron microscopy
µm	micron
CT	Conditioning time
CD	Collector dosage
SD	Soluble starch dosage
SPSS	Statistical Package for Social Sciences
DMS	Dense medium separation
SG	Specific gravity

Contents

List of figures

List of tables

List of tables in the appendix

1 CHAPTER 1: INTRODUCTION

1.1 Background

Iron is the fourth common mineral on earth's crust mainly found as a compound due to its high reactivity (Wills, 2006). It is primarily found as an oxide (hematite and magnetite), hydroxide (goethite and limonite) and to a lesser extent as a carbonate (e.g. side rite) (Filippov, et al., 2014). Metallic minerals are generally found associated with other minerals in igneous rocks or sedimentary rocks. The most common gangue minerals in iron ores are quartz, feldspar, clays, where the most undesirable constituents are alumina, silica and phosphorus (Wilson & Anhaeusser, 1998).

Mineral processing is therefore conducted to extract/concentrate the valuable minerals from gangue to produce a commercial end product. For a high grade ore (>65%Fe and minimum impurities) this simply includes crushing the ore to the required particle size, screening and directly feeding the screened ore into the blast furnace. Gradual depletion of high grade iron ore has necessitated miners to develop strategies for beneficiation of low grade iron ores, which normally is present at purities as low as <50%Fe.

Beneficiation of low grade ores has resulted in a need to grind the ores finer (even <250µm) in order to liberate the valuable mineral Low grade iron ore is characterised by low iron content (<60%Fe), high content of impurities and fine texture. These ores require a concentration method prior to feeding into the blast furnace. The general beneficiation process for low grade ores often includes excavation of sedimentary rock, crushing, grinding, subjecting to separation method to concentrate the valuable mineral, drying of the valuable mineral and rejecting of the gangue into the tailings pond, as shown in Figure 1.1. The first step of iron ore processing is comminution, where the ore is reduced to the required size with an aim to liberate valuables from gangue minerals and provide desired size range for the selected metallurgical treatment (Jain, 1985).

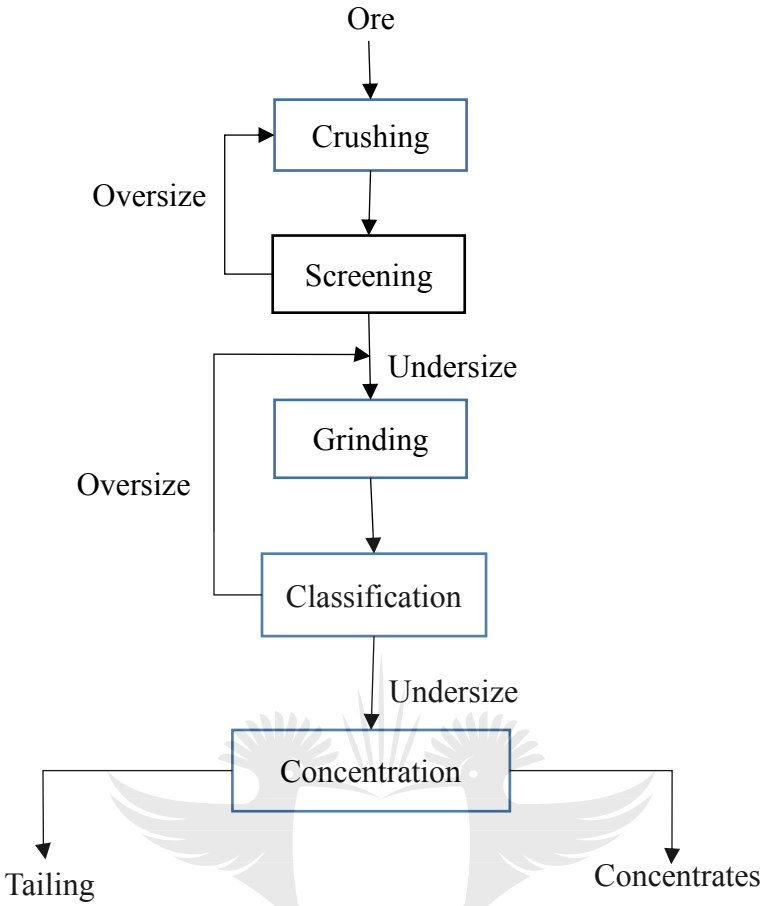

Figure 1.1: General beneficiation flowsheet of low grade iron ore

Typical liberations classes shown in Figure 1.2 where 1 is fully liberated valuable hence classed as concentrate. Minerals classed as 2 and 3 are termed middling and 4 is tailing.

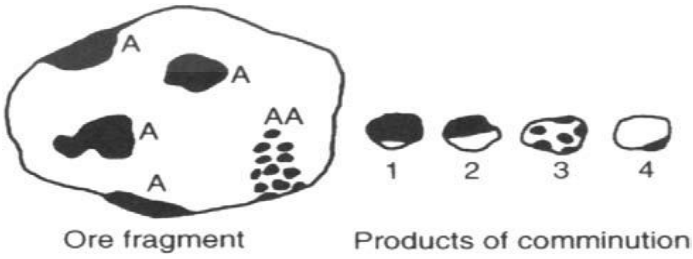

Figure 1.2**:** Typical liberation classes (Wills, 2006)

The beneficiation process, which normally takes place at the mine site, is critical since it reduces the transportation cost of the ore from the mine to the blast furnace site. The resulting iron ore concentrates from some beneficiation process could be very fine, hence requiring agglomeration for ease of transportation and better feeding to the blast furnace (Mbele, 2012).

Quality requirements for blast furnace feed is >63%Fe, alumina to silica ratio of <1, silica <3%, alumina <2%, calcium oxide to silica ratio of around 1, lumpy particles of size -32+6.3mm, for better blast furnace productivity and slag flow ability (Singh, et al., 2015; Zogo, 2009). Slag composition is critical in determining the physicochemical characteristics which affect coke consumption, slag handling, smoothness of operation, hot metal productivity and quality of the metal produced. Abbassi, et al., 2007 investigated the impact of phosphorus content in gray cast iron, where it was found that levels in phosphorus content changes the mechanical strength, hardness and other properties of the product. Different types of iron are produced for different end use e.g. pig iron, cast iron, wrought iron and iron alloy such as steel, hence grade requirements may vary.

The beneficiation method for low grade iron ores is selected based on the physical, chemical and mineralogical properties of the ore. The general separation methods for low grade iron ore are gravity separation, magnetic separation and flotation. Upon selection of the appropriate mineral separation method, experiments are conducted to obtain optimum conditions that would repeatedly obtain the required quality of iron concentrate. Due to a large number of parameters influencing a separation method, it would be difficult to study all possible combinations of factors as it would lead to uneconomically lengthy experiments and high consumption of resource (Bendell, et al., 1989).

It is thus imperative to approach the experimental activities with a well-designed plan to ensure focus, relevance and reliability of results. Statistical design of experiments is used for planning the experiments so that appropriate data will be collected and analysed by statistical methods, resulting in valid and objective conclusion (Montgomery, 2009). Experimental plan covers the selection of the sample, clear setting of the objectives, hypothesis, careful pairing of parameters under investigation and levels to which they will be varied, systemic execution of the experiments and collection of data. It also includes conducting repeatability tests to ascertain experimental errors, and considering the acceptable confidence levels required to deem results reliable (Fisher, 1942). Design of experiments (DOE) methods are used to statistically provide a predictive knowledge of a complex, multi-variable process using few trials (Hicks & Turner, 1999). DOE is largely used in the areas such as optimization of manufacturing processes; screening and identification of important factors and robustness testing of methods. Examples of DOE methods include full factorial design, fractional factorial design and Taguchi method. (Athreya & Venkatesh, 2012; Ryan, 2007).

1.2 Problem statement

Vergenoeg Mine, located 65km North East of Pretoria, South Africa, is the largest fluorspar mine in the world with production capacity currently at 240 000 tons per year (Vergenoeg Mining Company, 2016). Fluorspar is mined as the mineral fluorite (CaF_2) and is generally found associated with metallic minerals (such as hematite, magnetite, etc.) and other gangue minerals such as quartz, calcite, zinc sulphides, etc.

Typical fluorspar beneficiation process shows that recovery of fluorspar is done using flotation method, as shown Figure 1.3.

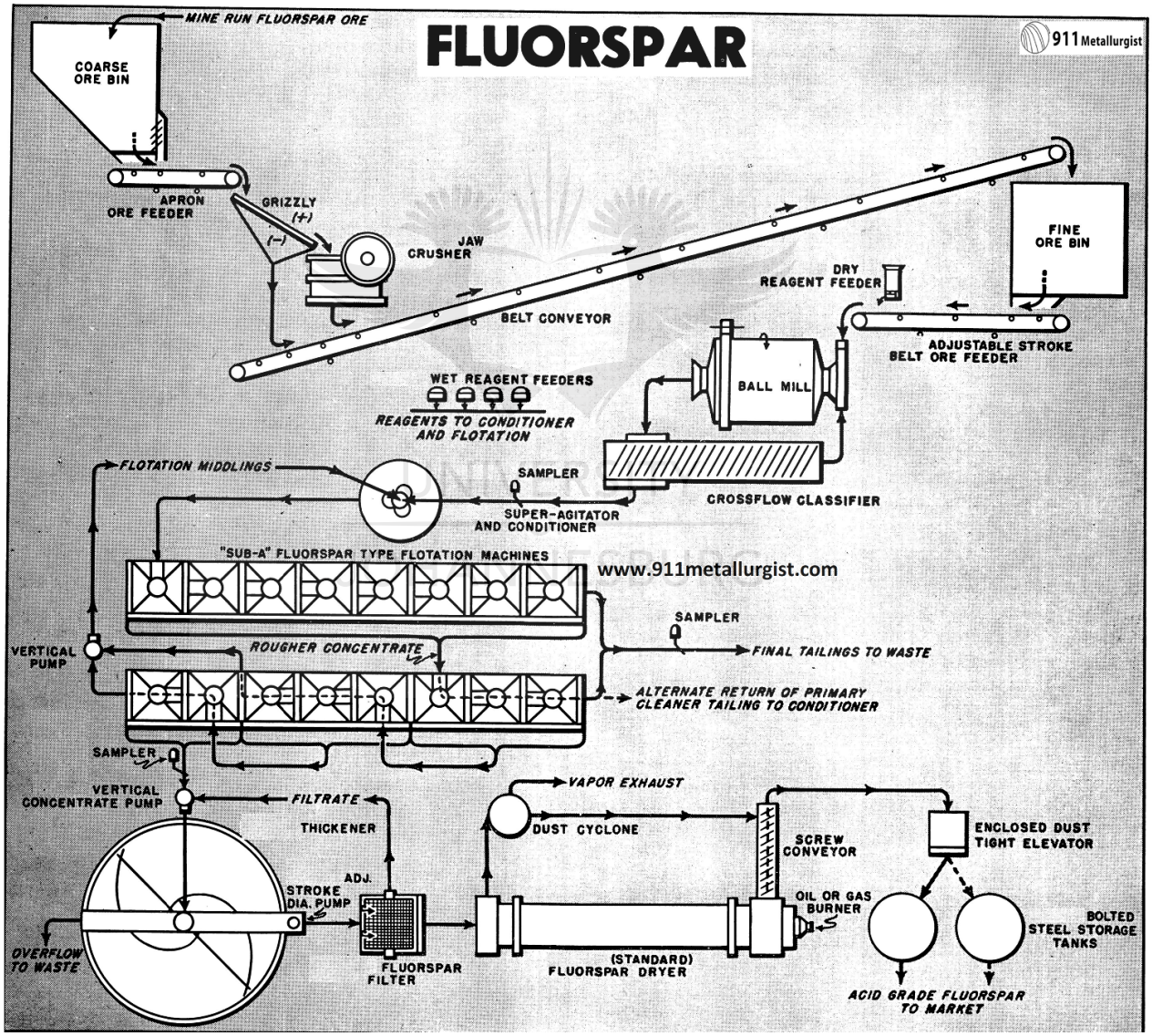

Figure 1.3: General fluorspar recovery flowsheet (Michaud, 2006)

Figure 1.3 shows the general fluorspar recovery process for a 100ton/day plant capacity for the production of Sub A fluorspar. According to this diagram the mined ore is crushed to a

manageable size followed by grinding to -297µm+ 230µm in order to liberate calcium fluoride from gangue particles. Thickening of the classifier overflow is necessary, to maintain proper density and feed regulation to flotation, in larger plants and where fine grinding is done. Conditioning of pulp is then conducted prior to the flotation process. The flotation circuit is arranged depending on the required product grade. The final product is filtered, dried and stored. The mine produces acid grade fluorspar and various metallurgical grades for domestic and export needs. Fluorspar is an important commodity with uses in areas such as the chemical industry, metallurgical and ceramic processes, e.g. manufacture of hydrofluoric acid, as a flux in smelting operations, manufacture of enamels, and optical products such as lenses amongst others (Wilson & Anhaeusser, 1998).

The final waste produced from the processing is disposed into the tailings ponds, as shown in Figure 1.4.

Figure 1.4: Tailings pond (Florian Neukirchen, 2016)

An estimated 480000 tons of tailings are annually disposed, by Vergenoeg Mine, into the tailing ponds. Mining and disposal of waste minerals have the potential to cause a number of environmental problems such as:

- loss of flora including direct losses through clearing

- loss of fauna as a results of vegetation clearing, reduction and fragmentation of habitat
- Acid mine drainage arising from disposal of sulphide product, which generate acid through bacterial oxidation when exposed to moisture and oxygen. This acid leachate may then mobilise heavy metals which can be released into nearby water streams.
- large landfill site requirements
- land rehabilitation challenges.

A number of bills, acts and regulation govern the environmental impact of South African industrial processes with an aim to impose stringent laws to enforce industries to adopt cleaner production and practice responsible operations that are safe to people and the environment. On national level there is the Water Act (NWA), National Environmental Management Act (NEMA) and Occupational Health and Safety Act (OSH Act). An example of waste management principle is section 2(4)(a)(ii) of NEMA, which states that industry must avoid or where it is not possible to avoid altogether, minimise and remedy pollution and degradation of the environment (Barclay, et al., 2011). Waste disposal therefore carries costs for the mining industries in general, which include; operational measures undertaken to implement pollution preventative measures, loss of profit, company image, management time, land, financial loss through fines, possible company closure as a results of non-compliance to regulations, etc. Cleaner production refers to waste minimisation, pollution prevention or eco-efficiency and its adoption by mining industries is vital for compliance with regulations, cost saving, public image and business sustainability.

It is therefore of interest for Vergenoeg Mine to explore waste minimization projects in order to comply to environmental laws, increase company revenue, reduce land requirements and position themselves as the responsible mine operators.

1.3 Research aim

The main thrust of this dissertation is to contribute to the ongoing treatment of tailings with an aim of recovering valuable minerals and reducing negative environmental impacts. The research would investigate the use of reverse cationic flotation on fluorspar tailings with an aim of recovering low grade iron found in the form of hematite. The optimisation of the process would consider parameters such as pH, collector type and dosage, depressant type and dosage, conditioning time, solids content, agitation speed, air rate, and impact of feed de-sliming.

Due to the number of parameters investigated, this research will make use of the Taguchi DOE method for optimisation of the flotation process. Taguchi is a well-accepted technique founded in 1966 by Genichi Taguchi. Taguchi method is based on Ronald's Fischer factorial design work, and is widely applied for product design and process optimization in manufacturing, marketing and engineering sectors worldwide. (Altan, 2010; Kumar et al 2015; du Plessis 2007).

1.4 Research objectives

The specific project objectives are to:

- Perform physical, chemical and mineralogical analysis of fluorspar tailings to identify the mineral phases and chemical contents in order to ascertain the appropriate method of concentrating the low grade iron.
- Develop a reverse cationic flotation procedure for experiments conducted using available laboratory equipment.
- Optimize the reverse cationic flotation of low grade iron oxide found in fluorspar tailings using Taguchi design of experiments.
- Determine the critical factors affecting the performance of reverse cationic flotation in achieving the required iron grade.

1.5 Research justification

Iron is an essential ingredient in steel making for domestic and foreign market consumption, with demand greatly increased in developing countries worldwide (Zogo, 2009). It is amongst the four most important minerals in the South African mining industry contributing to the country's economy, as shown in Figure 1.5. According to year 2012 sales contribution, iron ore sales contributed 14%, with coal leading mineral contributing 26% to the mineral sales.

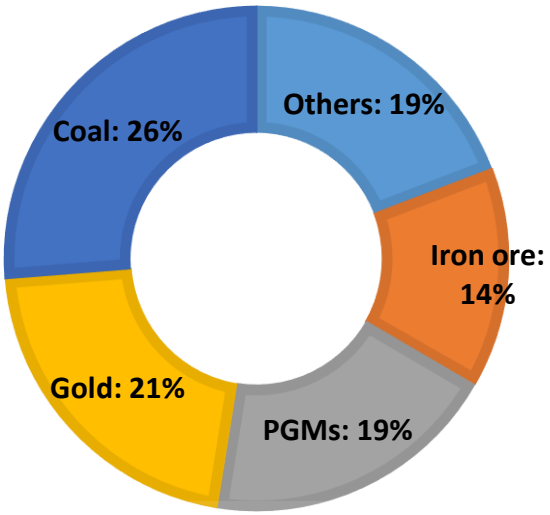

Figure 1.5: Important South African minerals (STATSSA, 2016)

Construction is the leading consumer of steel and iron where other uses include transportation industry, automotive, chemical industry, etc. Work done by Basov, 2015 showed that China is the highest consumer of steel with steel consumption increasing from year 1980 - 2010, as illustrated in Figure 1.6. It is further shown that there was a global increase in iron/steel consumption during 1995-2010, which is attributed to development of many countries.

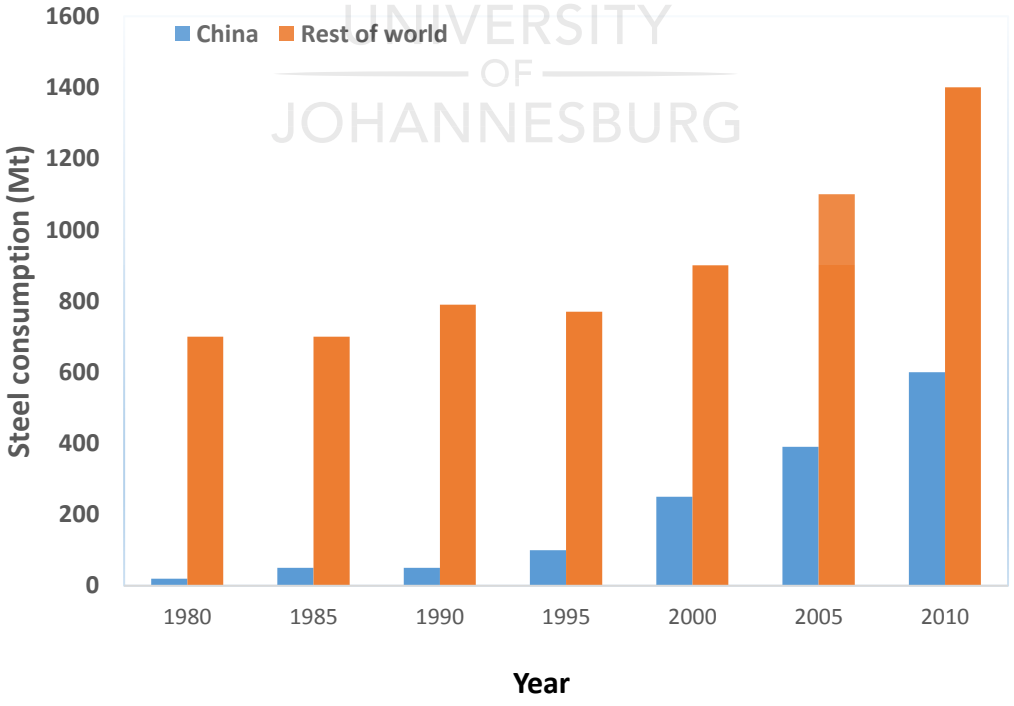

Figure 1.6: Steel consumption trend in China and the world (Basov, 2015)

Transparency Market Research, 2016 showed that China is the leader of global iron and steel market in terms of production with >50% of global volume with South Africa being number 7, as illustrated in Figure 1.7.

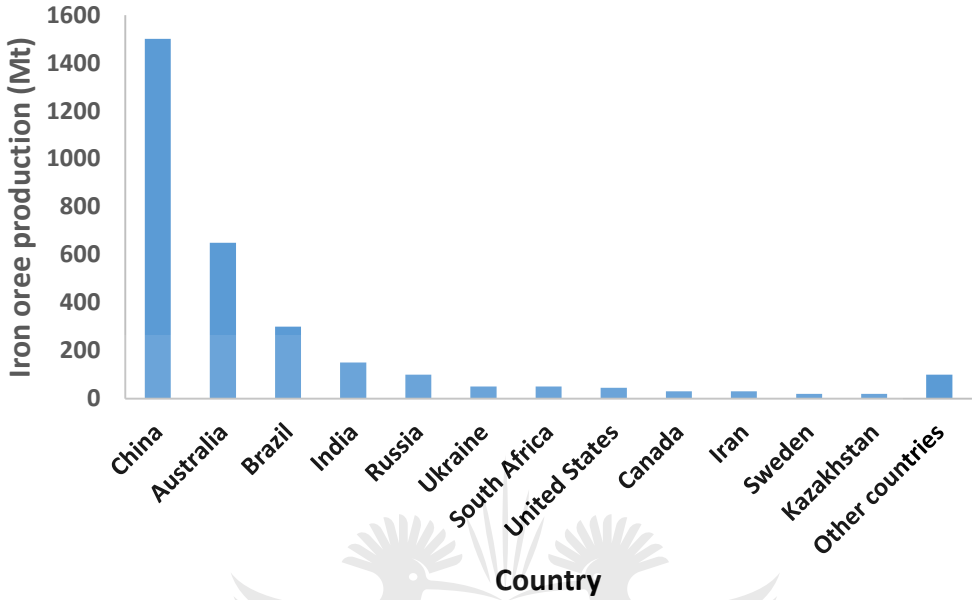

Figure 1.7: Top iron ore producing countries in 2014 (Transparency Market Research, 2016)

Since China is the largest consumer and producer of iron and steel (as shown in Figure 1.6 and 1.7), dynamics in the global market are therefore greatly defined by China. South Africa is the 7th largest producer of iron globally with production of 80.8Mt iron ore in 2014, however, production fell by 8.6% to 73Mt in 2015 (Statics, 2016). Large volatility in iron price over January 2008-January 2015 period is cited as the cause of poor performance in the iron mining industry. Data from International Monetary Fund (IMF) reflected in Figure 1.8 showed a 55% fall in iron price between Jan 2013- Jan 2015 (Kario & Brown, 2015). China's economic slowdown and subsequent weaker demand for iron are cited as the main cause of this price drop (Innace, 2016).

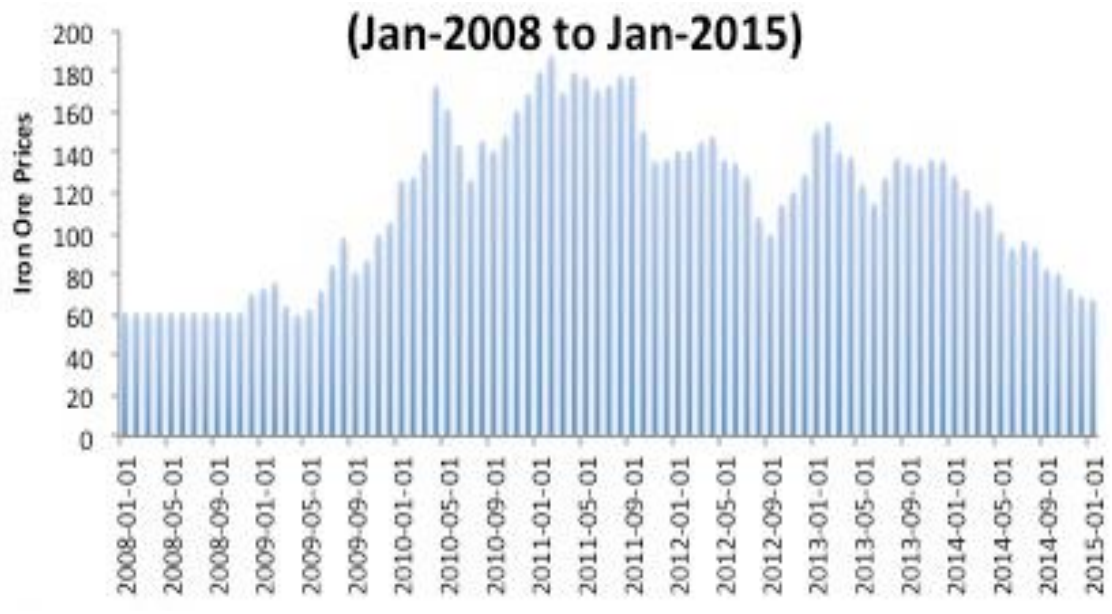

Figure 1.8: Monthly iron ore prices for Jan 2008 – Jan 2015 (Kario & Brown, 2015)

A weaker demand in iron has also been attributed to major companies (BHP, Vale and Rio) exercising expansion strategies that flooded the iron market, thus driving iron prices down. Some iron ore mines particularly in Africa, China and Canada have been forced to shut down due to inability to compete in such a low price environment (Kario & Brown, 2015). The top 10 producers of iron are tabulated in Table 1.

Table 1: Top 10 iron ore mining companies (2014)

	Major owner	Country	Province/State	Iron ore production, Mt
Hamersley	Rio Tinto	Australia	Western Australia	163
Carajas	Vale	Brazil	Para	120
Chichester Hub	Fortescue Metals	Australia	Western Australia	90
Yandi	BHP Billiton	Australia	Western Australia	79
Mount Whaleback	BHP Billiton	Australia	Western Australia	77
Solomon Hub	Fortescue Metals	Australia	Western Australia	58
Area C	BHP Billiton	Australia	Western Australia	57
Hope Downs	Rio Tinto/Hancock	Australia	Western Australia	43
Mariana Hub	Vale	Brazil	Minas Gerais	39
Sishen	Anglo American	South Africa	Northen Cape	36

Despite significant decline in iron prices, a demand for iron will exist for many years because iron is necessary for an economy to function and remain productive. There are predictions that iron demand will peak by year 2025-2030 (Innace, 2016). In fact, iron price has been reported to be on a steady increase, where iron price increased from $39.6 per Mt in December 2015 to $56.7per Mt in September 2016 (Statista, 2016). Large companies are already planning to increase supply taking market share from small miners in anticipation of major market growth as undeveloped countries develop and more urbanization of various areas occurs (Innace, 2016). Producers with operation costs that are far below current iron ore prices are well positioned to take market share.

Treatment of flotation tailings is generally cheaper than the conventional beneficiation process due to the activity of mining and comminution being omitted in the process (Wills & Finch, 2016). Iron ore mining is generally done using surface mining operations (open pit and open cut mining method), however a few underground iron ore mines are in operation around the globe. Recovery of low grade iron from the fluorspar tails would have the following benefits:

- reduced fluorspar tails disposal costs,
- reduced fluorspar tails quantities thus reducing landfill site requirement.
- increase company revenue at reduced operating costs, with elimination of mining and grinding step in the iron beneficiation process.
- reduce heavy metals content in the fluorspar tailing ponds and associated environmental risks such as acid mine drainage.
- elimination of risks associated with iron ore mining, which include drilling, blasting, land vibrations, and other safety risks (Golosinski, 2000).
- Position the company as the environmentally cautious thus improving its public image.

1.6 Dissertation layout

This dissertation consists of 5 chapters. Chapter 1 provides a background to low grade iron oxides, their treatment options, the aim and objectives of the project, as well as research justifications. Chapter 2 provides literature review of iron oxide separation techniques, with more focus on the principles of the selected reverse cationic flotation method and the Taguchi DOE method. The literature review also mentions some previous work done by various authors on different iron oxide flotation routes. Chapter 3 describes the experimental methods; which includes characterization of fluorspar tails, reverse cationic flotation experiments using Taguchi DOE and approach used in applying Taguchi DOE method. Chapter 4 presents and discusses characterisation and flotation results using SN ratio and ANOVA. Chapter 5 reflects on conclusions drawn from the research and recommendations. References are on Section 6 and the Appendices is reflected on Section 7.

2 CHAPTER 2: LITERATURE REVIEW

This chapter provides literature review for various beneficiation methods for low grade iron oxides with a focus on flotation. Principles of flotation are discussed with more focus on reverse cationic flotation used in this study. The importance of design of experiments (DOE) is highlighted with more emphasis on the studied Taguchi DOE.

2.1 Review of iron oxide beneficiation methods

Physical, chemical and mineralogical analysis of minerals are critical in the selection of appropriate separation method for concentrating valuable mineral. Generally, the upgrading of iron oxide ore is achieved using one or a combination of gravity separation, magnetic separation or flotation (Araujo, et al., 2005). The performance of the selected separation method is measured based on the achieved valuable mineral grade and recovery. Feasibility studies are further performed comparing the cost of production, losses incurred and price of the valuable commodity.

2.1.1 Gravity separation method

The gravity concentration method is the oldest technique used in mineral separation including that of iron ores. It is defined as the method used for separation of two or more minerals of different specific gravity, by their relative movement in response to the force of gravity and resistance to motion by viscous fluid such as water or any other suitable fluid (Burt, 1984). Gravity separation is suitable for processing iron ores – quartz minerals since there exists sufficient specific gravity difference between hematite and quartz (Voges, 1975). Besides specific gravity, this method is also affected by factors like weight, size and shape as they affect particle movement. It is efficient when a marked density difference exists between the mineral and the gangue (Das, et al., 2007).

Gravity separators are generally cheaper due to their simplicity and very low power requirements. Their environmental impact is lower due to the absence of organic chemicals. The limitation for gravity separators is that they are not efficient for the treatment of complex ores and fines (Rao, et al., 2009). A common problem in minerals processing is the efficient recovery of mineral values in the fines fraction, usually <75µm. In the fine size ranges, the fluid and viscous forces become dominant relative to the gravity and this in turn affects the separation efficiency. According to Wills & Finch, 2016 gravity separators are sensitive to presence of slimes (<10µm) due to increased slurry viscosity hence reduced separation efficiency and

obscure visual cut point for operators. The performance of gravity concentration generally increases with increased particle size. To reduce the size effect and to make the relative motion of the particles specific gravity dependent, a closely sized feed is desirable. However, significant development has been made in this field by introduction of enhanced gravity separators like Knelson, Falcon, Kelsey Jig, Multigravity separator, etc. Such equipment's generate higher gravity by application of centrifugal force and are capable of concentrating fines and ultrafine particles. The suitability of gravity concentration method for the processed minerals is determined by the difference in specific gravity (SG) of minerals and is measured using the concentration criterion (CC) (Wills, 2006):

$$CC = \frac{SG_{hm} - SG_{fluid}}{SG_{lm} - SG_{fluid}} \qquad \text{.....eqn 1.1}$$

Where SG_{hm} is heavy mineral's specific gravity, SG_{fluid} is specific gravity of the fluid and SG_{lm} is that of the light mineral. The concentration criterion is interpreted as follows;

CC > 2.5, suitable for separation of particles above 75µm in size

1.75 < CC < 2.5, suitable for separation of particles above 150 µm
1.50 < CC < 1.75, suitable for separation of particles above 1.7 mm
1.25 < CC < 1.50, suitable for separation of particles above 6.35 mm
CC < 1.25, not suitable for any size

Generally, when the quotient is >2.5 then gravity separation is relatively easy. The final gravity concentrate often needs cleaning by magnetic separation or some other method. Seifelnassr, et al. (2013) found that it was possible to upgrade iron ore using two stages (rougher and cleaner) of a gravity separation technique followed by magnetic separation or using two magnetic separation techniques. Examples of gravity concentrators for iron ores include dense media separation, jig concentrator, spirals, shaking tables, etc. (Wills & Finch, 2016).

- ***Dense media separators (DMS)****:* A fluid of specific gravity (SG) between the specific gravities of valuable and gangue mineral is used to float the lighter particles and the heavy particles settle, thus effecting separation of feed into gangue and concentrates. This process is applicable where there is adequate difference in specific gravities, liberated particles of +0.3mm size (Jain, 1985). Wills & Finch, 2016 recommended the use of DMS when processing coarse material of >4mm, in which case separation can be effected even on a

<0.1 difference in specific gravity. However, separation down to 500µm can be effected by inclusion of centrifugal separators.

The DMS is mainly used in laboratory for appraisal of gravity separation techniques on ores. DMS can be used in separation of hematite from mainly quartz gangue, however, consideration on selection of the fluid media is critical (Voges, 1975; Bosman, 2014). Generally, toxicity of the fluid media increases with increased SG which also impose limitations on the use of DMS. Sishen Iron Ore Mine used DMS to upgrade A-grade hematite ore (>60% Fe) of -90mm particle size to a final product grade of 66% Fe in lump and 65% Fe in the fine ore. However, its use on the B-grade (between 50% and 60% Fe) and C-grade material (between 35% and 50% Fe) was abandoned, owing to the inability of the existing DMS plant to beneficiate material at densities higher than 3600 kg/m^3 (Myburgh & Nortje, 2014). Instead, Sishen Mine considered jigging for B grade material.

- ***Jig concentrators****:* The separation of minerals of different SG is achieved in a particle bed which is fluidized by pulsating current of water producing stratification based upon density. A pulsation forces water up through the screen with adequate velocity to momentarily suspend all the particles resulting in fluidised condition. This pulsing causes the minerals with differing SG to arrange themselves according to the law of hindered settling (Jain, 1985). The stratification causes particles to be arranged in layers (concentrate, middling and tailing) with increasing density from the top to the bottom.

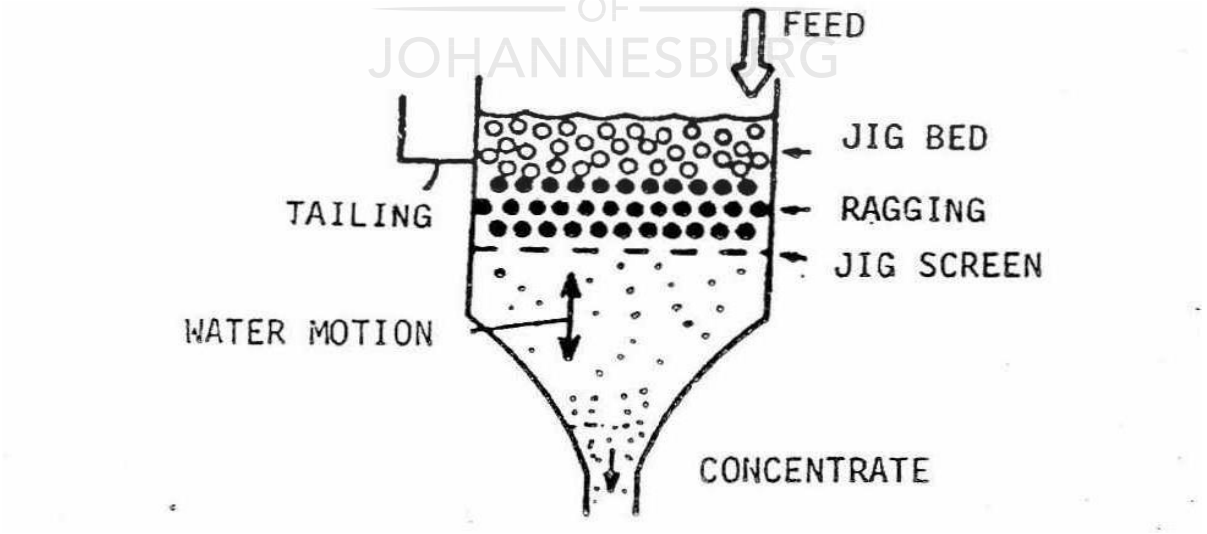

Figure 2.1: Basic construction of the jig (Michaud, 2006).

The size fraction of the required feed to the jigs is normally 0.5-30mm, however feed size as low as 75µm is possible with enhanced jigs. The jig is normally used to concentrate relatively coarse material and if the feed is fairly close-sized (e.g. 3-10mm) a good separation can be achieved even when a narrow difference in SG exists (Wills & Finch, 2016). The jig has advantages of low capital and operational costs, however, it is not suitable for fines. The presence of fines affects the jig performance in that fines tend to float thus reporting with the light/tailing layer. Sishen Iron Ore Mine investigated factors affecting jigging, studying a concentrate B-grade (50-60%Fe) hematite ore of coarse (-25+8mm), medium (-8+3mm) and fine (-3+1mm) texture (Myburgh & Nortje, 2014). Jigs are environmentally friendly with no use of reagents and cheaper to run. Das, et al. (2007) successfully used jigging to treat low grade iron of <5mm and 56-58%Fe into a concentrate of 63.7%Fe at 73.6% recovery.

- ***Spirals concentrators****:* The homogeneous feed slurry is introduced into the spiral channel and stratification occurs in a vertical plane as pulp flows around the helix of the spiral concentrator (Jain, 1985). This stratification is usually considered to be the result of a combination of hindered settling, interstitial trickling and centrifugal force in the helical trough (Wills & Finch, 2016). The heavies proceed to the lower velocity zones towards the inner side of the trough surface, while the lights tend to stratify in the higher velocity zones towards the outer side of the trough, as shown in Figure 2.2. The splitters are position at different locations on the through for collection of different streams (concentrate, middlings and tails)

Figure 2.2: Diagram showing spiral operation (Alibaba.com, 1999-2016)

The challenges of spirals concentrators have made industrial application of this process not fully utilized, though significant progress in the modelling of spiral concentrator has been made during the last decades (Vermaak, et al., 2008). These challenges include difficulty of splitter position adjustment to accommodate changes in feed parameters, low throughput (thus requiring large banks of spirals and large footprints), and large recycles due inefficiencies (Ramsaywok, et al., 2010).

2.1.2 Magnetic Separation method

This method uses magnetic intensity to separate paramagnetic minerals from diamagnetic minerals. The paramagnetic materials are those materials attracted along the lines of the magnetic field force to the point of greater magnetic field intensity. While diamagnetic materials are those repelled from the regions of greater field intensity along the magnetic field force lines to points of smaller magnetic field intensity (Jain, 1985). Figure 2.3 shows a powdered ore consisting of paramagnetic and ferromagnetic minerals being separated using magnetic rollers. The more magnetic susceptible mineral will stick to the roller until magnet is disable then it will fall off, while the less/none magnetic mineral will not stick to the roll hence drop off earlier.

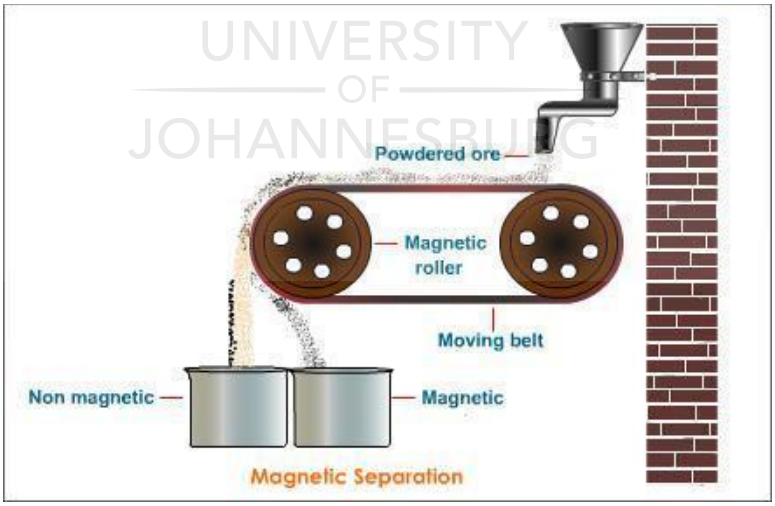

Figure 2.3: Magnetic separation operation (Tutorvista, 2016).

The magnetic response property of a target material to a magnetic field is therefore the determining factor in the efficiency of this process. The diamagnetic materials are concentrated using high intensity magnetic separators, while low intensity magnetic separators are used for paramagnetic minerals since these are greatly attracted to the magnetic force (Wills, 2006). The

other factors influencing separation is particle size, specific gravity of particles and freedom of movement of particles relative to moving stream (Jain, 1985). Magnetic separation is said to produce concentrates of superior physical nature for the blast furnace and achieves fairly complete recovery of iron, however, capital costs are high. Magnetic separators have lower capacity when compared to flotation method. Dworzanowski (2012) stated that recovery of fine iron ore by magnetic separation decreases with decreasing particle size because the magnetic susceptibility of magnetic particles decreases with a decrease in particle mass. Iron ore with low magnetic susceptible product (e.g. hematite) would require de-sliming while high magnetic affinity product (magnetite) would not require de-sliming**.** This is due to the fact that magnetic susceptibility of magnetite is on average 100 times greater than that of haematite for an equivalent mass of particle and that magnetite is ferromagnetic which means the mechanism of magnetic flocculation will apply (Dworzanowski, 2012).

Umadevi, et al. (2013) investigated the use of hydrocyclone, wet high intensity magnetic separator (WHIMS) and reverse flotation to concentrate low grade iron ore (≤50% Fe) slimes of d_{80}= <45µm. The findings revealed that gravity separation was unable to provide the required high grade concentrate possibly due to fine texture of the feed. WHIMS method was able to provide the high grade concentrate at reduced recovery and reverse flotation achieved high Fe recovery at lower grade.

Filippov, et al. (2014) recommended wet low-intensity for separation of magnetite and WHIMS as the best methods to process hematite ores with a high iron content, high liberation degree of iron oxide and where quartz is the major gangue mineral. Generally, gravity and magnetic separation methods are restricted to coarse grain size particles (Tripathy, et al., 2013). Rao, et al. (2009) recommend use of magnetic separation for magnetite/hematite ore that is not too fine and recommended flotation for ores that contain fine grains.

Figure 2.4 shows a guideline to the separation method recommended for a particular range of particle size. It is reflected that froth flotation is applicable for particle as fine as 5µm, whereas high intensity magnetic separation and gravity separation require minimum particle size of 20µm and 80µm respectively. This graph further shows that separation process efficiency generally increases with coarse particles, where in the lighter shade means the process is not as efficient in that size range and the darker shade reflects size ranges where the process performs well.

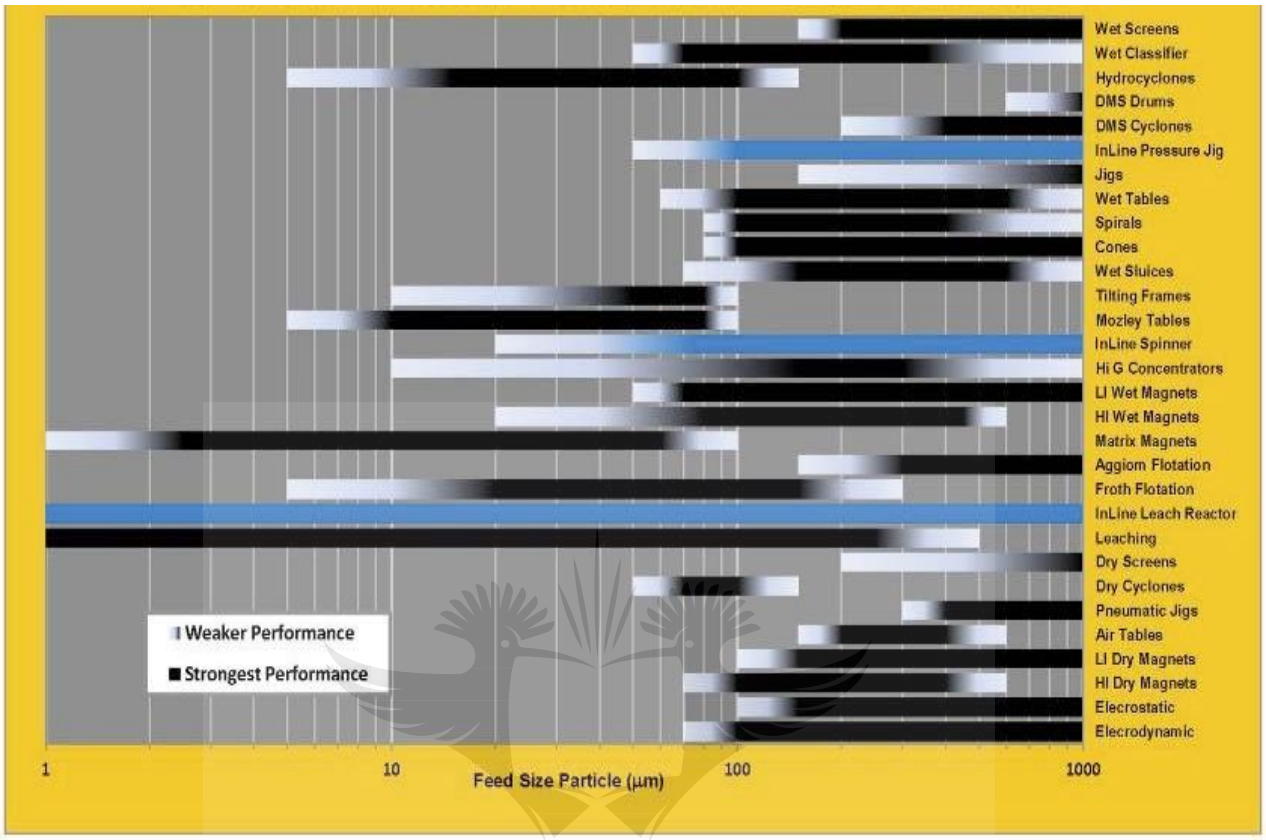

Figure 2.4: Effective particle size range for various mineral separation techniques (Gekko, n.d.)

2.1.3 Flotation method

Flotation is the physico-chemical separation process that utilises the difference in surface properties of valuable minerals and the unwanted gangue minerals. The flotation method uses differences in surface wettability, whereby the hydrophobic mineral in an aqueous medium is carried by air into the pulp surface thus effecting separation (Xu & Zhou, 2013). It was initially introduced for the treatment of sulphides of copper, lead and zinc but has now been expanded to include platinum, nickel, oxides such as hematite, non-metallic ores such as fluorite, etc. (Wills & Finch, 2016). The use of flotation has been extended to waste paper deinking, water treatment, flotation of plastics, etc. (Nguyen, 2013).

Flotation is the preferred method of separation for finely disseminated ore, due to its high selectivity (Filippov, et al., 2014). Wide use of flotation had come with the gradual depletion

of high grade ore bodies internationally, which has resulted in a need to grind ores into finer size (<149µm) in order to enable improved liberation of valuable mineral (Araujo, et al., 2005). Wide use of flotation has also come with increased processing of tailings as industries attempt to increase company revenue and lower environmental risks associated with heavy metals disposal (Wei, et al., 2015). Flotation is the recommended separation method for concentration of low grade iron ores (Kumar, et al., 2010). The general flotation routes for iron oxides are direct anionic flotation, reverse cationic flotation and reverse anionic flotation. Some work has been done on these flotation routes (Quast, 2005; Filippov, et al., 2014; Ma, et al., 2011). Recent development on flotation is concentration of iron oxide minerals using column flotation. (Lin, et al., 2009; Preas, et al., 2013).

2.2 Principles of froth flotation

Froth flotation is a recommended separation method for upgrading low grade iron oxide due to its high selectivity and therefore ability to produce super concentrates (Filippov, et al., 2014). Separation of solid particles is achieved using differences in their affinity for air bubbles in an aqueous solution (Parrent, 2012). Figure 2.5 shows a schematic diagram of the conventional froth flotation cell.

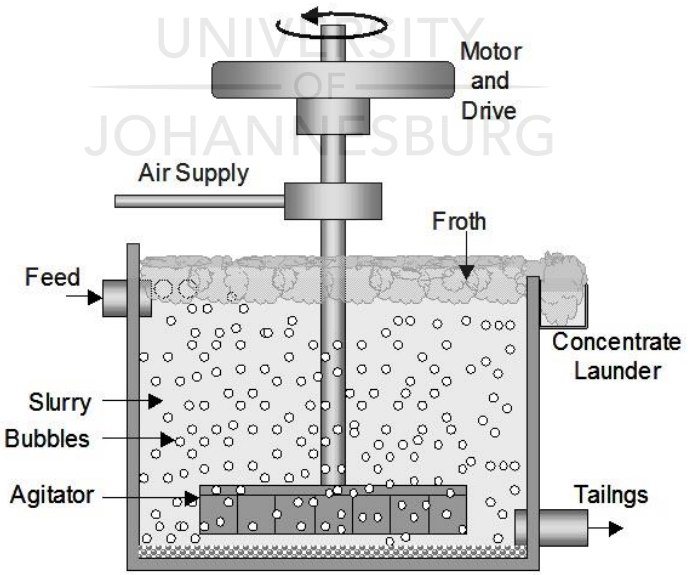

Figure 2.5: Conventional flotation cell (Trade Channel, 2014)

The flotation feed is crushed to an optimum size (10-250µm) that allows for sufficient liberation of valuable mineral from gangue (Filippov, et al., 2014). The feed is mixed with

water where the solids content is typically 20-40%, though solid content of up to 55% have also been reported (Wills, 2006). The pulp is introduced into the flotation cell and agitated at a specific speed for specific time while stage wise addition of flotation reagents is done. Reagents are added to effect apparent difference in surface properties for effective separation to occur. After the condition period has lapsed, air is introduced into the cell to start flotation. Small bubbles used in froth flotation produce very high specific area per unit volume of the gas-liquid interface for particles attachment, which makes flotation the most efficient technique for separation of especially low grade ores of fine texture (Nguyen, 2013).

The valuable hydrophobic mineral attaches to the bubble upon contact and is carried into the froth phase where it is collected as "concentrate". The froth layer contains inter-bubble water, hydrophobic particles and a small fraction of hydrophilic particles which get into froth by entrainment. The gangue mineral, being hydrophilic, is left in solution and is discharged as "tailings" at the bottom of the cell. This is termed direct flotation, where the valuable mineral is in the floats. Reverse flotation is when the valuable mineral is collected in sinks and is recommended when the amount of valuables exceeds that of gangue which is prevalent in iron oxides ores (Wills & Finch, 2016).

The theory of froth flotation is complex as it involves three phases viz; solids, liquid and gas. The process of recovering material from pulp by flotation comprises three mechanisms, viz:

(a) Selective attachment of target solids to air bubbles (or true flotation)
(b) Entrainment of solids in the water which passes through the froth
(c) Physical entrainment of solids between particles in the froth attached to air bubbles.

2.2.1 Selective attachment of mineral to the bubble

Selective attachment of target solids to air bubbles is the most important and dominant mechanism in flotation. Both valuable and gangue mineral can be transported to the froth area by entrainment and entrapment thus these mechanisms are not selective (Wills, 2006). The ability of a mineral surface to displace water and attach to air bubble is described by the contact angle, as shown in Figure 2.6.

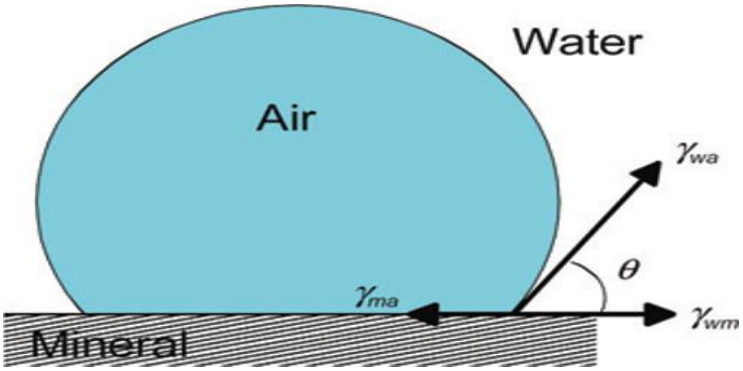

Figure 2.6: Bubble-air contact angle in an aqueous medium (Nguyen, 2013).

The general thermodynamic relationship between solid, liquid and gas interface at equilibrium is described using Young's equation:

$$\gamma_{wm} + \gamma_{wa}cos\theta = \gamma_{ma} \quad \therefore \cos\theta = \frac{\gamma_{wm}-\gamma_{ma}}{\gamma_{wa}} \qquad \text{.....eqn 2.1}$$

where γ_{wm}, γ_{wa} and γ_{ma} are the surface energies between solid and air, solid and water and water and air respectively, and θ is the contact angle between mineral surface and bubble. A mineral-air interface must be created, for flotation to occur, with simultaneous destruction of water-air and mineral-water interfaces of equal area. Thus for bubble-mineral attachment to occur, the contact angle must be finite and equation 2.1 gives

$$\gamma_{ma} - \gamma_{wm} \leq \gamma_{wa} \qquad \text{..... eqn 2.2}$$

A variety of methods used to measure contact angle are explained in Nguyen (2013). Most works, however, agree that contact angle does not fully describe the floatability of a mineral. The actual floatation of mineral particles depends on a large number of interacting variables such as kinetics, hydrodynamics and mineral particle size (Fuerstenau, et al., 2007). The force required to break the particle-bubble interface is called work of adhesion, W_{ma} and is equal to the work required to separate the solid-air interface and produce separate air-water and solid-water interface:

$$W_{ma} = \gamma_{wa} + \gamma_{wm} - \gamma_{ma} \qquad \text{.....eqn 2.3}$$

Combining with equation 2.1 gives:

$$W_{ma} = \gamma_{wa}(1 - cos\theta) \qquad \text{.....eqn 2.4}$$

It is seen that the greater the contact angle the greater is the work of adhesion between particle and bubble and the more resilient the system is towards disruptive forces. The hydrophobicity of a mineral therefore increases with the contact angle (Wills, 2006).

2.2.2 Hydrophobicity created by addition of flotation reagents

Flotation reagents are added into the system to effect selectivity of the process by adsorbing on the mineral surface thus modifying/intensifying the surface properties of a target mineral, making valuable mineral more hydrophobic or hydrophilic (Xu & Zhou, 2013). Reagents are also added to stabilise the froth phase so it retains the targeted mineral until it is collected thus minimizing mineral detachment. Reagents used in flotation can be classified into the following four categories:

- ***Depressants:*** They are those reagents that increase selectivity of flotation by rendering certain mineral hydrophilic thus preventing their flotation. Starch is the mostly used depressant for iron oxides due to its wide availability as it can be extracted from several vegetables such as corn, potato, wheat, cassava (Araujo, et al., 2005). Turrer & Peres (2010) suggested that the depressant action of starch on iron oxide is due to coating of a natural low energy hydrophilic surface with a hydrophobic film thus preventing attachment of air bubbles. An investigation conducted by Kar, et al. (2013) indicated that depressing activity of starch on hematite is due to interaction of hydroxyl groups of starch with that of the OH group on the hematite surface as per Figure 2.7.

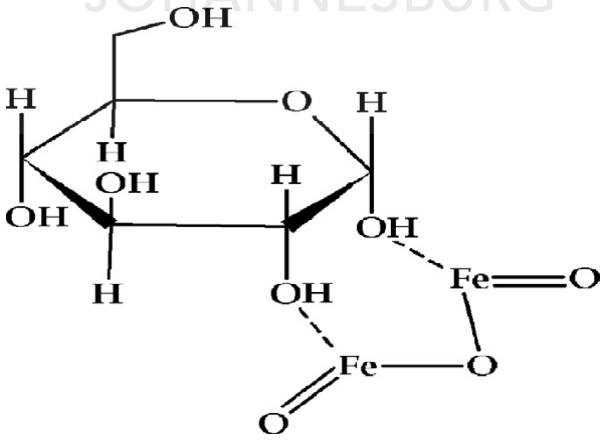

Figure 2.7: Hematite – starch interaction structure. (Kar, et al., 2013)

- ***Frothers:*** They are water soluble organic reagents that absorb at the gas-liquid interface, helping in the formation of a stable froth to ensure particles will not fall back into the

flotation pulp (Pearse, 2005). They are heteropolar molecules, with a polar group bonding with the water molecules and nonpolar hydrocarbon group for adsorption on a bubble as shown in Figure 2.8.

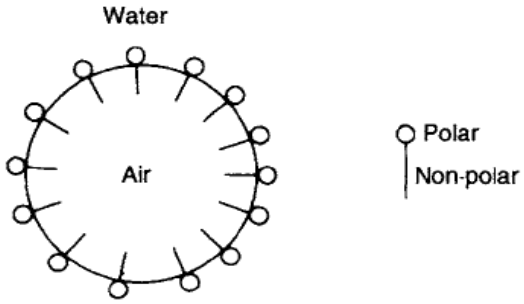

Figure 2.8: Action of the frother (Wills, 2006)

Froth structure and stability are known to play a significant role in determining the mineral grade and recovery achieved from froth flotation (Farrokhpay, 2011; Ata, 2012). Most collectors have frothing power. Alcohols are the most widely used and preferred frother in iron ores since they display no collector properties. A wide range of synthetic frothers, based on high molecular weight alcohols, are used in plants. A widely used synthetic alcohol frother is methyl isobutyl carbinol (MIBC), however, other range of synthetic frothers based on polyglycol ethers have been found very effective. It is also common to blend all three chemical groups (alcohols, polyglycols and polyglycol ether) together to provide a specific frother for a particular flotation circuit. (Araujo, 2005)

- ***Collectors:*** These are heterogeneous organic compounds that contain an active inorganic group (polar) coupled with a hydrocarbon chain (non-polar), as shown in Figure 2.9. The inorganic group is the portion of the collector molecule that adsorbs on the mineral surface, and the non-ionic hydrocarbon chain provides hydrophobicity to the mineral surface after collector adsorption by attaching on to air-bubble on contact (Xu & Zhou, 2013).

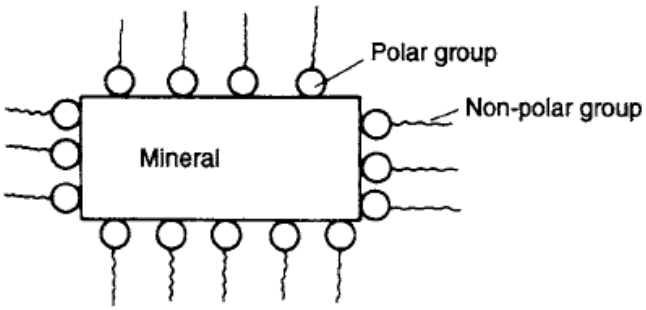

Figure 2.9: Collector adsorption on mineral surface (Wills, 2006).

The collectors are broadly categorized as non-ionizing and ionizing. The ionizing collectors are further categorized as cationic and anionic collector depending on the active site. Figure 2.10 below depicts classification of collectors.

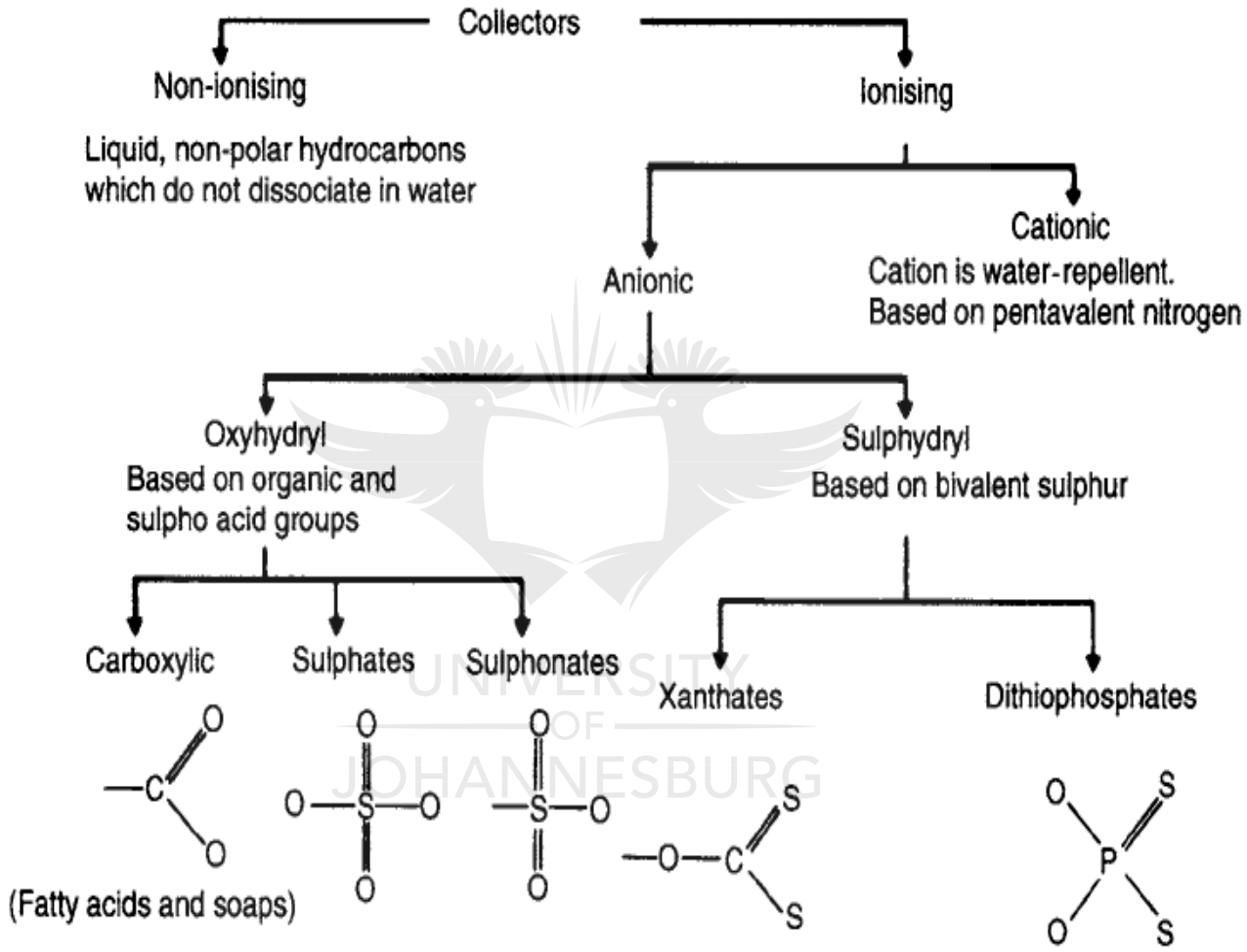

Figure 2.10: Classification of collectors (Wills 2006)

- **Cationic collectors** are used for floating oxides, carbonates, silicates and alkali earth metals such as barite, etc. (Wills 2006). Widely used cationic collectors for iron oxides are amines and they obtain their water repulsion characteristics from the polar group based on pentavalent nitrogen, as seen in Figure 2.11.

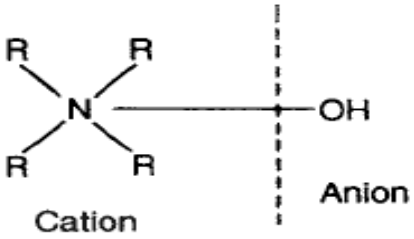

Figure 2.11: Cationic amine collectors. (Wills, 2006)

The amines are considered to adsorb from a solution below critical micelle concentration onto the negatively charged oxide or silicate surface primarily due to electrostatic attraction between the polar head of the collector and the charged electrical double layer on the mineral surface (Xu & Zhou, 2013). Cationic collectors ionize in aqueous solution by protonation, as follows;

$$RNH_{2(aq)} + H_2O \leftrightarrow RNH_3^+ + OH^- \qquad \text{eqn 2.5}$$

- **Anionic collectors** are classified into two types according to the structure of the polar group, viz; oxyhydryl and sulphydryl type, as shown in Figure 2.10. The sulphydryl collectors have bivalent sulphur as a polar group and are powerful in flotation of sulphides (Wills, 2006). The oxyhydryl collectors are used for the flotation of the silicates and iron oxide amongst others. Anionic collectors have been reviewed by Quast (2005) in direct anionic flotation of iron oxide.

- **Collector mixtures** are the mixtures containing the cationic and anionic collector and also those with non-ionic surfactants (Rao & Forssberg, 1997). Use of collector mixtures is on the rise as they have shown improved flotation selectivity and recovery compared to each separate reagent. The research done by Filippov, et al. (2010) showed that selected mixtures of ether amines with primary monoamines or with alcohols provided flotation of Fe-bearing gangue minerals which could not be floated by ether amines nor primary monoamines individually. A study done by Vidyadhar, et al. (2012) showed an increased adsorption of a cationic collector

(C12 amine) onto hematite surface in the presence of anionic collector compared to each collector working individually.

- ***Regulators or modifiers****:* They are used to intensify/reduce the collector action on the mineral surface. They are classed as:

    - *Activators* which are those reagents that alter mineral surface property such that mineral surface becomes hydrophobic due to the action of the collector. An example of activator is calcium oxide (CaO) used to render silica hydrophobic in reverse anionic flotation of iron oxides (Lin, et al., 2009).
    - *pH regulators* are those reagents which modify process pH. The common reagents used include caustic soda, soda ash, lime and sulphuric acid. Reverse cationic flotation of iron ores is usually conducted at basic condition (pH 10-10.5) (Araujo, et al., 2005).

2.2.3 Mechanism of reagent adsorption on oxide mineral surface

Selective adsorption of collector and modifying reagents in flotation of oxides and silicates is controlled by the electrical double layer at the mineral-water interface surface. Ions from the solution that are oppositely charged will be attracted and form a bound layer around the mineral surface. A diffuse layer of counter ions is also formed and it decreases in concentration with increase in distance (Carlson, 2010). These layers of ions constitute the electrical double layer (as shown in Figure 2.12) and each time particle moves there is a shear between the bound layer and the diffuse layer and that the plane of shear is called the zeta potential.

The magnitude of zeta potential depends on surface potential, concentration and charge of counter ions. King (1982) highlighted that the electrical double layer is critical in flotation and can affect flotation in many different ways, including that:

- The sign and magnitude of the surface charge controls the adsorption of physically adsorbing flotation reagents.
- Flocculation and dispersion of mineral suspensions is controlled by the electrical double layer interactions.
- Slime coating is controlled by electrical double layer interactions and hydrodynamics phenomena.
- Fine particle-air interactions are dominated by the surface charge effects.

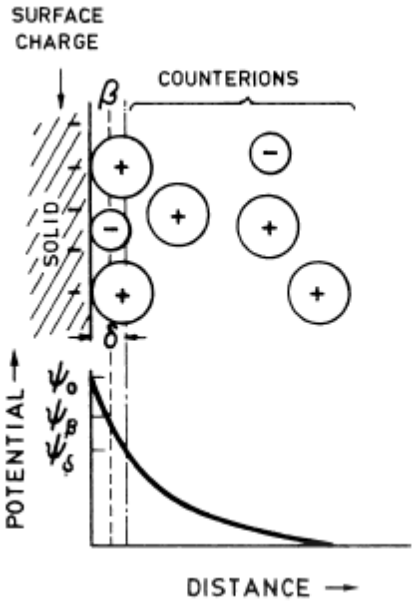

Figure 2.12: Schematic representation of the electrical double layer and potential drop across the double layer at a solid-water interface. The planes represent the inner and outer Stern planes (Fuerstenau & Pradip, 2005)

The ionic surfaces of oxide minerals are amphoteric and can take up either H^+ or an OH^- ion depending on the pH, which will determine the surface charge on the oxide. Amphoteric minerals have one particular pH at which the potential is zero because electro-neutrality has been reached, which means the density of positive sites is equal to that of negative sites. This point is called the point of zero charge (pzc) or iso-electric point (iep) (Nguyen, 2013). IEP is defined as pH at which particles carries neutral net surface charge. Whereas the pzc, refers to the absence of any type of charge. Ideally pzc and iep of the specific mineral should not be different if no other species has been adsorbed on the mineral surface, hence the reason Nguyen 2013 refers to pzc and iep as being the same. The mineral is negatively charged at pH above pzc value and is positively charged at pH value below pzc (Parrent, 2012).

Work done by Quast (2000) showed a variation in pzc and iep of relatively pure hematite, where the pzc 6.7 and iep of 2.7. The zeta potential measurement, done by Vidyadhar, et al. (2012), on pure hematite and quartz showed hematite iep of pH 6.7 and that of quartz at pH 2. Fuerstenau & Pradip (2005) measured pzc of natural and synthetic hematite to be 6.7 and 8.6 respectively. Filippov, et al. (2010) measured the iep of hematite at pH 7.7. The variations in pzc have been attributed to heterogeneity, where heterogeneity refers to coating of iron oxides by silica (Quast, 2005). Coating of course silica with ultrafine iron oxide (goethite and

hematite) was investigated by Rusch, et al. (2010) and it was observed that surface reactivity and pzc value were modified by presence of such coatings. Typical approximate pH ranges of the pzc of silica and hematite are pH 2-3 and pH 5-8 respectively (Nguyen, 2013).

2.3 Important factors affecting flotation

2.3.1 pH modifiers

These reagents are critical but yet their role is complex (Wills, 2006). In non-sulfide mineral flotation, the importance of pH is that hydroxyl and hydrogen ions modify the electrical double layer and zeta potential surrounding the mineral particle hence the hydration of the mineral surface and their floatability is affected. The variation of pH therefore affects the sign and the magnitude of charge of oxide. Flotation is often carried out under alkaline conditions since most collectors are stable under these conditions and metal corrosion is minimised. Sodium hydroxide is used in iron ore flotation, as a pH modifier, to limit effects of calcium (Wills & Finch, 2016).

Ma, et al. (2009) reported that cationic flotation of silica and iron oxides is stronger at alkaline medium, due to surface charge growing more negative as pH increases. The importance of pH is also demonstrated by work done by Ma, et al. (2011), which showed that reverse anionic flotation is less sensitive to the presence of fines when compared to reverse cationic flotation. This was shown by better recoveries of Fe observed in the ultrafine range of <10µm when using reverse anionic flotation. Reverse anionic flotation is typically conducted at pH 11.5, which makes hematite and quartz ultrafine particles highly negatively charged and repelling each other thus preventing heterogeneity. Unlike in reverse cationic flotation conducted at pH 10.5, where the hematite surface is only slightly negatively charged since its pzc is around pH 8 (Ma, et al., 2011).

2.3.2 Collector type and dosage

The choice of collector is determined by the mineral surface charge, collector's ability to dissolve in water and its hydrocarbon chain length and structure (Filippov, et al., 2014). Quast (2006) investigated the use of C6-C18 saturated fatty acids in hematite direct anionic flotation. It was discovered that the gradation increases with increase in collector carbon chain length, however, reduced solubility of longer carbon chain fatty acid make these reagents ineffective

as flotation reagents. Filippov, et al. (2014) reported that flotation of silicates from iron ores is mainly conducted using amines with hydrocarbon chain length of C10-C16. The hydrocarbon chain length of a collector is important because the chain to chain association enhances the adsorption once the surfactant ions aggregate to form hemi-micelles at the surface (Fuerstenau & Pradip, 2005).

The collector dosage is important for flotation as an increase in collector dosage will increase the process selectivity until a point when the recovery will plummet as the collector starts precipitating out of solution (Wen-gang, et al., 2009). Another cause of poor recoveries at excessive collector concentrations is the formation of a surfactant hemi-micelles on the mineral surface thus reducing the proportion of hydrocarbon radicals oriented into the bulk solution (Wills, 2006; Fuerstenau, et al., 2007).

2.3.3 The particle size

The mineral particle size plays a critical role in flotation. Particle recovery by true flotation involves collision, attachment and formation of a stable attachment to bubbles. Flotation behaviour of particles is therefore driven by hydrodynamic conditions and chemical environment and the behaviour of the froth zone (Nyambayo, 2014). Fine particles have insufficient inertia to cross the streamlines around the coursing bubble thus lead to decreased rate of flotation hence lowered recovery. Increased exposure of the fine particles to bubbles will however favour flotation of fine particles. This can be achieved by increasing air or increasing impeller speed (Wills, 2016). High presence of fines (<20µm) reduces selectivity of the flotation process as they tend to agglomerate on the target mineral thus altering surface properties. Too fine particles also tend to increase reagent consumption due to increased adsorption area (Ma, et al., 2011)

On the other hand, coarse particles may signal reduced liberation of the targeted mineral. The mineral size must be sufficient to allow for bubbles to lift the weight of the mineral until mineral is collected in the froth phase. Some strategies have been implemented to accommodate the different needs of fine and coarse particles, e.g. low collector concentration at the head of the bank is sufficient for the fast floating intermediate size particles followed by further collector dosage down the bank to recover the slow floating coarse particles (Wills, 2016). Typical recovery trend as a function of particle size is given in Figure 2.13.

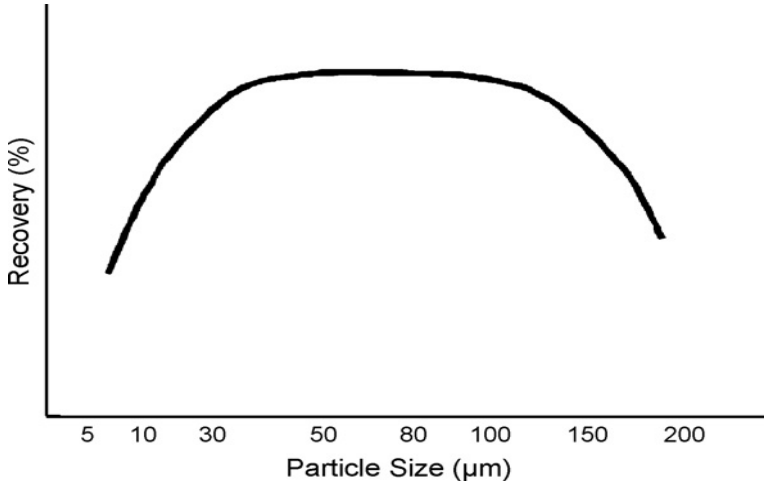

Figure 2.13: Typical view of flotation of different size fractions. (Santana, et al., 2008)

The trend depicted in Figure 2.13 shows that the recovery increases with increase in particle size until a plateau is reached after which a sudden drop in recovery is observed. Particles must be coarse enough to allow for bubble to lift the weight of the particle to the froth phase, whilst the target mineral must be liberated sufficiently to allow for selective attachment of the respective reagents onto the mineral surface (Santana, et al., 2008).

2.3.4 Conditioning time

Conditioning time refers to the time allocated for addition of reagents and stirring of pulp prior to introduction of air. Conditioning time has a significant effect on flotation of oxides since this is the first point of interaction between the targeted minerals and the flotation reagent (Quast, 2015). Work done by Molwa, et al. (2008) showed that the longer the conditioning time the better the separation efficiency of hematite until an optimum point of 5-6 minutes after which the separation efficiency plummets.

2.3.5 Pulp density

Pulp concentration refers to the percentage solids content in pulp. It plays an important role in recovery. Generally, recovery would increase with increase in pulp concentration until an optimum point is reached where the recovery drops. This recovery reduction at high pulp concentration may be due to deterioration in pulp aeration, poor floatability of larger particles, and increased floatability of fines (Jain, 1985). Pulp density is usually controlled between 15-40%, however, pulp density of 55% have been reported. Higher pulp density increases flotation machine output. An increased pulp density may require volumetric reagent concentration increase in order to avoid reagent starvation.

2.4 Flotation routes for iron oxides

The three flotation routes for iron ores are direct anionic flotation, reverse anionic flotation and reverse cationic flotation.

2.4.1 Direct anionic flotation

Direct flotation achieves separation of iron from gangue by floating iron oxide using anionic collectors such as fatty acids, hydroxamates and petroleum sulphonates. Direct flotation method is generally used for processing ores with vast amount of quartz, such as those in tailings (Quast, 2005). The use of direct flotation of iron oxides is still attractive in processing of low grade ores, and also in the recovery of material stored in tailings which contain vast amounts of quartz (Ma, et al., 2012). However, several laboratory investigations show that use of direct anionic flotation yields concentrates with high silica content (Araujo, et al., 2005). The challenges of direct flotation include its negative impact on the wettability of the iron during agglomeration process (Ivesona, et al., 2004).

2.4.2 Reverse anionic flotation

Reverse anionic flotation concentrates the iron mineral by first activating quartz with the use of lime, and then floating the quartz using mostly anionic fatty acids as collectors. Calcium oxide is added to activate quartz via ionization of CaO in water into Ca^{2+} and H^{+} ions, whereby Ca^{2+} will react with quartz at pH>11 (Lin, et al., 2009). NaOH is used to adjust the pH value of pulp, change surface potential of mineral and to provide stable conditions for other reagents. Starch is adsorbed on the surface of the iron mineral and is used as a depressant for iron mineral.

The advantages of reverse anionic flotation in comparison with reverse cationic flotation include its lower sensitivity to the presence of slimes (<10μm) and lower reagent costs since fatty acids are the main component from waste paper (Ma, et al., 2011). However, despite the success of reverse anionic flotation of iron ore in China, reverse cationic flotation remains the most popular flotation route used in the iron ore industry (Ma, 2012). Vidyadhar, et al. (2012) found quartz not responding to flotation with anionic collectors and that its response to C12 amine was observed to be pH and collector concentration dependent.

2.4.3 Reverse cationic flotation

Reverse cationic flotation refers to concentration of iron oxide by floating the gangue mineral (SiO_2 in this case) using cationic collector and depressing the valuable mineral (Fe-oxide in this case) thus recovering the iron oxide in the sinks. Reverse cationic flotation of low grade iron oxide is normally conducted at pH 10-10.5 (Ma, et al., 2011). Polymeric depressant mainly such as starch is used to depress the iron oxide mineral and cationic collectors such as amines adsorb on the negatively charged quartz. Starch absorbs extensively on hematite and has lower affinity for quartz at higher pH, while the amine adsorbs strongly on quartz than on hematite (Pavlovic & Brandao, 2003). Research show that there are numerous alternative depressants used in hematite separation. These include humic acid as a better depressant for hematite, when compared to starch, in the presence of dodecylamine (DDA) collector (Santos & Oliveira, 2007). Research done by Kar (2013) on usage of corn starch, potato starch, rice starch and soluble starch as depressants indicated that all starches are good depressants for hematite, however, quartz was better floated in the presence soluble starch and DDA collector.

Various amines are used as cationic collectors during reverse flotation of iron oxides. Amines are alky-derivatives of ammonia (NH_3). Primary amines are those where one hydrogen atom is replaced by the alkyl group and tertiary amines are those where all three hydrogen atoms are replaced by alkyl groups, which enables higher molecular weight in tertiary amines. Primary amines are said to have higher basicity than tertiary amines and are said to form hydrogen bonds easier and are more stable than tertiary amines when dissolved in water (Matthews, 1992). Hydrolysed reagents are the most efficient cationic collectors as they present both ionic and molecular species in the aqueous phase where this is will depend on system pH (Filippov et al., 2014). However, solubility of amines in water is reduced with increased length of the carbon chain.

Use of DDA in reverse cationic flotation of iron oxides has produced reputable results and is well published however has a challenge of low solubility (Kar, et al., 2013; Ma, et al., 2012). In early years the primary amines such as DDA were used as quartz collectors, however due to their low solubility in pulp they were replaced by the more soluble ether amines (Ma, et al., 2012). The insertion of a hydrophilic group in ethers improves solubility thus facilitating access to solid-liquid and liquid-gas interfaces and also enhances the elasticity of the liquid film around the bubbles (Araujo, et al., 2005). Quaternary ammonium salts have in recent years been reported to be more selective than primary amines. Filippov, et al. (2010) compared

primary monoamine (DDA) with an ether diamine and observed that ether diamine is a stronger collector for quartz than the primary monoamine. However, the amines are generally costly compared to fatty acids used in anionic flotation. Yuhua & Jianweig, (2005) conducted an investigation using combined quaternary ammonium salt for flotation of quartz and observed that it was a better collector for quartz in iron ore separation when compared to primary amines.

Research done by Filippov, et al. (2014) showed that reverse cationic flotation of iron ores is the best separation method when compared to anionic flotation due to higher process selectivity and flotation rate as well as satisfactory results when hard water is used. The work done by Ma, et al. (2011) showed that the reverse cationic flotation is sensitive to the presence of ultrafine particles (<10µm) while its performance was slightly better than reverse anionic flotation at coarse particle range (>210µm). Reverse anionic flotation is conducted at pH 11 where both hematite and quartz are highly negatively charged thus the fines having sufficient repulsion to prevent hetero-coagulation (Wills & Finch, 2016). The importance of de-sliming fines <20µm was emphasized by Fillipov, et al. (2014), however, it led to hematite loss of 7.6-16.6%. Lima, et al. (2013) recommended that the reverse cationic flotation feed particle size must range between 10-150µm, the slimes (<10µm) to be removed and the top size limited to 5-10% >150µm as wide range of particle size impairs process selectivity. The impaired selectivity may be due to differences in hydrophobicity, specific surface area and weight.

Flotation rate is significantly faster in reverse cationic flotation than reverse anionic flotation (Ma, et al., 2011). Reverse cationic flotation has also been investigated by Peres & Mapa (2008) who suggested that reverse cationic flotation is critical for producing pellets feed fines at all iron ore processing plants in Brazil.

2.5 Design of experiments – Taguchi Method

Due to multiple parameters influencing flotation, it is difficult to study all possible combinations of factors as it would lead to uneconomically lengthy experiments and high consumption of resources (Bendell, et al., 1989). Design of experiments (DOE) is a statistical approach that attempts to provide a predictive knowledge of a complex, multi-variable process with few trials (Athreya & Venkatesh, 2012). There are various DOE methods available such as full factorial design, fractional factorial design and Taguchi method. The minimum number of observations (N) required for the above-mentioned DOE methods is given by equations 2.5-2.7:

Full factorial doe, $N = l^k$ …….eqn 2.5

Fractional factorial doe, $N = l^{k-p}$ …….eqn 2.6

Taguchi doe, $N = 1+k(l-1)$ ……..eqn 2.7

Where l is the number of levels, k is the number of parameters and p is the number of generators.

Unlike full factorial design which tests all possible combinations, the fractional factorial design tests a fraction of the full factorial design. The Taguchi DOE method test a fraction of the fractional factorial design by testing pairs of combinations using orthogonal arrays to organize the parameters affecting the process and the levels at which they are varied (Athreya & Venkatesh, 2012). The Taguchi therefore allows for a small number of observation required to find the main factors effects on output while all the parameters and their levels appear the same amount of time in the orthogonal matrix. Due to the number of parameters investigated, this research will study use of Taguchi DOE method for optimisation of the flotation process. Taguchi is a well-accepted technique founded in 1966 by Genichi Taguchi. This method is based on Ronald's Fischer factorial design work, and is widely applied for product design and process optimization in manufacturing, marketing and engineering sectors worldwide (Altan, 2010; Kumar et al 2015; du Plessis 2007). Taguchi method was used in optimization of nickel – copper sulphide ore flotation (Masiya & Nheta, 2014). Taguchi method has applications in various processes such as welding, marketing, etc.

It uses orthogonal arrays to arrange parameters and levels to which they shall be varied such that it tests pairs of combinations thus allowing for a smaller number of required observations. (Athreya & Venkatesh, 2012). Taguchi is recommended for processes with intermediate number of variable (3-50) where there are few interactions between variables and where only a few variables contribute significantly. The analysis of data is conducted using tools such as signal-noise ratio (SN ratio) and analysis of variance (ANOVA). Taguchi method uses the Signal-Noise ratio to show optimum conditions for the desired output response, where the system is robust (less sensitive to variations). Higher values of the signal-to-noise ratio (SN) would identify control factor settings that minimize the effects of the noise factors (Sapakal & Telsang, 2012). The SN ratio is able to also rank the parameter according to relative significance. ANOVA is a tool used to determine the relative importance of each factor under investigation (Tofighy & Mohammadi, 2012). It is also used to identify and quantify the errors resulting from deviations of a set of results (Altan, 2010). A variety of software that can be

used for fractional factorial DOE can also be used for computing/analysis of Taguchi DOE results. These include Minitab 17 and Statistical Package for the Social Science (SPSS).

3 CHAPTER 3: METHODOLOGY

This chapter describes the steps followed in characterisation of the tailing sample and concentration of the valuable mineral found using flotation. These include sample preparation, sample characterisation analysis procedures and flotation experiments. It further explains the use of Taguchi DOE method for the selected parameters and levels investigated. Variety of hazards exist in the laboratory. Specific risk assessment, as in Table 1 of the appendix, was conducted before commencement of flotation experiments to ensure compliance to safe work procedures

3.1 Materials

Laboratory testing of a concept prior to implementation on a large scale is critical in mineral processing industry. Approximately 400kg wet fluorspar tails sample was received from Vergenoeg Mine in plastic bags. Random bags of wet sample, measuring total of 120kg, were selected. This sample was oven dried at 70^{o}C, de-lumped, mixed and sub sampled using a combination of random sampling, cone-quartering and rotary splitting. The sample was dried at 70^{o}C to ensure that the sample composition is not changed due to loss of organics or denatured due to high heat.

Batch rougher reverse cationic flotation experiments were conducted on the fluorspar tails using two amine collectors, 98% pure Dodecylamine (DDA) and 99% Betacol 373. Betacol 373 is composed of a mixture of octa-dodecane, tri-ethoxydecane and di-alkyl ammonium chloride. The difference between the two amines is that DDA is a primary monoamine and Betacol 373 is a tertiary amine. The general structures of primary and tertiary amines are shown in Figure 3.1.

Figure 3.1: Structure of a primary and tertiary amine, respectively (Matthews, 1992)

Though Araujo et al., 2005 recommended the use of ether amines over mono amines, the cost of ether amines was found to be very high. Preliminary test were conducted to check the feasibility of the reagents. This included investigating the use of the anionic reagent Betacol 290, dodecyl amine. From the pre-liminary results it was observed that cationic reagent was a

better collector, hence the dodecyl amine and Betacol 373 were selected for further investigation. The selected collectors were further selected based on availability and cost, where the Betacol 373 was supplied by local company free of charge and dodecyl-amine was a stock item at University of Johannesburg laboratory.

The two depressants under investigation were dextrin (Betachem 30D) and soluble starch (SS). The difference between the two depressants is that Betachem 30D is a dextrin which is a group of low-molecular weight carbohydrates made from hydrolysis of starch (Matthews, 1992).

3.2 Methods

3.2.1 Characterization of fluorspar tails

Characterization results are essential in selection of appropriate separation method for minerals. Characterisation of fluorspar tails was conducted using a combination of physical, chemical and mineralogical analysis. The analysis done for characterisation of fluorspar tails sample was adapted from works of Tripathy et al., 2013; Srivastava et al., 2001 and Nheta et al., 2015.

- ***Particle size distribution analysis***

Particle size distribution in the head sample was determined using Microtrac Particle Size Analyser (PSA), which makes use of the three precisely placed laser diodes to characterise particles from 0.02-2800µm.

- ***Density and chemical analysis***

A representative sample was classified into different size fractions, viz; +150µm, -150+106µm, -106+75µm, -75+53µm, -53+45µm, -45+38µm and -38µm for the purpose of examining mineral distribution in the sample. The Micromeritics AccuPyc III 1340 gas pycnometer utilizing N_2 gas was used to measure the density of the head sample and density across the different size fractions to assess valuable mineral distribution.

The chemical composition, of the head sample and of different size fractions, was determined using a Rigaku ZSX Primus II X-Ray fluorescence (XRF).

- ***Loss on ignition analysis***

The moisture, organic and carbonates content was determined in the head sample using the loss on ignition (LOI) method published by National Lacustrine Core Facility, 2013. Three 1.7g sample were placed in weighed crucibles and weighed. The samples were heated at 100ºC for 8 hours to remove moisture. The samples were removed from the oven and cooled down in a desiccator. The samples were heated at 550ºC for four hours in a furnace to remove organic matter. The samples were removed from the furnace, cooled and weighed. The samples were heated to 1000ºC for two hours to remove carbonates, after which, the samples were cooled in a desiccator and weighed.

The moisture, organics, carbonates and loss on ignition (LOI) was calculated as follows:

$$Moisture\ content,\% = \frac{Initial\ mass(g) - Final\ mass_{100^{o}C}(g)}{Initial\ mass(g)} \times 100 \quad \text{…….. eqn 2.8}$$

$$Organics\ content,\% = \frac{Final\ mass_{100^{o}C}(g) - Final\ mass_{550^{o}C}(g)}{Final\ mass_{100^{o}C}(g)} \times 100 \quad \text{…….. eqn 2.9}$$

$$Carbonates\ content,\% = \frac{Final\ mass_{550^{o}C}(g) - Final\ mass_{1000^{o}C}(g)}{Final\ mass_{550^{o}C}(g)} \times 100 \quad \text{…….. eqn 2.10}$$

$$Loss\ on\ ignition,\% = \frac{Initial\ mass(g) - Final\ mass_{1000^{o}C}(g)}{Initial\ mass(g)} \times 100 \quad \text{…….. eqn 2.11}$$

- ***Mineral phases analysis***

The mineralogical phases present in the sample were determined using the Rigaku Ultima IV X-ray diffractometer (XRD).

- ***Mineral abundance using QEMSCAN***

QEMSCAN was used in combination with x-ray powder diffraction (XRD) and geochemical analyses to identify and quantify mineralogical characteristics of the tailings. X-Ray diffraction is only a semi-quantitative technique which identifies crystalline minerals with concentrations >3mass% in the sample. QEMSCAN BMA was conducted on two traverse-cut polished sections from the sample in order to quantify their mineral. In addition, QEMSCAN Particle

Map Analysis (PMA) was conducted on the polished section with an aim of characterising Fe-oxides in terms of the Fe-oxide grain size dimension, Fe-oxide liberation, Fe-oxide exposure and mineral association.

3.2.2 Flotation experiments method

Reverse cationic flotation using rougher stage only was use to concentrate the valuable mineral (iron). The optimization of the process considered parameters such as collector type and dosage, depressant type and dosage, pH, solids concentration, conditioning time, agitation speed, air rate and presence of fines. Taguchi method was employed for planning and arrangement of experiments. Minitab 17 was used as a software to compute data and analysis of results using signal-to-noise ratio and ANOVA.

The performance of the flotation test was measured by measuring the iron grade in the concentrate, calculating metal recovery and metal loss as follows:

$$Metal\ recovery, R = \frac{Cc}{Ff} \times 100 \quad \text{.....eqn 2.12}$$

$$Metal\ loss, M = 100 - R \quad \text{.....eqn 2.13}$$

Where C is the concentrates mass in grams, c is the iron assay in the concentrates (mass %), F is the feed mass in grams and f is iron assay in the feed (mass%). Metal loss refers to metal in the tails and also miscellaneous losses (e.g. losses due to spillages, washings, materials left in filter papers, etc). Related measures to grade and recovery include: the ratio of concentration, the weight recovery/yield, the enrichment ratio and separation efficiency. (Wills & Finch, 2016).

- ***Reagents preparation***

De-ionised water was used for reagents preparations. The 98% dodecylamine (DDA) from Merc was prepared to 1%weight solution, heated to 40^{o}C while mixing and addition of few drops of hydrochloric acid was done to ensure a dissolved solution. Lumps in the collector solution lead to uneven distribution of the collector (Araujo et al., 2005). The second cationic collector used, Betacol 373, was kindly supplied by Betachem in a liquid form hence required no preparation. Sodium hydroxide was prepared to 5% weight solution and HCl to 5% solution. The depressants, Soluble Starch (SS) and dextrin Betachem 30D, were prepared to 3% solution. The dextrin was heated to 40^{o}C while mixing was done to ensure a dissolved solution. The

frother, Dowfroth 200 was supplied by Betachem. All reagents were prepared on the day of experiment.

- ***Flotation equipment description***

Flotation was carried out in Laboratory Denver D12 mechanical flotation machine with 2.5lt cell capacity, shown in Figure 3.2. The Denver D12 machine is fitted with the variable speed agitator, and air pipe.

Figure 3.2: Denver D12 conventional flotation equipment

- ***Flotation experiment description***

A combination of L25, L16, L9 orthogonal arrays and full factorial designs were used throughout the project depending on the number of parameters and levels to which they were varied. The flotation procedure followed is depicted in Figure 3.3.

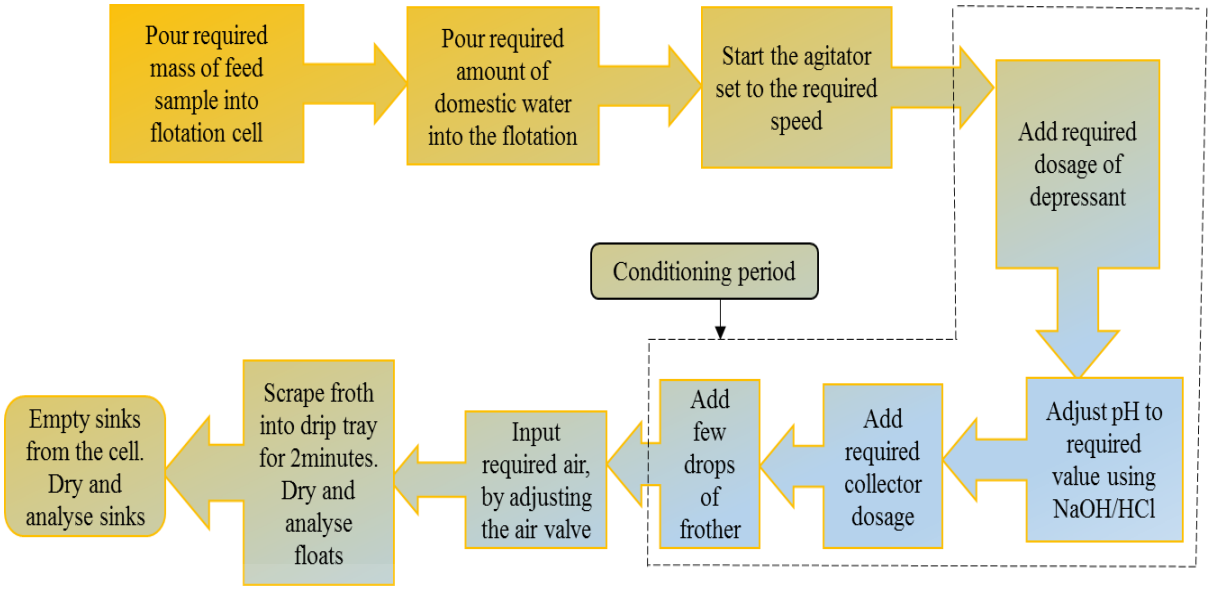

Figure 3.3: Flowsheet depicting flotation procedure

The required pulp was prepared in the flotation cell using domestic water, where solid content was varied from 35-55%. The rotor was started and speed varied between 1200-1400rpm. The measured depressant was poured into the pulp, whereby soluble starch was varied from 750-2000g/t and 300-2000g/t Betachem 30D. Pulp pH was measured using Hannah pH meter and adjusted to the required value, between 4-12, using NaOH/HCl. The collector was then added and a few drops of frother were then added while agitating for the required conditioning time of 3-20 minutes. The DDA collector dosage was varied from 200-600g/t, Betacol 373 from 2500-8000g/t and few drops of frother. The pulp level was kept at about 10-15mm below the froth overflow launder. Collection plate was placed for the collection of froth. After the desired conditioning time had lapsed the desired air was opened into the cell to create bubbles for attachment of hydrophobic minerals. Froth was collected into the drip tray using froth paddles to scrap the froth into the collection plate. Flotation was carried out for 2 minutes after which the floats and sinks were filtered and oven dried at 70^{o}C. The dried floats and sinks were cooled, weighed and analysed for oxide content using XRF machine.

3.3 Taguchi Method - Design of experiments

The approach to planning of experiments using Taguchi was done according to Figure 3.4, where control and noise factors under investigation and the levels to which they will be varied were identified (du Plessis & de Villiers, 2007). The choice of orthogonal arrays matrix

selected was based on minimum number of required observation, N, as determined by the degree of freedom. Minitab 17 was used for computing of Taguchi data and data analysis.

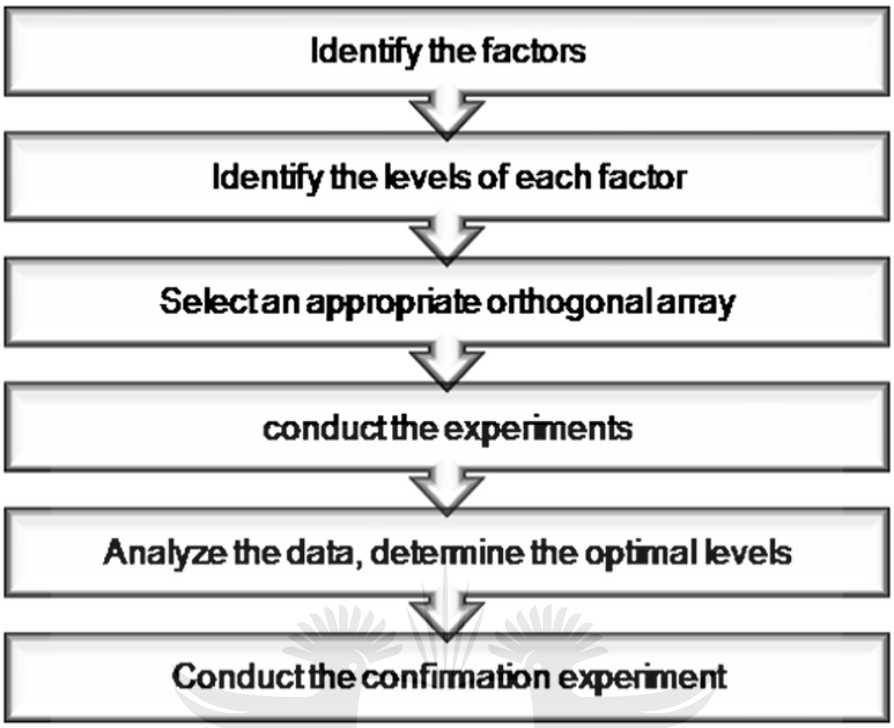

Figure 3.4: Taguchi method steps (Bendell, et al., 1989).

3.3.1 DOE setup for the Soluble starch – DDA system

The selected parameters and the levels to which variation was made for the soluble starch (SS) and DDA system, is shown in Table 2. The fixed parameters were agitation speed at 1200rpm and air valve half open.

Table 2: Experimental parameters and their levels.

Parameters	Level 1	Level 2	Level 3	Level 4	Level 5
Starch dosage (g/t)	750	1000	1300	1500	2000
DDA dosage (g/t)	200	300	400	500	600
pH	4	6	8	10	12
Solids content %	35	40	45	50	55
Condition time, min	3	6	10	15	20

As five parameters and five levels were under investigation, this experimental programme required 3125 observations to conduct full factorial design, as per equation 2.5. The minimum

required number of Taguchi observations was calculated using equation 2.7 to be 21. Hence L25 Taguchi orthogonal array (OA) matrix was selected. The L25 worksheet showing the experimental arrangement for soluble starch and DDA is given in Table 3, where SD is the soluble starch dosage, CD is the collector dosage and CT is conditioning time.

Table 3: L25 orthogonal array matrix for DDA and soluble starch experiments

	Operating conditions				
Exp. no.	**SD g/t**	**CD, g/t**	**pH**	**%solids**	**CT, min**
1	750	200	4	35	3
2	750	300	6	40	6
3	750	400	8	45	10
4	750	500	10	50	15
5	750	600	12	55	20
6	1000	200	6	45	15
7	1000	300	8	50	20
8	1000	400	10	55	3
9	1000	500	12	35	6
10	1000	600	4	40	10
11	1300	200	8	55	2
12	1300	300	10	35	10
13	1300	400	12	40	15
14	1300	500	4	45	20
15	1300	600	6	50	3
16	1500	200	10	40	20
17	1500	300	12	45	3
18	1500	400	4	50	6
19	1500	500	6	55	10
20	1500	600	8	35	15
21	2000	200	12	50	10
22	2000	300	4	55	15
23	2000	400	6	35	20
24	2000	500	8	40	3
25	2000	600	10	45	6

The output columns (Fe grade) were added into the worksheet and tests repeated randomly. The optimization was conducted by studying the control factors only, with the targeted output being "highest Fe grade", with SN ratio is given as follows:

$$\frac{S}{N} = -10 \log\left[\frac{\Sigma\left({}^{1}/_{y_i{}^{2}}\right)}{n}\right] \qquad \text{.....eqn 2.14}$$

Higher values of the signal-to-noise (SN) ratio would identify control factor settings that facilitate desired output results (Sapakal & Telsang, 2012). The signal – noise ratio was also used to rank parameters according to relative significance. A confirmation test was conducted at the optimum conditions predicted by Taguchi SN ratio.

Further optimization exercises were conducted until the required result was obtained. Analysis of data using ANOVA was done to identify and quantify the errors resulting from deviations of a set of results (Altan, 2010). ANOVA can also be used to determine the relative importance of each factor under investigation (Tofighy & Mohammadi, 2012).

3.3.2 DOE setup for the Betachem 30D – DDA system

The information obtained from the SS - DDA experiments was used in planning experiments for Betachem 30D and DDA. This experiment used L9 OA matrix whereby the Betachem 30D dosage, DDA dosage, air rate and agitation speed were studied. The parameters such as pH, solids content and conditioning time were fixed at 10, 50% and 6 minutes respectively. The varied parameters and their levels is shown in Table 4.

Table 4: Betachem 30D - DDA system parameters setting

Parameters	**Level 1**	**Level 2**	**Level 3**
Betachem 30D (g/t)	300	1000	2000
DDA (g/t)	200	400	500
Agitation speed (rpm)	1200	1300	1400
Air	½ open	¾ open	Fully open

L9 orthogonal array matrix was used since there were four parameters and three levels, as shown in Table 5.

Table 5 : L9 orthogonal array matrix for DDA and Betachem 30D experiments

Betachem 30D (g/t)	DDA (g/t)	Air rate	Agitation speed (rpm)
300	200	1/2	1200
300	300	3/4	1300
300	500	1	1400
1000	200	3/4	1400
1000	300	1	1200
1000	500	1/2	1300
2000	200	1	1300
2000	300	1/2	1400
2000	500	3/4	1200

The flotation experiments were conducted, as per Figure 3.3, then the SN ratio was used to determine optimum operating conditions for achievement of higher Fe grade and ranking of parameters.

3.3.3. DOE setup for the Betachem 30D – Betacol 373 system

The L9 orthogonal array matrix was used to determine optimum conditions for high iron grade. The parameters investigated were Betachem 30D dosage, Betacol 373 dosage and solid content. Dextrin dosage was varied 300-2000g/t, Betacol 373 dosage 380 – 3328g/t and solid content 35-55%. The parameters pH, agitation speed, air rate and conditioning time were fixed at 10, 1300rpm, ¾ air vale open and 15minutes as adapted from the SS-DDA system.

4 CHAPTER 4: RESULTS AND DISCUSSION

This chapter presents fluorspar characterization results whereby the chemical analysis, physical analysis and mineralogical analysis results are discussed. It also includes results obtained through rougher flotation of flurosar tails using DDA and Betacol 373 cationic collectors. The two iron oxide depressants used (soluble starch and Betachem 30D) are compared. The results were analyzed using the Taguchi SN ratio and ANOVA.

4.1 Characterisation of fluorspar tailings

4.1.1 Particle size analysis

The particle size distribution of the fluorspar sample showed that the sample is fine with 80% passing 155µm, as illustrated in Figure 4.1. This confirms that the sample is from a flotation circuit and has been already milled since it is of fine texture. It was also observed that 10% of the particles were slimes, <20µm.

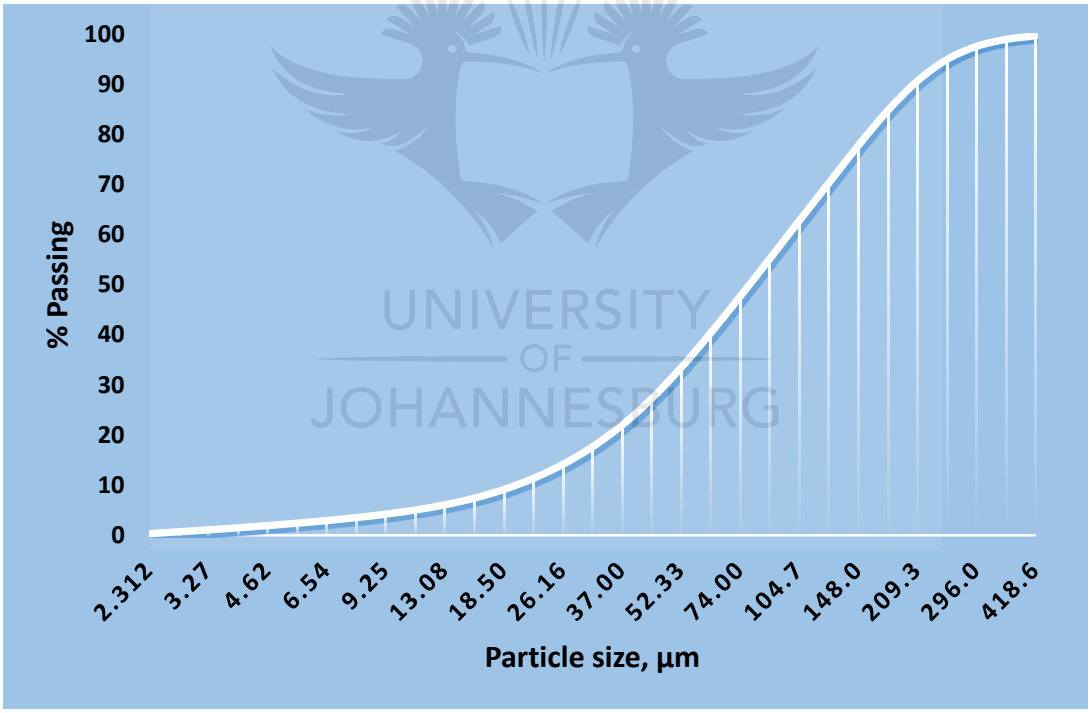

Figure 4.1:Particle size distribution

4.1.2 Chemical assay results

Chemical results showed that the most valuable mineral in the head sample is Fe in the form of hematite assaying 48.9%Fe. The major gangue minerals found were 16.8%SiO_2, 3.8%CaO with 2.25%F and remaining oxides all occurred in concentrations <1 wt.%. The Fluorine was measured as an element. Detailed chemical analysis for feed received are shown in Table A2 of the appendix. The sample was classified as low grade since iron assayed <50%.

4.1.3 Mineral distribution analysis results

A combination of density measurement and chemical analysis conducted to measure size wise distribution of hematite in the sample showed the results reflected in Figure 4.2. Hematite and quartz have specific gravity of 5.1g/cm^3 and 2.65g/cm^3 respectively (McMurry, 2014). It was observed that the density increases as particles becomes finer. Density measurement of 3.51g/cm^3 was obtained at +150µm size fraction and 4.42g/cm^3 obtained in the -38µm size fraction. From these results it was anticipated that the hematite will be more concentrated in the finer sizes. Numerical details of mineral distribution results are shown in Table A4 of the appendix.

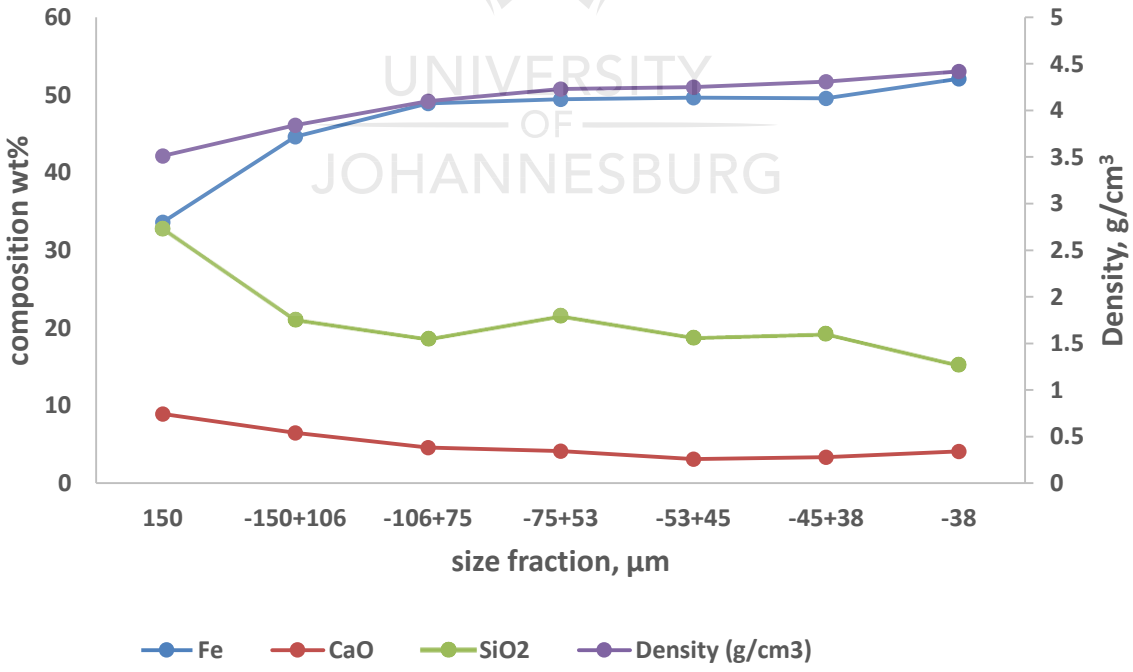

Figure 4.2: Mineral distribution in fluorspar sample collected

The prediction was confirmed by chemical analysis results where a concentration of iron was observed to be increasing in the finer size range, as shown in Figure 4.2. A lower concentration 33.59%Fe was found in the +150µm and higher concentration of 52.09%Fe in the -38µm, which collaborated with density results. The silica and calcium oxide content was observed dropping in the finer size range. It must be noted that frequent flooding problems were experienced during size classification using vibrating wet screening, hence the mass distribution across the selected size fraction was not studied.

The concentration ratio of 2.48 was calculated using equation 1.1. Generally, a concentration ratio of 2.5 implies the mineral can be separated with ease using gravity separation for minerals that are >75µm in size. However, since chemical analysis shown in Figure 4.2 illustrated that iron is more concentrated in the finer ranges (<75µm), gravity separation (specifically jigs, spirals and DMS) does not become an ideal separation method for this product. According to effective range of mineral processing techniques application shown in Figure 2.4, gravity separation is efficient at >80µm size particles. High intensity magnetic separation is another option for enrichment of hematite-quartz system, however, magnetic separation is not recommended for low grade iron oxides and for ores that are too fine (Filippov, et al., 2014; Rao, et al., 2009).

The results depicted by chemical assay analysis that iron is richer in the fines, eliminated the use of gravity separation and magnetic separation techniques since the fluorspar tailings will require uneconomic settling times during gravity separation and is not coarse enough for effective magnetic separation.

4.1.4 Loss on ignition results

The head sample total LOI obtained, using equation 2.11, was 2.7wt%. From these results it was anticipated that the iron would be present in predominantly anhydrous oxide form. Leonel & Peres, 2013 investigated the impact of high LOI in the pelletizing of iron ores. Their research concluded that low grade iron ores with LOI above 3.5wt% present challenges of decreased yield in the beneficiation stage and high loss of productivity in the pelletizing process. The resulting LOI of 2.7wt% would permit the use of flotation as a better Fe concentration method, since negligible presence of hydrated oxides and carbonated oxides is anticipated.

4.1.5 Chemical and mineralogical composition using XRD

The major mineral assemblage, as well as the semi-quantitative mineral abundance of the fluorspar tails was investigated using XRD. The semi-quantitative results showed major component was hematite, which was in agreement with chemical results using XRF. The results are represented in Table 6 and graphically in Figure 4.3.

Table 6: Semi-quantitative mineral abundances determined from XRD.

Mineral Name	Approximate chemical formula	XRD Abundance (wt %)
Hematite	$Fe^{3+}{}_2O_3$	>50
Quartz	SiO_2	10-20
Geothite	$Fe^{3+}O(OH)$	3-10
Magnetite	$Fe^{3+}{}_2Fe^{2+}O_4$	3-10
Fluorite	CaF_2	3-10
Siderite	$Fe^{2+}(CO_3)$	≤3
Pyrite	$Fe^{2+}S_2$	≤3
K-feldspar	$KAlSi_3O_8$	≤3
Monazite	$(Ce,La,Nd,Th)PO_4$	≤3

The results depicted in Table 6 and Figure 4.5 indicated that the head sample is composed predominantly of hematite at >50%, with quartz being the main gangue at 10-20%. The sample also contains minor amounts of goethite, magnetite and fluorite, at 3-10%. Trace minerals within the sample are made up of pyrite, K-feldspar and monazite. Minor concentration of hydrated and carbonate oxides found were in agreement with loss on ignition results.

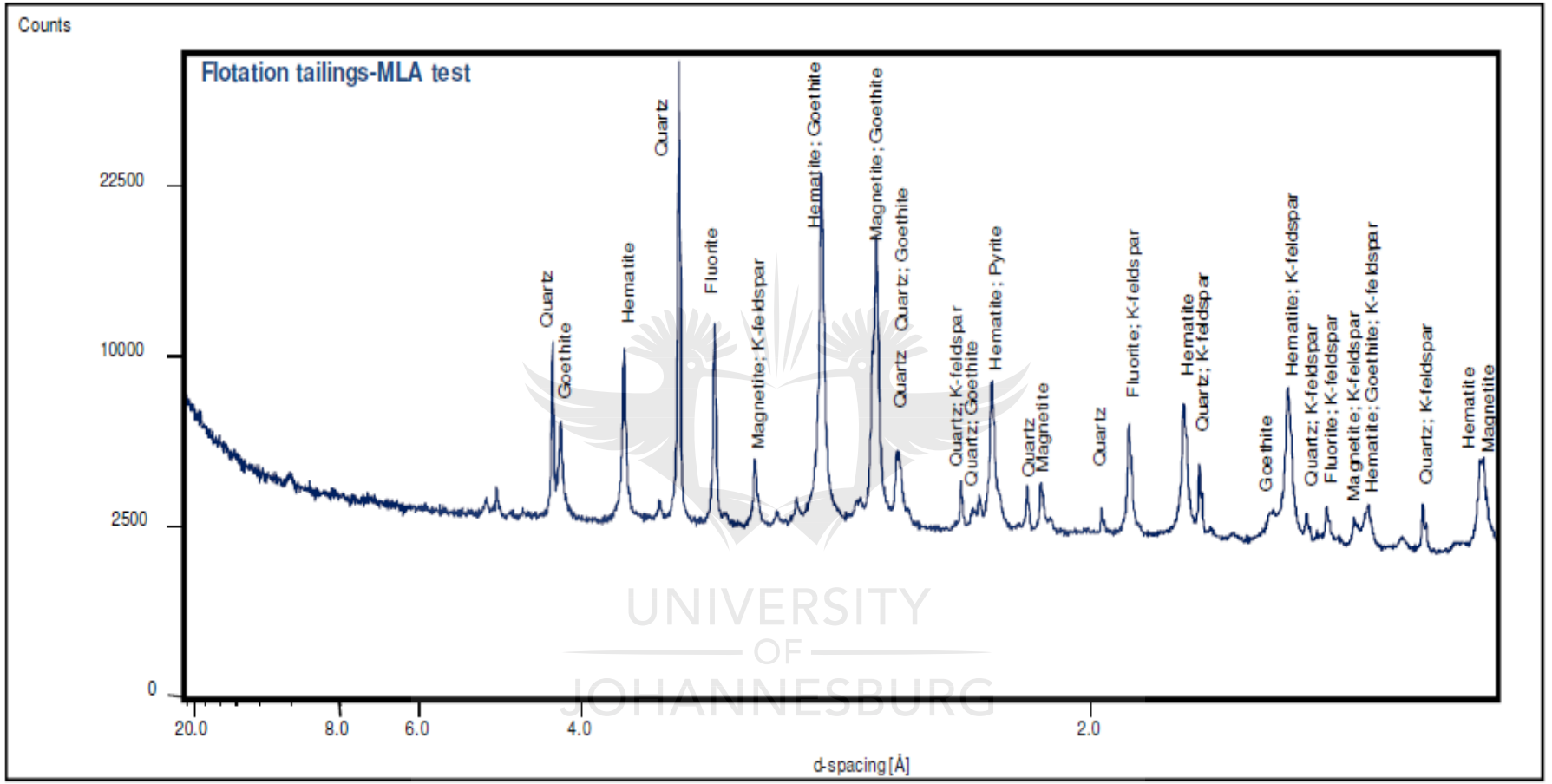

Figure 4.3: XRD pattern for fluorspar tails

4.1.6 QEMSCAN Bulk Modal Analysis

The BMA results quantified the various iron phases present in the sample, since it has the ability to differentiate iron oxide forms unlike XRF. The results were consistent with both chemical assay and XRD mineral abundance as it revealed that the fluorspar tails sample is dominated by iron oxide, mainly hematite. Detailed BMA result are shown in Table 7.

Table 7: Bulk Modal Analysis composition (mass%)

Mineral	**Mineral Formula**	**Mineral mass Abundance (%)**
Hematite	$Fe^{3+}_2 O_3$	60.83
Geothite	Fe^{3+} O(OH)	9.76
Magnetite	$Fe^{3+}_2 Fe^{2+}O_4$	5.91
Other oxide	Fe^{2+} TiO_3,Fe^{2+} Cr_2O_4	0.10
Total Oxide		**76.60**
Quartz	SiO_2	12.52
Plag-Feldspar	(Ca,Na) $AlSi_3O$-$KAlSi_3O_8$	0.74
Muscovite	$KAl_2(AlSi_3O_{10})(OH)_2$	0.42
Other Silicate		0.70
Total silicate		**14.38**
Pyrite	Fe^{2+} S_2	0.57
Other Sulphides	_	0.03
Total Sulphides		**0.60**
Fluorite	CaF_2	6.21
Monazite	$(Ce,La,Nd,Th)PO_4$	1.53
Siderite	$Fe^{2+}(CO_3)$	0.54
Carbonate,Phosphate,Sulphates	$CaCO_3$,$Ca_5(PO_4)_3(F,Cl,OH)$, $BaSO_4$	0.54
TOTAL		**100**

BMA results are in agreement with LOI predictions whereby data revealed that the fluorspar tails sample predominantly contains anyhydrous iron oxide. BMA results further revealed the sample was composed of quartz (12.52%) which accounts for the major mineralogical gangue phase, with minor content of fluorite (6.21wt%). The total oxides accounted for 76.6% which is comparable with the 70% found using XRF. Minor presence of goethite and carbonates allows ease of flotation separation method.

4.1.7 Iron oxide distribution in grain size

The grain size distribution shown in Figure 4.4 indicated that the largest portion of iron oxides (12.04wt%) occurred between 40-50µm and that the majority of Fe-oxide in the sample occurred between 10-70µm. These results agree with size wise chemical analysis results which depicted that majority of Fe-oxide in finer size ranges.

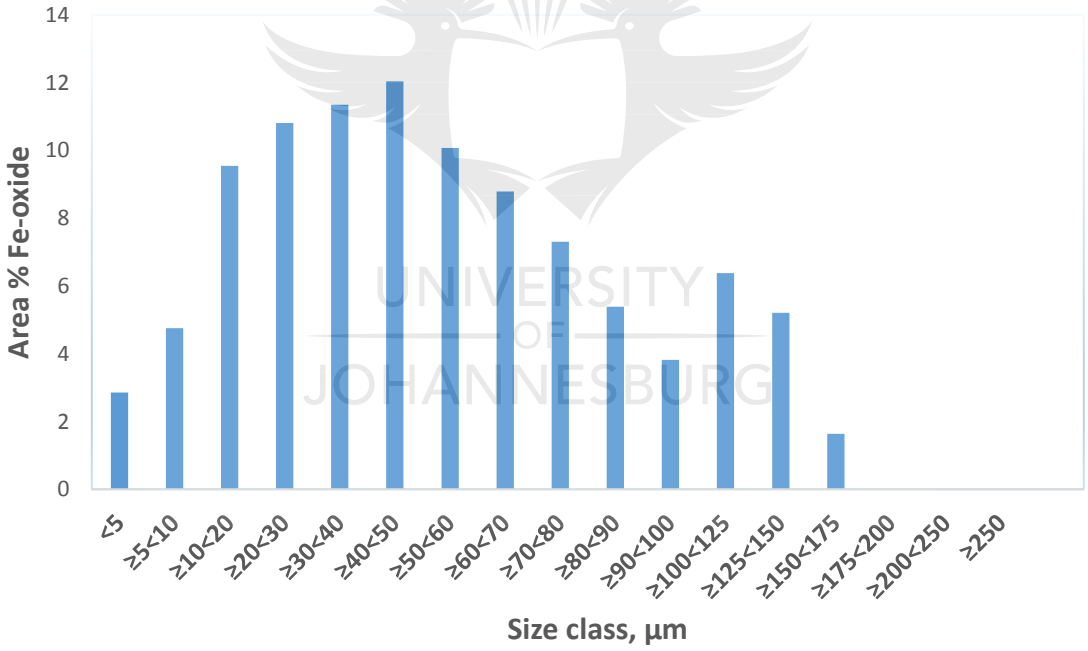

Figure 4.4: Iron oxide distribution per grain size dimension

4.1.8 Mineral exposure and mineral liberation analysis

The mineral exposure classes shown in Figures 4.5(a) indicated that majority (81%) of Fe-oxide within the sample occur within ≥80% exposure class with 18% of Fe-oxides occurring within the ≥10%<80% class. The exposure classes and mineral liberation classes are explained in Figure A2 and A3 in the appendix.

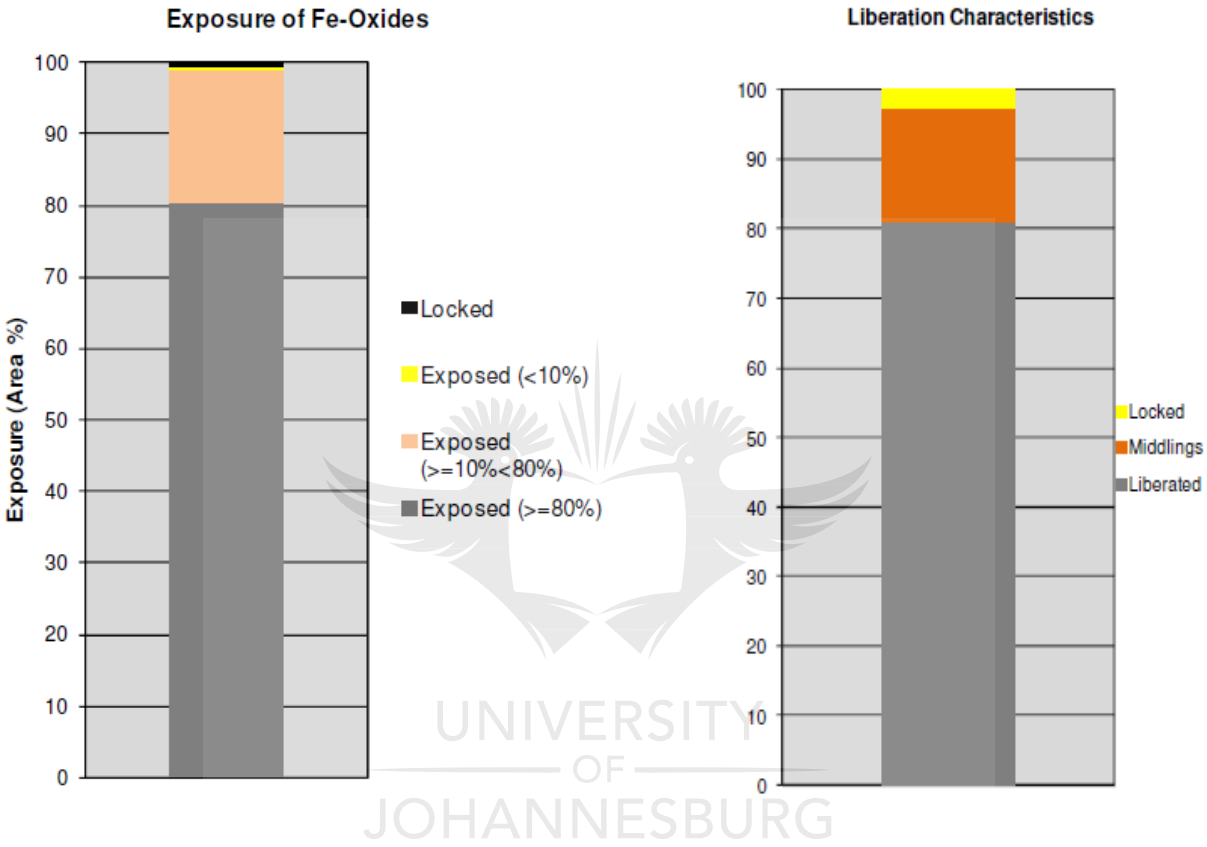

Figure 4.5: (a) Results of exposure characteristics of Fe-oxides (b) Mineral liberation analysis results

Figure 4.5(b) showed that 81% of the iron oxide is liberated, while 16% and 3% were in middlings and locked respectively. Only 0.5% of all Fe-oxide was locked and 0.39% of total locked Fe-oxide was in silicates and fluorites. Detailed exposure and mineral association characteristics of Fe-oxides is shown in Table A5. From the results it was decided that there is no need for grinding the feed sample further. An image grid highlighting the exposure of Fe-oxide at various grain size classes in Figure 4.6 showed that the locked particles are in the <20µm size range.

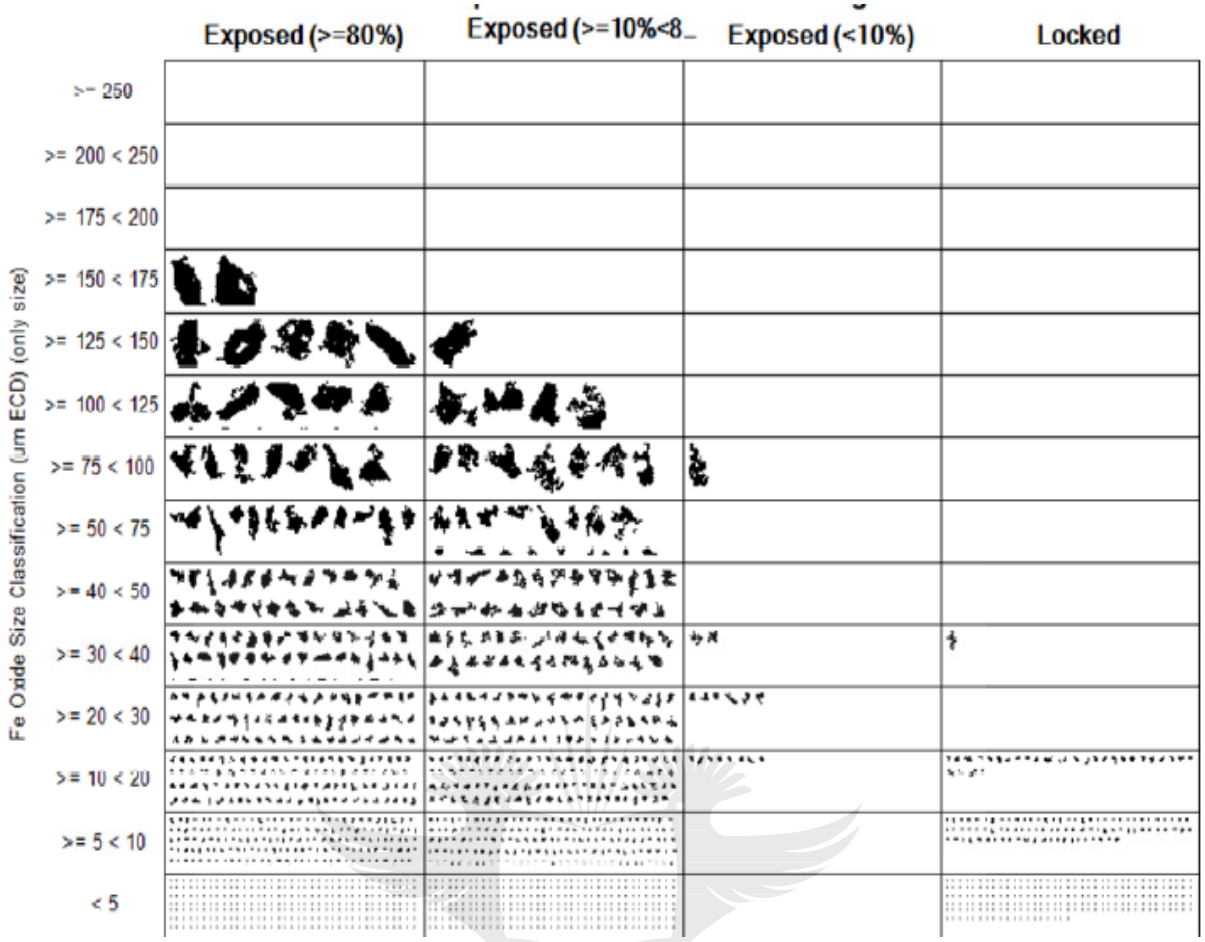

Figure 4.6: Exposure and association categories

4.2 Flotation Results

4.2.1 Optimum conditions predictions for soluble starch - DDA system

Minitab 17 software was used to capture the flotation experiments output (iron content in concentrates) data. The SN ratio was used to interpret results, as shown in Figure 4.7. An example of the Taguchi spreadsheet showing data obtained by running Soluble starch – DDA experiments, according to Table 3, is shown in Table A7 of the appendix. The graphical representation of information compiled from Table A7 is shown in Figure 4.7

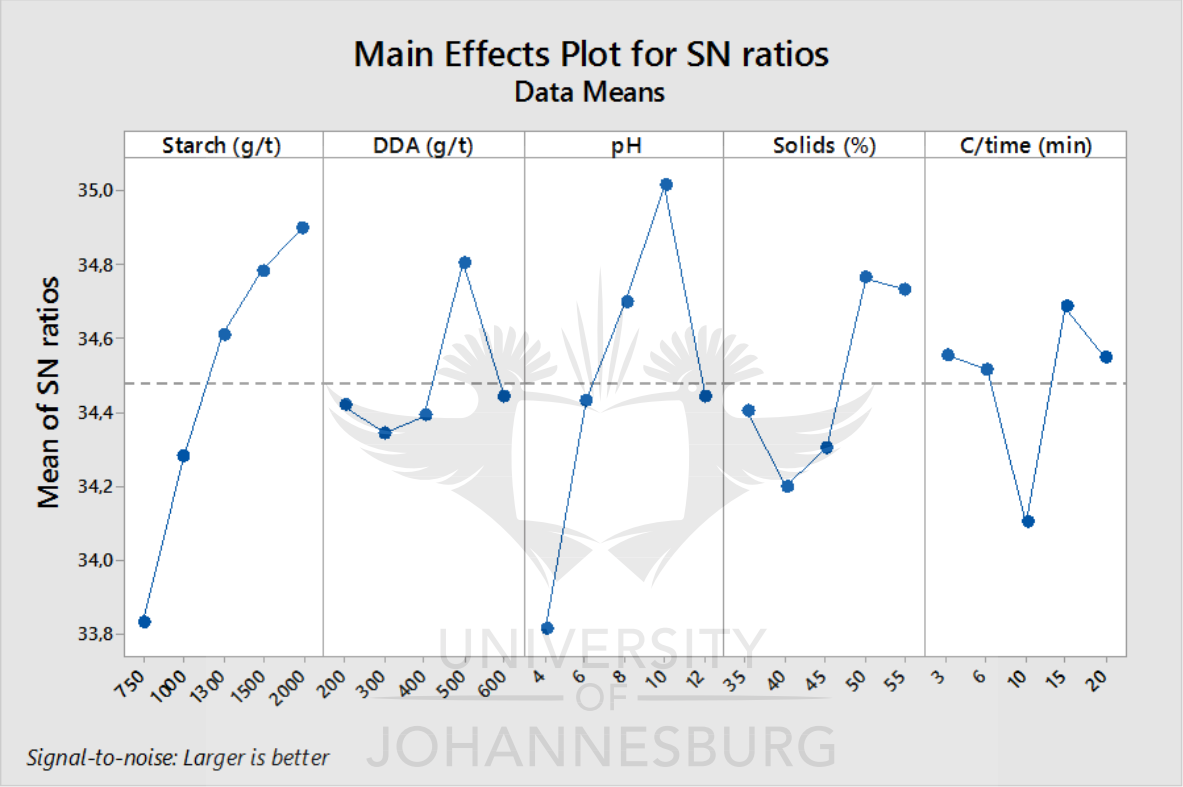

Figure 4.7: SN ratio response for soluble starch-DDA system

The data analysis using SN ratio was used to identify optimum conditions to achieve higher Fe grade. The graph in Figure 4.7 showed that the optimum condition for the desired output of larger Fe grade were obtained at soluble starch 2000g/t, DDA collector 500g/t, pH 10, 50% solids content, and conditioning time of 15minutes. The results for optimum condition as depicted by the SN ratio were observed to be mostly in line with existing literature condition for reverse cationic flotation of iron oxides.

- ***Soluble starch dosage - SN ratio trend***

The soluble starch dosage – SN ratio trend in Figure 4.7 showed that the efficiency of the process generally increases with increased starch dosage. The highest SN ratio was predicted at 2000g/t starch dosage. Work done by Kar, et al. (2013) showed that depressing action of hematite increased with increase in starch dosage. It was noted that the 2000g/t soluble starch obtained as the optimum soluble starch dosage in this study is much higher than the previously recorded dosages of 400-600g/t reported by Nheta, et al. (2015) and Kar, et al. (2013). Due to general high cost of soluble starch, a decision was made not to investigate higher soluble starch dosage.

- ***DDA dosage – SN ratio trend***

The DDA collector dosage-SN ratio trend in Figure 4.7 showed that flotation performance increased with increasing collector dosage from 300-500g/t after which a sudden decline was observed at 600g/t. Generally, the floatability of quartz increases with increased collector dosage until an optimum point is reached where a decline occurs possibly due to formation of hemi-micelles at the solid-liquid interface (Filippov, et al., 2014). The optimum collector dosage of 500g/t depicted by the SN ratio is more that of 300g/t depicted by preliminary results of Nheta, et al. (2015) and the 48g/t depicted by Kar, et al. (2013). The higher collector dosage requirement could be attributed to differences in feed quality, water quality, etc.

- ***Pulp pH – SN ratio trend***

The pH – SN ratio trend in Figure 4.7 showed that the efficiency of the flotation experiments increased with increasing pH whereby the highest SN ratio was reached at pH 10. Work done by Ma, et al. (2011) conducted reverse cationic flotation at pH 10.5. It is normal practice to conduct reverse cationic flotation of iron ore at pH 10-10.5 (Turrer and Peres, 2010; Kumar, et al., 2010). The pH-SN ratio trend statistically predicts a sudden drop in system efficiency at pH>10. A similar trend was reported by Huang, et al. (2014), where it was observed that flotation of quartz increased gradually with increasing pH but decreased at pH > 10. The flotation of quartz is said to increase with increasing pH as the quartz becomes more negatively charged when the point of zero charge (pzc) of pH 2-3 is passed.

- ***Solids content – SN ratio trend***

The solids -SN ratio trend in Figure 4.7 predicted the process performance to increase with increased solids content in pulp until an optimum point is reached at 50% solids content after which the performance drops. A reduction of flotation efficiency at high solids content was attributed to the detachment of bubbles from particle surfaces and also reduction of bubble numbers with increasing of pulp density for a given air flow rate. (Mowla, et al., 2008).

- ***Conditioning time – SN ratio trend***

The conditioning time – SN ratio in Figure 4.7 predicted optimum Fe grade at 15 minutes conditioning time. This was a deviation from 5-6 minutes recommended by Molwa, et al. (2008) and the 6 minutes used by Ma, et al. (2011). Based on the works of Molwa, et al. (2008) and Ma, et al. (2011), a decision was made to conduct experiments at 6 minutes conditioning time.

- ***Ranking of parameters***

The parameters under investigation were ranked according to relative importance and the results are shown in Table 8. The ranking looks at the difference between the lowest SN ratio and the highest SN ratio as the parameter setting level is varied (Masiya & Nheta, 2014). The parameter with the highest difference is deemed the most critical as its variation effected the most change in the output response.

Table 8: Parameter ranking results using SN ratio

Level	Starch	DDA	pH	Solids	C/time
1	33.83	34.42	33.81	34.41	34.55
2	34.28	34.34	34.43	34.20	34.52
3	34.61	34.39	34.70	34.30	34.10
4	34.78	34.81	35.02	34.76	34.69
5	34.90	34.44	34.44	34.73	34.55
Delta	1.07	0.46	1.20	0.57	0.59
Rank	2	5	1	4	3

The response table of SN ratio to higher iron grade was conducted to rank the parameters according to significance. The ranking of process parameter, indicated in Table 8, showed that the relative significance of the parameter was in the order of pH being the most significant parameter followed by starch dosage, conditioning time, solids content and collector dosage respectively. This means that the system is most sensitive to pH changes. This finding is in line with literatures since pH is known to be critical in flotation of iron oxides as it affects the surface charge of oxide minerals (Fuerstenau & Pradip, 2005)

- ***Confirmation test for SS-DDA system***

A confirmation test for soluble starch and DDA was conducted at predicted optimum conditions. With soluble starch at 2000g/t, DDA dosage of 500g/t, pH 10, solids content of 50% and conditioning time of 6 minutes. The result showed a 56.87%Fe grade in the concentrate stream. The metal recovery of 78% was obtained when using equation 2.12 and metal loss was 22% when using equation 2.13. This iron assay was far below the required ≥63%Fe for pellets making. Detailed chemical analysis of this SS-DDA confirmation test are shown in Table A8 of the appendix.

4.2.2 Optimum condition prediction for Betachem 30D and DDA system

Figure 4.8 showed that the optimum condition for the desired output of larger Fe grade were obtained at dextrin (Betachem 30D) 300g/t, DDA collector 500g/t, ¾ air valve opening and 1300rpm agitation speed. The results for optimum condition as depicted by the SN ratio were observed to be mostly in line with existing literature condition for reverse cationic flotation of oxides.

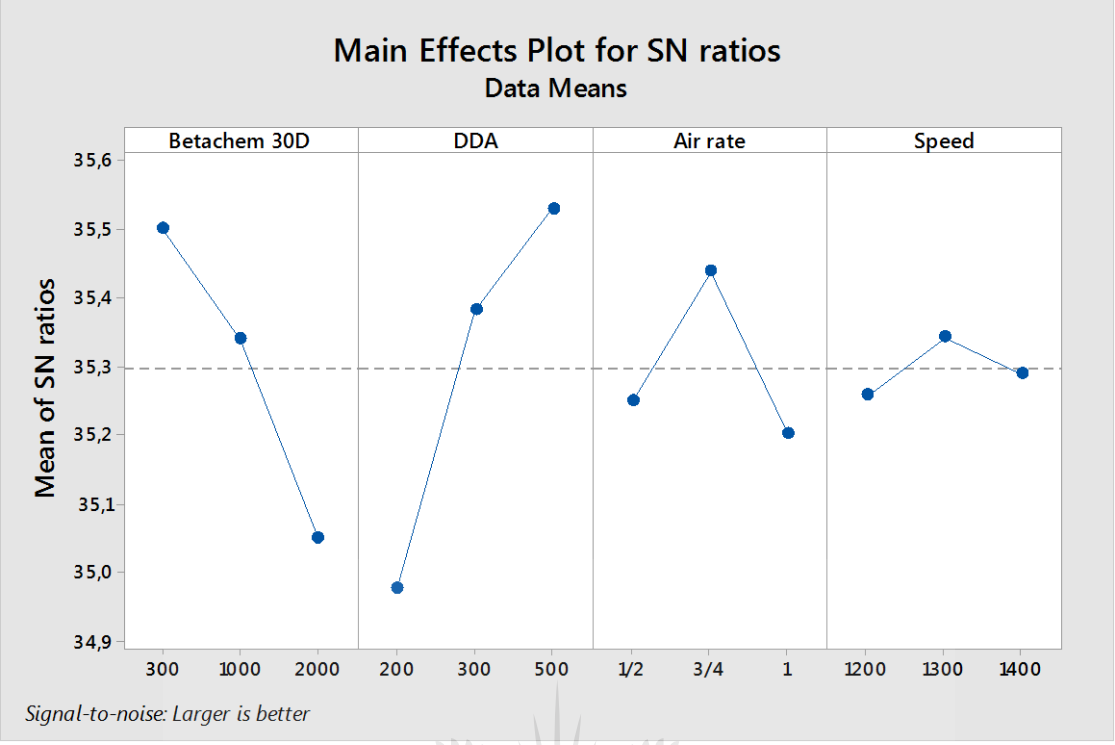

Figure 4.8: SN ratio response for Betachem 30D-DDA system

- ***Dextrin dosage – SN ratio trend***

Betachem 30D dosage – SN ratio, in Figure 4.8, showed the optimum dextrin dosage for lager Fe grade output is at 300g/t, which is much lower than the 2000g/t predicted when soluble starch is used. The SN ratio graph showed a decline in flotation performance at increased dextrin dosage, which could be due to clathrate. This is when quartz hydrophobicity is reduced at increased starch and amine dosage due to the interaction of free starch molecules with amine molecules thus resulting in amine acting rather as a depressant (Lima et al., 2013)

- ***DDA dosage – SN ratio trend***

It was observed that the optimum DDA dosage was not reduced by the introduction of parameter such as air rate, agitation speed and a different type of depressant. The DDA dosage – SN ratio in Figure 4.8 showed an increase in flotation efficiency with increased collector dosage with optimum dosage being 500g/t.

- ***Air rate and agitation speed – SN ratio trend***

The air rate – SN ration graph in Figure 4.8 showed an improvement in system efficiency as air rate is increased from valve half open to valve 3/4 open and a sudden drop when the air valve is fully open. A similar trend was observed with agitation speed – SN ratio graph where the performance is seen to increase when the agitation speed is increased from 1200-1300rpm and it dropped suddenly when the speed is increased to 1400rpm. Air rate and agitation speed are critical for efficient performance in flotation as high air rate increase the available area for attachment of targeted mineral and the increased agitation speed increases contact opportunities of air with the target mineral. With flotation rate driven by factors; collision, adhesion and detachment, increased performance is anticipated as agitation speed is increased due to increased rate of collision and adhesion between particles and bubbles (Abd El-Rahiem, et al., 2009). However, at the highest impeller speed of 1400rpm the rate of detachment could be greater than that of collision and adhesion leading to poor flotation of quartz thus reduction in the sinks iron grade.

- ***Ranking of parameters (Betachem 30D and DDA)***

The response table of SN ratio to higher the better iron grade was conducted to rank the parameters according to significance. The ranking of process parameter, indicated in Table 9, showed that the relative significance of the parameter was in the order of collector dosage being the critical parameter followed by depressant dosage, air rate and agitation speed.

Table 9: Parameter ranking results using SN ratio.

Level	Betachem 30D	DDA	Air rate	Speed
1	35.50	34.98	35.25	35.26
2	35.34	35.38	35.44	35.34
3	35.05	35.53	35.20	35.29
Delta	0.45	0.55	0.24	0.08
Rank	2	1	3	4

- ***Confirmations tests results for Betachem 30D – DDA system***

A confirmation test for the dextrin Betachem 30D and DDA was conducted at predicted optimum conditions. With Betachem 30D at 300g/t, DDA dosage of 500g/t, pH 10, solids

content of 35%, conditioning time of 6 minutes, air rate at valve ¾ open and rotor speed of 1300rpm. The results showed a 58.38%Fe grade at 68.5% recovery.

Since figure 4.8 showed explicitly that flotation performance was low at 1000g/t when compared to 300g/t and it was known that a large gap existed in the studied Betachem 30D dosage (300g/t and 1000g/t), a decision was made to investigate other dosages in-between. The studied dosages were 300, 500 and 750g/t. The results shown in Figure 4.9 indicated that better grade of Fe is observed as the depressant dosage is increased from 300-750g/t with higher Fe grade recorded 500g/t after which the Fe grade started dropping.

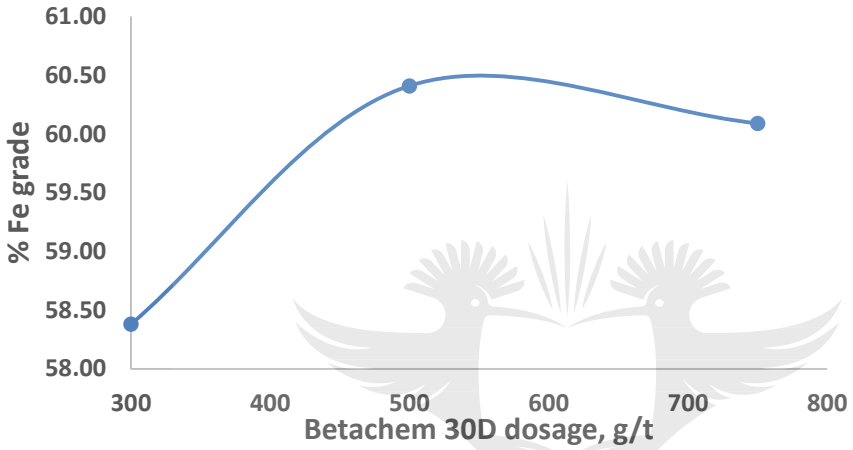

Figure 4.9: Effect of dextrin dosage on flotation performance

A 2.02% increase in Fe grade was observed when increasing Betachem 30D dosage from 300-500g/t. A decline in iron grade was observed at 750g/t dextrin dosage. Detailed chemical analysis results for Figure 4.9 are shown in Table A9 of the appendix. According to Kar, et al. (2013) and Lima, et al. (2013) depressing action of a depressant would increase with increased dosage until an optimum concentration is reached where the performance drops due to possible clathrate.

4.2.3 Comparing soluble starch and Betachem 30D depressants

Since the optimum flotation conditions for soluble starch and DDA excluded agitator speed and air rate factors, they were therefore not compatible for comparison with Betachem 30D-DDA results. The information received from Betachem 30D – DDA system, regarding agitation speed and air rate, was therefore added into the SS-DDA system for comparison sake. The confirmation test of SS-DDA system was conducted using the optimum; soluble starch dose 2000g/t, DDA dosage of 500g/t, solid content of 50%, conditioning time of 6 minutes,

agitation speed of 1300rpm and ¾ open air valve. Increasing agitation speed and air rate showed an improvement in performance from 56.87% Fe to 61.2%Fe at a recovery of 69.70% with 3.6%SiO_2 in sinks. This means that by adjusting the air rate and agitation speed, an increase of 2.5% in iron grade was observed. The quality of final concentrates found from flotation using soluble starch showed an Fe assay of 61.2% and 60.41% when using Betachem 30D. Hence it was apparent that both starch and dextrin are good depressants for hematite.

Flotation kinetics using the depressants (soluble starch and Betachem 30D) was then conducted using the obtained optimum conditions and results are shown in Figure 4.10. The aim was to observe a trend of Fe assay concentration in the floats with time. The flotation kinetics of the soluble starch-DDA and Betachem 30D-DDA system showed that iron loss to floats increased with increasing flotation period for both depressants.

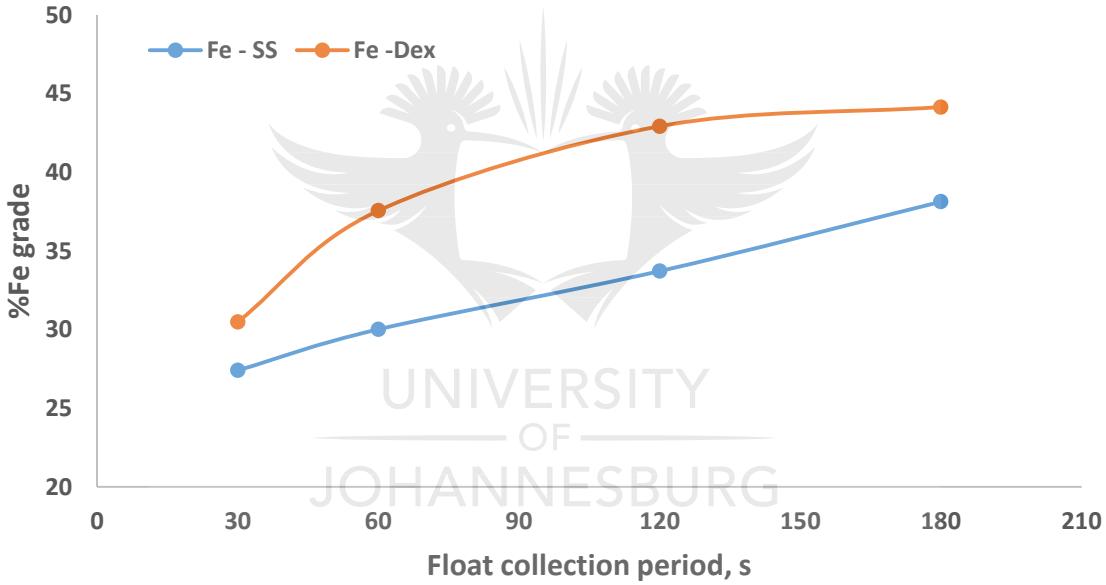

Figure 4.10: Flotation kinetics of dextrin and soluble starch systems

In the first 30 seconds of flotation, Betachem 30D showed 30.48%Fe in the floats while soluble starch showed lower value of 27.4%Fe assay in the floats. Detailed chemical analysis results for the conducted flotation kinetics is shown in Table A11 and A12 of the appendix. Soluble starch showed superior depressing power when compared to Betachem 30D, as shown in Figurer 4.10. Research done by Kar, et al., 2013 on usage of corn starch, potato starch, rice starch and soluble starch as depressants indicated that all starches are good depressants for hematite, however, quartz was better floated in the presence soluble starch and dodecylamine

collector. High cost of soluble starch, however, led to selection of dextrin for further optimisation.

4.2.4 Further optimisation of Betachem 30D – DDA system

- ***De-sliming of feed***

Further optimisation of Betachem 30D – DDA system was done by de-sliming the feed removing the <20µm size fraction. The metal loss due to de-sliming was measured at 13%, where chemical analysis showed that slimes contained 53.5%Fe. No major changes in the feed quality was observed by the removal of the slimes, since the Fe assay was reduced by 1.3%.

Considering that the iron oxide in this size range was locked, the aim of de-sliming was to reduce effect of slime coating, sludge formation and possibly reduce collector consumption. Flotation of de-slimed feed was conducted at varied collector dosage and the results reflected in Figure 4.11. Detailed chemical analysis results are illustrated in Table A14 of the appendix.

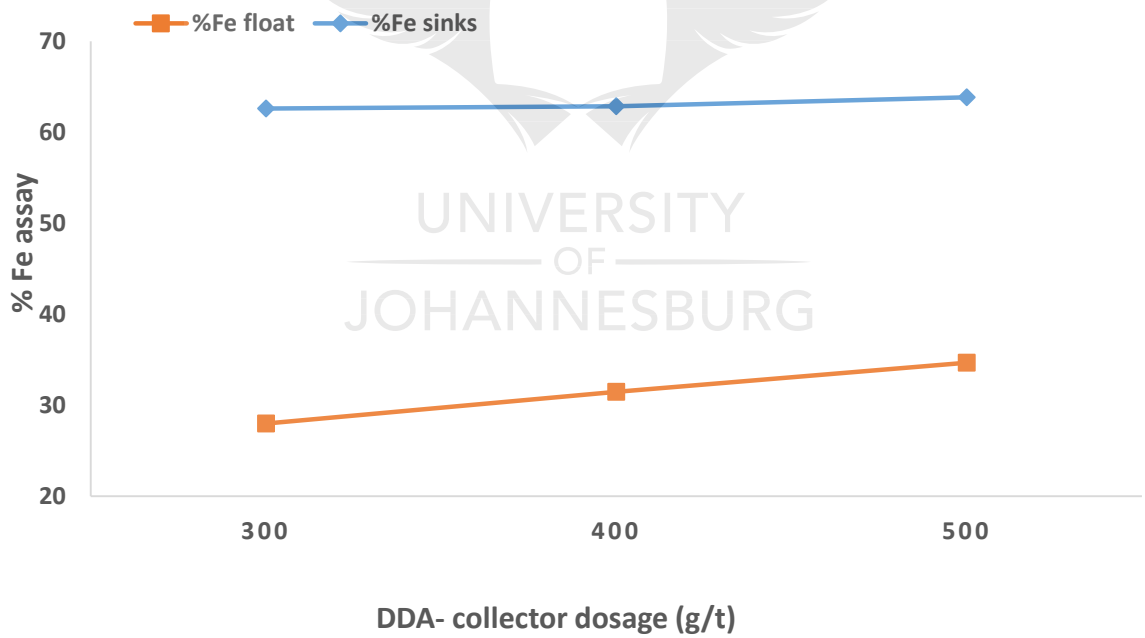

Figure 4.11: Impact of de-sliming on iron grade

Figure 4.11 showed that iron grade of 62.6% is achievable with 300g/t collector dosage when the feed is de-slimed. This is an improvement from the 60.41%Fe assay achieved when using 500g/t collector on feed that was not de-slimed. The iron assay in the concentrate was seen to be increasing slightly with increased collector dosage, however, bigger increases in iron assay in floats was observed with increased collector dosage. The highest iron grade of 63.86% at

75.16% recovery, was, observed at 500g/t collector dosage. The metal loss at 500g/t collector dosage using de-slimed feed were at 25% and 38% when adding the 13% lost by action of de-sliming alone.

Though some reagent saving was observed with de-sliming, high metal losses were however observed hence it was decided that the action of de-sliming was not beneficial for this project.

- ***Increasing conditioning* time**

Further optimisation of dextrin-DDA system was done by increasing the conditioning time of the original feed without de-sliming, from 6 minutes to 15minutes. This resulted in the better performance of the system whereby the iron grade was increased from 60.83%Fe to 63.79%Fe, which indicated a 3% grade increase. The comparison between concentrate quality obtained from processing de-slimed feed and that obtained from increasing the conditioning time gave the results tabulated in Table 10.

Table 10: Comparison between de-sliming and increased conditioning time

	Concentrate at 15min conditioning time	**Concentrate from de-slimed feed**
Fe assay	63.79%	63.84%
SiO_2	3.76%	3%
CaO	1.01%	1.97%
F	0.65%	1.02%
Al_2O_3	0.87%	0.63%
Recovery	72.44%	75.16%
Total metal loss	27.56%	38%

It must be noted that reflected in this table are only those components at concentrations >0.5mass%, detailed chemical analysis results are shown in Table A15. From the results above, it was decided to accept Betachem 30D – DDA at 15 minutes as the final optimum results for

this system. The detailed results comparing the different conditioning times are shown in Table A16 of the appendix.

4.2.5 Optimum conditions prediction for Betachem 30D- Betacol 373 system

The L9 orthogonal array was selected for experimental set up and Taguchi used for analysis of results. The optimum conditions predicted by SN ratio analysis showed that best performance for Betachem 30D – Betacol 373 was at dextrin dosage 500g/t, BET 373 dosage of 3328g/t and 35% solids content. A confirmation test was conducted at the obtained optimum conditions and a concentrate with 62.08%Fe at 69.07% recovery was achieved. Seeing that Taguchi picked the maximum setting of BET 373 dosage, a decision was taken to investigate further dosages.

4.2.6 Further optimisation of BET 30D – BET 373 system

- ***Collector dosage variation***

The dosages 3328g/t, 5548g/t and 7770g/t were investigated and the results are displayed in Figure 4.12.

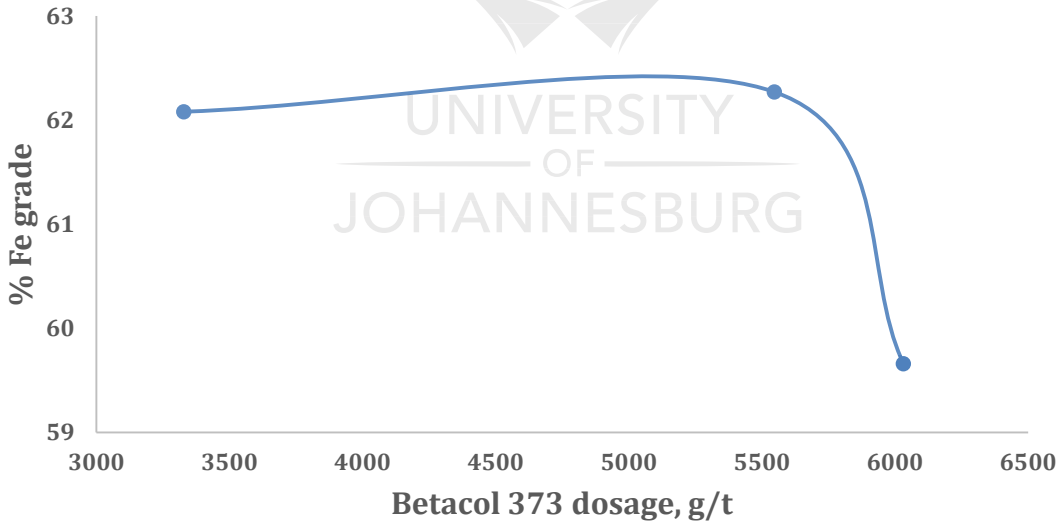

Figure 4.12: Impact of collector dosage on iron grade

An increase in collector dosage was observed resulting in a slight increase in iron grade until an optimum point of 5548g/t, where after the performance suddenly dropped, as shown in Figure 4.12. The Fe grade of 62.28%Fe at a reduced recovery of 61.01% in sinks was observed at 5548g/t. When compared to 62.08%Fe and 69.07% recovery obtained at 3328g/t collector dosage, an increase to 62.27%Fe signals a slight improvement in results and does not justify

increasing collector dosage from 3328g/t to 5548g/t. Detailed results are reflected in Table A17.

- ***Increased solids content***

The solids content was increased from 35% to 45% with an aim to increase recovery and increase cell capacity while the collector dosage was also varied from 2560 -7770g/t. The results are shown in Figure 4.13.

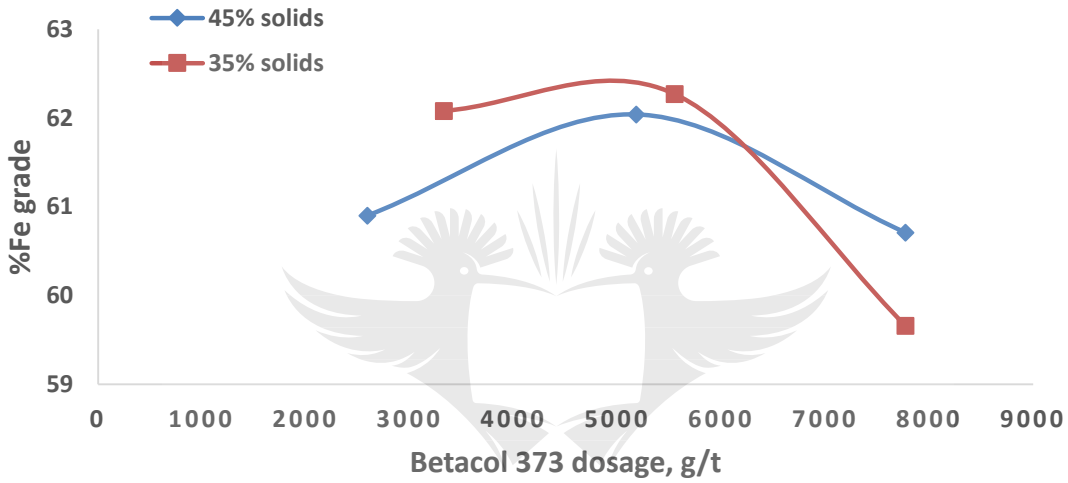

Figure 4.13: Impact of increasing solids content on iron grade

Similar trend in iron grade with increased collector dosage, as observed with operating at 35% solids, was observed at 45% solids content as shown in Figure 4.13. It was shown that mostly higher Fe grade was achieved when operation at 35% solids content. This verifies optimum solids content obtained by the SN ratio.

4.2.7 Comparing cationic amines (DDA and Betacol 373) results

Table 11 shows comparison between the concentrates obtained at operation at optimum conditions for DDA and Betacol 373, where Betachem 30D was the used depressant. Results tabulated in Table 11 show that both Betacol 373 and DDA were able to reduce silica in the concentrate significantly from the feed with 16.8% to concentrates with 3.76% and 3.39% respectively. Betacol 373 system was also able to concentrate the iron in the feed significantly

from 48.9% to 62.08%Fe grade at 67.02% recovery. The alumina and phosphorus were reported at <1%.

However, a system of Betachem 30D - DDA was able to produce results with higher iron grade (63.79%) in concentrate, which is within the required ≥63%Fe. The recovery was higher (70.78%) when compared to the 67.02% obtained with Betacol 373. The alumina and phosphorous were at <1wt%. Table A18 shows detailed chemical analysis results for collector comparison.

Table 11: Dodecylamine and Betacol 373 comparison

Description	DDA	Betacol 373
Fe in sinks	63.79%	62.08%
Si in sinks	1.76%	1.58%
Ca in sinks	0.71%	2.2%
Fe in floats	40.43%	40.07%
SiO_2	3.76%	3.39%
Al_2O_3	0.87%	0.60%
Fe Recovery	70.78%	67.02%
Metal loss	29.22%	32.98%
%Mass in sinks	54.26%	53.15%
Betachem 30D dosage	500g/t	500g/t
Collector dosage	500g/t	3328g/t
pH	10±0.5	10±0.5
Solids content	50%	35%
Conditioning time	15min	15min
Agitation speed	1300rpm	1300rpm
Air valve opening	¾ open	¾ open

4.3 ANOVA analysis

The flotation experiments in the selected orthogonal array matrix were conducted two times and the mean results compared to each other using One Way Repeated Measures ANOVA analysis, as in Table 12.

Table 12: Mean results

	Mean	Std. deviation	Number of subjects
% Fe in sinks 1	53.1208	4.13950	25
% Fe in sinks 2	53.0452	4.07979	25

The Statistical Package for the Social Science (SPSS) software was used for ANOVA analysis. The following results were obtained for Soluble starch and DDA system. Hypothesis testing was done using the P-value approach (Pallant, 2010). The following hypothesis were made, with α = 0.05 (Level of significance);

- Null hypothesis, H_0: There is no change in percentage of iron in sink over two repeats experiments.
- Alternative hypothesis, H_A: There is change in percentage of iron in sink over two time periods.

P-value approach determines the likeliness or un-likeliness of observing a test statistic in the direction of either a null nor am alternative hypothesis. If P-value is ≤ α, then the null hypothesis is rejected in favour of the alternative hypothesis.

The results for the effect of %Fe in sinks are shown in Table 13 below, where b is the exact statistics:

Table 13: Results for multivariate tests

Method	Value	F	Hypothesis df	Error df	Significance, p-value.	Partial Eta Squared
Pillai's Trace	0.105	1.351[b]	2.000	23.000	0.279	0.105
Wilks' Lambda	0.895	1.351[b]	2.000	23.000	0.279	0.105
Hotelling's Trace	0.117	1.351[b]	2.000	23.000	0.279	0.105
Roy's largest root	0.117	1.351[b]	2.000	23.000	0.279	0.105

The P-value, P = 0.279, was obtained. According to Ramsey, 2011 a p value >0.05 indicates weak evidence against the null hypothesis hence failure to reject null hypothesis. With p=0.279>0.05, the null hypothesis was not rejected, hence, there was sufficient evidence to conclude that there is no change in percentage of iron in the sinks.

5 CHAPTER 5: CONCLUSIONS AND RECOMMENDATIONS

5.1 Conclusions

It was concluded that the fluorspar waste is of fine texture, with a grind size of 80% passing 155µm. Hematite was the main Fe-oxide with minor presence of goethite and magnetite. Silica was found as the main gangue mineral. Majority of Fe-oxide grains within the sample occur between the sizes of 10-70µm. The sample was classified as low grade iron oxide since chemical analysis results using XRF showed that the sample had low iron content 48.9%Fe and high impurity content of 16.8% SiO_2, minor content of fluorine (2.25%) and CaO (3.8%) with all other elements at <1% composition. There was no need for grinding of the sample since mineral liberation analysis results showed that 81% of all Fe-oxide were liberated while the locked Fe-oxide occurred in the <20µm particle size. From the characterisation results it was concluded that reverse flotation is the suitable separation process to concentrate the Fe in the fluorspar tailings to acceptable levels of >63wt%Fe required for pig iron production in the blasting furnaces. Reverse cationic flotation is generally recommended for beneficiation of low grade iron ores due to its high flotation rates and high selectivity. (Filippov et al., 2014)

Reverse cationic flotation was conducted using amine collector (DDA and Betacol 373) and two types of depressants (Betachem 30D and soluble starch). The relative significance of flotation parameters using SN ratio indicated that pH has the most significant effect on iron grade during reverse cationic flotation. Reverse cationic flotation efficiency increases with increased pH, however, it drops at alkaline conditions (pH12). Depressant dosage and conditioning time also play a significant role in increasing flotation performance.

Soluble starch was the best iron depressant, however, when considering a combination of factors (e.g. performance, cost and availability) Betachem 30D was the preferred depressant. Both Betacol 373 and DDA performed well in concentrating iron in fluorspar tails, however, DDA showed superior results under the investigated conditions. A concentrate of 63.79%Fe at 70.78% recovery was achievable using BET 30D – DDA for flotation. The obtained SiO_2 and Al_2O_3 levels achieved in the concentrate were 3.78% and 0.87% respectively.

This was achieved at DDA dosage of 500g/t, Betachem 30D dosage of 500g/t, 50% solids content, pH 10, agitation speed of 1300rpm and air valve ¾ open. It was concluded that reverse cationic flotation is suitable for concentration of iron in fluorspar tailings to acceptable quality required for agglomeration.

It was concluded that use of Taguchi method in optimization of flotation process is effective and produces reliable results. ANOVA showed that results obtained had acceptable levels of error with 95% confidence level.

5.2 Recommendations

- Further trials using a cheaper and locally available cationic reagents are recommended due to high cost of DDA.
- Agglomeration process is recommended to make the concentrate suitable for blast furnace feed.
- Bentonite is the common binder for iron oxide concentrate. It however contains SiO_2 which will affect the pellets quality, since it would increase impurities in the product. It is there recommended that an investigation into organic binders must be considered for agglomeration of the Fe concentrate.
- Production of a higher Fe grade and lower silica grade by introduction of cleaner cells is recommended.
- The project can be investigated at pilot plant level.

6 References

Abbasi, H. R., Bazdar, M. & Halvaee, A., 2007. Effect of phosphorus as an alloying element on microstructure and mechanical properties of pearlitic gray cast iron. *Materials Science and Engineering A,* Volume 444, pp. 314-317.

Abd El-Rahiem, F., Selim, K. & Abdel-Khalek, N., 2009. Some parameters affecting beneficiation of fine Kaolin particles. *The Journal of ORE DRESSING,* 11(21), pp. 1-8.

Altan, M., 2010. Reducing shrinkage in injection moldings via the Taguchi, ANOVA and neural network methods. *Materials and Design* , Volume 31, pp. 599-604.

Amikiya, C. A., 2014. *Characterisation of iron ore - A case study of Mount Tokadeh, Western Nimba area, Liberia,* Liberia: Kwame Nkrumah University of Science and Technology.

Arantes, R. & Lima, R., 2013. Influence of sodium silicate modulus on iron ore flotation with sodium oleate. *International Journal of Minerals Processing,* Volume 125, pp. 157-160.

Araujo, A., Viana, P. & Peres, A., 2005. Reagents in iron ores flotation. *Minerals Engineering* , Volume 18, pp. 219-224.

Ata, S., 2012. Phenomena in the froth phase of flotation — A review. *International Journal of Mineral Processing,* Volume 102-103, pp. 1-12.

Athreya, S. & Venkatesh, Y., 2012. Application of Taguchi Method for optimization of process parameters in improving the surface roughness of Lathe facing operation. *International Refereed Journal of Engineering and Science,* 1(3), pp. 13-19.

Barclay, S., Trusler, G., von Blottnitz, H. & Buckely, C. A. K. B. J. C., 2011. *Cleaner production: A guidance document for the mining industry in South Africa,* Gezina: Water Research Commision.

Basov, V., 2015. *True giants of mining: World's top 10 iron ore mines.* [Online] Available at: http://www.mining.com/true-giants-of-mining-worlds-top-10-iron-ore-mines/ [Accessed 12 November 2016].

Bendell, A., Disney, J. & Pridmore, W., 1989. *Taguchi methods: Application in world industry.* New York: IFS Publications.

Bosman, J., 2014. The art and science of dense medium separation. *The Journal of The Southern African Institute of Mining and Metallurgy,* Volume 114, pp. 529-536.

Burt, R. O., 1984. *Gravity concentration technology.* New York: Elsevier.

Carlson, J. J., 2010. *Surface chemistry of hematite slurries,* Michigan Technological university: Joshua James Carlson.

Das, B., Prakash, S., Das, S. & Reddy, P., 2007. Effective Beneficiation of low grade iron ore through jigging operation. *Journal of Minerals & Materials Characterization & Engineering,* 7(1), pp. 27-37.

Dobbins, M., Dunn, P. & Sherrell, I., 2009. Recent advances in magnetic separator designs and applications. 7th International Heavy Minerals Conference. *The Southern African Institute of Mining and Metallurgy,* pp. 63-70.

du Plessis, B. J. & de Villiers, G., 2007. The application of the Taguchi method in the evaluation of mechanical flotation in waste activated sludge thickening. *Resources, Conservation and Recycling ,* Volume 50, pp. 202-210.

Dworzanowski, M., 2012. Maximizing the recovery of fine iron ore using magnetic separation. *The Southern African Institute of Mining and Metallurgy,* 112(3).

Filippov, L., Filippova, I. & Severov, V., 2010. The use of collectors mixture in the reverse cationic flotation of magnetite ore: The role of Fe-bearing silicates. *Minerals Engineering,* Volume 23, pp. 91-98.

Filippov, L., Severov, V. & Filippova, I., 2014. An overview of the beneficiation of iron ores via reverse cationic flotation. *International Journal of Minerals Processing,* Volume 127, pp. 62-69.

Fisher, R., 1942. *The design of experiments.* 3 ed. London: Oliver and Boyd.

Forsmo, S., Björkman, B. & Samskog, P., 2008. Studies on the influence of a flotation collector reagent on iron ore green pellet properties. *Powder Technology ,* Volume 182, pp. 444-452.

Fuerstenau, D. & Pradip, T., 2005. Zeta potentials in the flotation of oxide and silicate minerals. *Advances in Colloid and Interface Science,* Volume 114-115, pp. 9-26.

Fuerstenau, M. C., Jameson, G. & Yoon, R.-H., 2007. *Froth flotation: A century of innovation.* Johannesburg: Society for Mining Metallurgy and Exploration Inc.

Golosinski, T. S., 2000. *Mining in the new millenium: Challenges and opportunities.* Las Vegas: A.A. Balkema.

Hicks, C. R. & Turner, K. V. J., 1999. *Fundamental concepts in the design of experiments.* 5 ed. New York: Oxford University Press Inc..

Huang, Z. et al., 2014. Investigations on reverse cationic flotation of iron ore by using a Gemini surfactant: Ethane-1,2-bis(dimethyl-dodecyl-ammonium bromide). *Chemical Engineering Journal,* Volume 257, pp. 218-258.

Innace, J., 2016. *S&P Global Platts 2016: Global metal trends.* [Online] Available at: http://platts.com [Accessed 02 November 2016].

Ivesona, S., Holt, S. & Biggs, S., 2004. Advancing contact angle of iron ores as a function of their hematite and goethite content: implications for pelletising and sintering. *International Journal of Mineral Processing,* Volume 74, pp. 281-287.

Jain, S., 1985. *Mineral processing.* 2 ed. New Dehli: CBS Publishers.

James Cook University, 2005. *Element-to-stoichiometric oxide conversion factors.* [Online]

Available at: https://www.jcu.edu.au
[Accessed 12 January 2017].

John, P. W., 1971. *Statistical design and analysis of experiments*. First printing ed. New York: Collier-Macmillan Ltd.

Kamaruddin, S., Khan, Z. A. & Wan, K., 2004. The use of the Taguchi method in determining the optimum plastic injection moulding parameters for the production of a consumer product. *Jurnal Mekanikal,* Volume 18, pp. 98-110.

Kar, B., Sahoo, H., Rath, S. S. & Das, B., 2013. Investigations on different starches as depressants for iron ore flotation. *Minerals Engineering,* Volume 49, pp. 1-6.

Kario, P. & Brown, A., 2015. *How the iron ore market works: Supply and market share.* [Online]
[Accessed 02 November 2016].

King, R., 1982. *Principles of flotation.* Jhb: South African Institute of Mining and Metallurgy.

Krishna, S. J. G. et al., 2014. Characterisation and Processing of Some Iron Ores of India. *J. Inst. Eng. India Ser. D,* 94(2), pp. 113-120.

Kumar, T. et al., 2010. Reverse flotation studies on an Indian low grade iron ore slimes. *International Journal of Engineering Science and Technology,* 2(4), pp. 637-648.

LacCore, N. L. C. F., 2013. *Loss on Ignition Standard Operating Procedure,* s.l.: LacCore, National Lacustrine Core Facility.

Lima, N. P., Valadão, G. E. & E.C.Peres, A., 2013. Effect of amine and starch dosages on the reverse cationic flotation of an iron ore. *Minerals Engineering,* Volume 45, pp. 180-184.

Limited, S., 2016. *Sepfluor.* [Online]
Available at: http://sepfuor.co.za/fluorspar
[Accessed 11 November 2016].

Lina, L. et al., 2009. Experimental research on anionic reverse flotation of hematite with a flotation column. *Procedia Earth and Planetary Science ,* Volume 1, pp. 791-798.

Lin, L. et al., 2009. Experimental research on anionic reverse flotation of hematite with a flotation column. *Procedia Earth and Planetary Science ,* Volume 1, pp. 791-798.

Liu, W., Moran, C. & Vink, S., 2013. A review of the effect of water quality on flotation. *Minerals Engineering ,* Volume 53, pp. 91-100.

Loenel, C. & Peres, A., 2013. Calcination as additional unit operation in the pelletizing of iron ores presenting high contents of loss on ignition. *Revista De La Facultad De Ingeniera,* Volume 29, pp. 1-12.

Lubisi, T. P., Nheta, W. & Ntuli, F., 2016. *Physical, Chemical and Mineralogical Characterization of Fluorspar.* Proceedings of Materials, Minerals and Energy, South Africa, Elsevier.

Ma, M., 2012. Froth flotation of iron ores. *International Journal of Mining Engineering and Mineral Processing,* 1(2), pp. 56-61.

Masiya, T. T. & Nheta, W., 2014. *Flotation of Nickel-Copper Sulphide Ore: Optimisation of Process Parameters Using Taguchi Method.* Czech Republic.

Matthews, P. S., 1992. *Advanced chemistry.* Cambridge: Cambridge University Press.

Ma, X., Marques, M. & Gontijo, C., 2011. Comparative studies of reverse cationic/anionic flotation of Vale iron ore. *International Journal of Minerals Processing,* Volume 100, pp. 179-183.

Mbele, P., 2012. Pelletizing of Sishen concentrate. *Journal of Southern African Institute of Mining and Metallurgy,* 112(3), pp. 221-228.

McMurry, J., 2014. *General chemistry : atoms first.* 2 ed. Boston: Pearson.

Mead, R., 1988. *The design of experiments - Statistical principles for practical application.* New York: Press Syndicate of the University of Cambridge.

Michaud, L., 2006. *911 Metallurgist.* [Online] Available at: https://www.911metallurgist.com/blog/fluorspar-beneficiation-process-flotation-plant
[Accessed 21 November 2016].

Montes-Sotomayor, S., Houot, R. & Kongolo, M., 1998. Technical note flotation of silicated gangue iron ores: Mechanism and effecte of starch. *Minerals Engineering,* 11(1), pp. 71-76.

Montgomery, D. C., 2009. *Design and analysis of experiments.* 7 ed. Arizona: John Wiley and Sons.

Mowla, D., Karimi, G. & Ostadnezhad, K., 2008. Removal of hematite from silica sand ore by reverse flotation technique. *Separation and Purification Technology ,* Volume 58, pp. 419-423.

Myburgh, H. A. & Nortje, A., 2014. Operation and performance of the Sishen jig plant. *The Journal of The Southern African Institute of Mining and Metallurgy,* Volume 114, p. 574.

Nayak, N. P., November 2013. Mineralogical Constraints in Beneficiation Of Low Grade Iron Ores of Barsua, Eastern India. *International Journal of Engineering and Innovative Technology,* 3(5), pp. 1096-113.

Nguyen, A., 2013. *Froth Flotation,* The University of Queensland, Australia: Elsevier.

Ng, W. S., Sonsie, R., Forbes, E. & Franks, G. V., 2015. Flocculation/flotation of hematite fines with anionic temperature-responsive polymer acting as a selective flocculant and collector. *Minerals Engineering,* Volume 77, pp. 64-71.

Nheta, W., Lubisi, T. P., Masemola, S. & Makhatha, M. E., 2015. *Beneficiation of Haematite from Fluorspar Tailings by Reverse Flotation.* Proceedings of the World Congress on Mechanical, Chemical and Materia Engineering, Paper no 346, page 1-6.

Nyambayo, C. K., 2014. *The use of mixed thiol collectors in the flotation of Nkomati sulfide ore,* Cape town: University of Cape Town.

Pallant, J., 2010. *SPSS survival manual : a step by step guide to data analysis using SPSS.* 4th ed. Maidenhead: Open University Press.

Parrent, M., 2012. *Separation of pyrolusite and hematite by froth flotation,* Edmonton: University of Alberta..

Pavlovic, S. & Brandao, P., 2003. Adsorption of starch, amylose, amylopectin and glucose monomerand their effect on the flotation of hematite and quartz. *Minerals Engineering,* Volume 16, pp. 1117-1122.

Pearse, M., 2005. An overview of the use of chemical reagents in mineral processing. *Minerals Engineering ,* Volume 18, pp. 139-149.

Quast, K., 2005. Flotation of hematite using C6–C18 saturated fatty acids. *Minerals Engineering ,* 19(6-8), pp. 582-597.

Quast, K., 2015. Use of conditioning time to investigate the mechanisms of interactions of selected fatty acids on hematite. Part 1: Literature survey. *Minerals Engineering,* Volume 79, pp. 295-300.

Rachappa, S., Prakash, Y. & Amit, 2015. Iron ore recovery from low grades by using advanced methods. *Procedia Earth and Planetary Science,* Volume 11, pp. 195-197.

Ramsaywok, P., Vermaak. M., K. G. & Viljoen, R., 2010. Case study: high capacity spiral concentrators. *The Journal of The Southern African Institute of Mining and Metallurgy,* Volume 110, pp. 637-642.

Rao, D. S. et al., 2009. Mineralogy and Geochemistry of a low grade iron ore sample from Bellary-Hospet Sector, India and their implications on beneficiation. *Journal of Mineral & MaterialsCharacterization & Engineering,* 8(2), pp. 115-132.

Rao, H. K. & Forssberg, K., 1997. Mixed collector systems in flotation. *International Journal of Mineral Processing,* Volume 51, pp. 67-79.

Rusch, B., Hanna, K. & Humbert, B., 2010. Coating of quartz silica with iron oxides: Characterization and surface reactivity of iron coating phases. *Colloids and Surfaces A: Physicochem and Engineering Aspects,* Volume 353, pp. 172-180.

Santana, R. C., Anna C.C., Farnese, Marilia C.B. Fortes, Carlos, H. Aaide, Marcos. A.B. Barrozo. 2008. Influence of particle size and reagent dosage on the performance of apatite flotation. *Separation and Purification Technology ,* Volume 64, pp. 8-15.

Santos, I. D. & Oliveira, J. F., 2007. Utilization of humic acid as a depressant for hematite in the reverse flotation of iron ore. *Mineral Engineering,* Volume 20, pp. 1003-1007.

Sapakal, S. & Telsang, M., 2012. Parametric optimization of MIG welding using Taguchi design method. *International Journal of Advanced Engineering Research and Studies,* 1(4), pp. 28-30.

Seifelnassr, A. A. S., Moslim, E. M. & Abouzeid, A.-Z. M., 2013. Concentration of a Sudanese low-grade iron ore. *International Journal of Mineral Processing,* Volume 122, pp. 59-62.

Singh, G. et al., 2015. Iron Ore Pelletization Technology and its Environmental Impact Assessment in Eastern Region of India - A Case study. *Procedia Earth and Planetary Science,* Volume 11, pp. 582-597.

Srivastava, M., Pan, S., Prasad, N. & Mishra, B., 2001. Characterization and processing of iron ore fines of Kiriburu deposit of India. *International Journal of Mineral Processing ,* Volume 61, pp. 93-107.

Statics, S. A., 2016. *Statics South Africa - Iron ore.* [Online] Available at: http://www.statssa.gov.za [Accessed Thursday September 2016].

Statista, 2016. *Iron ore prices from September 2015 to September 2016.* [Online] Available at: https://www.statista.com/statistics/300419/monthly-iron-ore-prices/ [Accessed 12 November 2016].

Tofighy, M. A. & Mohammadi, T., 2012. Application of Taguchi experimental design in optimization of desalination using purified carbon nanotubes as adsorbent. *Materials research bulletin,* Volume 47, pp. 2389-2395.

Tombell, D., 2011. *Flotation of cobalt bearing minerals from a copper mixed copper-cobalt oxidised ore,* SA: University of JHB.

Transparency Market Research, 2016. *Iron and steel market - Global industry analysis, seze, share, growth, trends and forecast 2016-2024.* [Online] Available at: http://www.transparencymarketresearch.com/iron-steel-market.html [Accessed 02 November 2016].

Tripathy, S. K., Murthy, Y. R. & Singh, V., 2013. Characterisation and separation studies of Indian chromite beneficiation plant tailing. *International Journal of Mineral Processing ,* Volume 122, pp. 47-53.

Turrer, H. & Peres, A., 2010. Investigation on alternative depressants for iron ore flotation. *Minerals Engineering,* Volume 23, pp. 1066-1069.

Tutorvista, 2016. *Concentration - Enrichment of Ores.* [Online] Available at: http://www.tutorvista.com/content/science/science-ii/metals-non-metals/enrichment-ores.php [Accessed 11 November 2016].

Umadevi, T. et al., 2013. Recovery of Iron Bearing Minerals from Beneficiation Plant 2 Thickner Underflow of JSW Steel Limited. *Journal of Minerals and Materials Characterization and Engineering, 2013, 1, 55-60,* Volume 1, pp. 55-60.

Vergenoeg Mining Company, 2016. *MinerSA group.* [Online] Available at: http://www.minersa.com/eng/vergenoeg_mining.php [Accessed 11 November 2016].

Vermaak, M. K. G., Visser, H. J. & Bosman, J. B., 2008. A simple process control model for spiral concentrators. *The Journal of The Southern African Institute of Mining and Metallurgy,* Volume 108, pp. 147-153.

Vidyadhar, A., Kumari, N. & Bhagat, R., 2012. Adsorption mechanism of mixed collector systems on hematite flotation. *Minerals Engineering,* Volume 26, pp. 102-104.

Vidyadhar, A., Kumari, N. & Bhagat, R. P., 2012. *Flotation of quartz and hematite: Adsorption mechanism of mixed cationic/anionic collector systems,* India: IMPC, New Dehli.

Voges, H., 1975. The use of heavy-medium separation in the processing of iron ore. *Journal of the South African Institute of Mining and Metallurgy,* pp. 303-306.

Wei, S. N., Rowan, S., Forbes, E. & Franks, G. V., 2015. Flocculation/flotation of hematite fines with anionic temperature responsive polymer acting as a selective flocculant and collector. *Minerals Engineering,* Volume 77, pp. 64-71.

Wen-gang, L. et al., 2009. A new collector used for flotation of oxide minerals. *Transactions of Nonferrous Metals Society of China,* Volume 19, pp. 1326-1330.

Wills, B.A, 2006. *Will's Mineral Processing Technology: an introduction to the practical aspects of ore treatement and mineral recovery.* 6 ed. Canada: Elsevier.

Wills, B.A & Finch, J., 2016. *Will's Mineral Processing Technology: An introduction to the practical aspects of ore treatement and mineral recovery.* 8 ed. Canada: Elsevier.

Wilson, M. G. C. & Anhaeusser, C. R., 1998. *The mineral resources of South Africa: Handbook.* 6 ed. Pretoria: Council for Geoscience.

Xu, Z. & Zhou, Z., 2013. *FLOTATION | Historical Development,* Canada: Elsevier.

Yuhua, W. & Jianwei, R., 2005. The flotation of quartz from iron minerals with a combined quaternary ammonium salt. *International Journal of Mineral Processing,* Volume 77, pp. 116-122.

Zhou, Y. et al., 2014. Comparative study on the adsorption interactions of humic acid onto natural magnetite, hematite and quartz: Effect of initial HA concentration. *Powder Technology,* Volume 251, pp. 1-8.

Zogo, J.-C. B., 2009. *Beneficiation potential of low grade iron-ore from a discard lumpy stockpile and fines tailings dam at Beeshoek Mine, Northern Cape Province, South Africa,* University of Jhb.

7 APPENDIX

7.1 Laboratory activities risk analysis

Table A 1: Risk assessment

Task	Hazard	Risk	Risk rating	Risk control measures taken	Recommendations
Charactesization of fluorspar tails	Handling heavy sample bags	Back injuries	High	Flat trolley was used; assistance was requested where necessary and sample was scooped in manageable quantities	
	Drying of sample at 70°C	Burns	Low	Heat resistant gloves were worn	
	Dust during delumping and sub-sampling	Dust inhalation	Medium	Dust musk was worn.	
	Dust during pulvurising of sample	Dust inhalation and eye irritation	Medium	Dust musk and eye goggles were worn	Dust extraction in pulveriser room is required
	Noise during pulverising of sample	Hearing problems due to prolong exposures	Medium	Ear muffs were worn.	
	Working on vibrating machinery during pulverising	Injuries due machinery de-coupling	Medium	Training was obtained from the lab technician and the incubent kept a safe standing distance from a vibrating pulveriser.	
	Handling pulveriser metal rings and rods	Possible pintching of fingers	Low	Gloves were worn and caution applied	
	High furnace temperature during LOI determination	Injuries due to burns	High	Heat resistant gloves were worn and thongs were used to collect crucibles form the hot furnace	
Flotation	Handling chemicals such as HCl, NaOH	Eye irritation and skin burns	Medium	Gloves and eye goggles were worn	
	High agitational speed in the flotation cell	Injuries	High	The incubent avoided inserting rigid materials/hands into the cell while agitation was ON	
	High pressure during filtration	Injuries when lid not properly clamped or when lid is open before pressure escapes the vessel	High	Training was obtained from the lab technician and the incubent ensure safe working procedure was followed.	
	Slippery floors from possible spillages	Slippery floors	Medium	Good housekeeping was kept	

7.2 Characterization data

7.2.1 Detailed chemical analysis of feed

Table A 2: Chemical analysis of fluorspar tails sample

Component	Composition, %wt
F	2.25
Na_2O	0.12
MgO	0.05
Al_2O_3	0.91
SiO_2	16.8
P_2O_5	0.48
SO_3	0.06
Cl	0.21
K_2O	0.14
CaO	3.80
TiO_2	0.11
Cr_2O_3	0.01
MnO	0.23
Fe_2O_3	69.9
CuO	0.62
As_2O_3	0.21
Y_2O_3	0.11
MoO_3	0.11
SnO_2	0.32
CeO_2	0.15
Nd_2O_3	0.03

7.2.2 Conversion of oxides values to element values

The chemical analysis results obtained from XRF required conversion from oxide to element form. The generic conversion factors for various compounds are given in Table A3.

Table A 3: Element-to-stoichiometric oxide conversion factors (James Cook University, 2005)

Oxide name	Conversion factor	Oxide name	Conversion factor
Ag_2O	1.0741	HgO	1.0798
Al_2O_3	1.8895	HO_2O_3	1.1455
As_2O_3	1.3203	In_2O_3	1.2091
As_2O_5	1.5339	IrO	1.0832
Au2O	1.0406	K_2O	1.2046
B_2O_3	3.2202	La_2O_3	1.1728
BaO	1.1165	Li_2O	2.1527
BeO	2.7758	Lu_2O_3	1.1371
Bi_2O_5	1.1914	MgO	1.6582
CO_2	3.6644	MnO	1.2912
CaO	1.3992	MnO_2	1.5825
CdO	1.1423	MoO_3	1.5003
Ce_2O_3	1.1713	N_2O_5	3.8551
CeO_2	1.2284	Na_2O	1.3480
CoO	1.2715	Nb_2O_5	1.4305
Cr_2O_3	1.4615	Nd_2O_3	1.1664
Cs_2O	1.0602	NiO	1.2725
CuO	1.2518	OsO	1.0841
Dy_2O_3	1.1477	P_2O_5	2.2916
Er2O3	1.1435	PbO	1.0772
Eu_2O_3	1.1579	SO_3	2.4972
FeO	1.2865	SeO_3	1.6079
Fe_2O_3	1.4297	SiO_2	2.1392
Ga_2O_3	1.3442	SnO_2	1.2696
Gd_2O_3	1.1526	TiO_2	1.6681
F	1	Y_2O_3	1.2699
HfO_2	1.1793	Yb_2O_3	1.1387
ZnO	1.2448	Cl	1

Conversion of oxide results into element form was done by dividing the oxide value by the respective conversion factor given in Table A2. An example of such calculation is that of converting 69.9% Fe_2O_3 found in feed sample into %Fe;

$$Fe = \frac{69.9}{1.4297}$$
$$= 48.9\, wt\%$$

7.2.3 Mineral distribution data

The feed sample was classified into different size fractions to determine mineral distribution. The chemical composition of the feed showed the results in Table A3, where the reflected results are of those compounds present in concentrations >0.5%

Table A 4: Mineral distribution data

Component	**Fe**	**SiO_2**	**CaO**	**Al_2O_3**	**F**
Feed	48.90	16.80	3.80	1.21	2.25
+150µm	33.59	32.78	8.90	1.27	2.54
-150+106µm	44.61	21.07	6.48	1.23	4.50
-106+75µm	48.91	18.61	4.58	1.08	3.36
-75+53µm	49.42	21.53	4.12	1.25	1.25
-53+45µm	49.66	18.78	3.10	1.02	1.10
-45+38µm	49.55	22.50	3.33	1.25	1.00
-38µm	52.09	15.22	4.09	1.42	1.90

7.2.4 QEMSCAN Particle Map Analysis (PMA)

- *Iron oxide association*

The SEM-EBS, QEMSCAN map and semi-quantitative SEM-EDS showed the following;

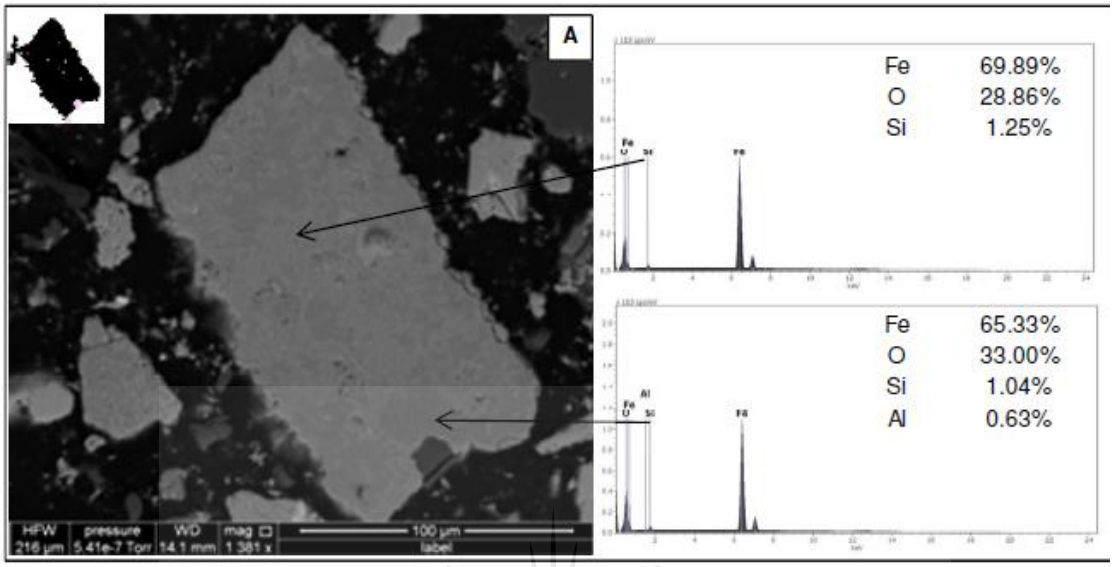

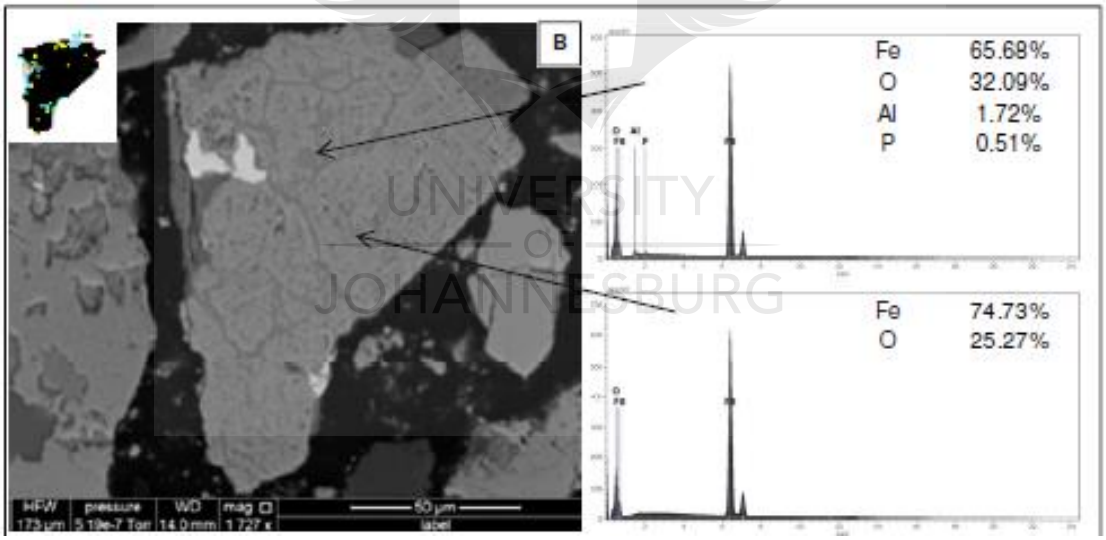

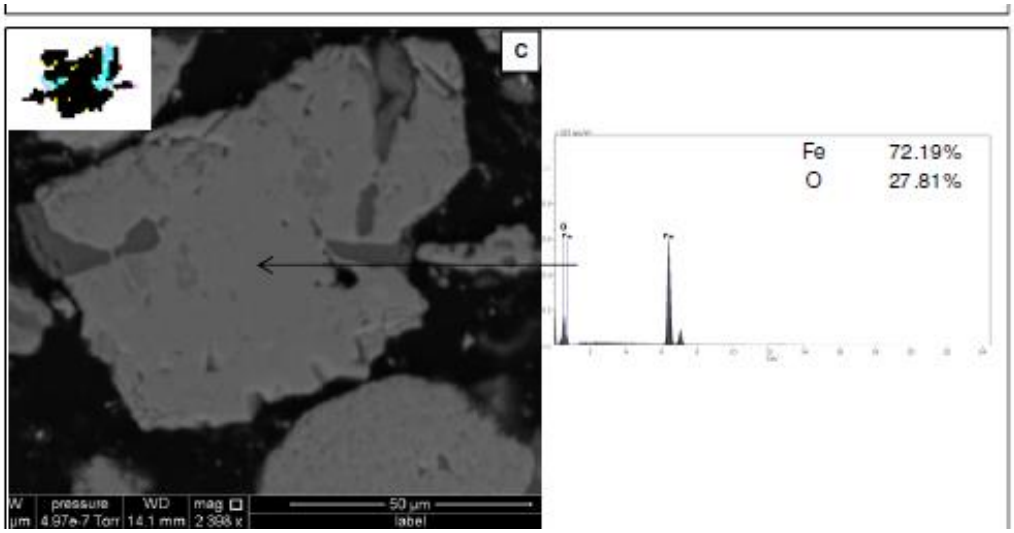

Figure A1: SEM-EDS diagram showing association of Fe-oxide

- *Exposure characteristics*

The exposure classes are explained below;

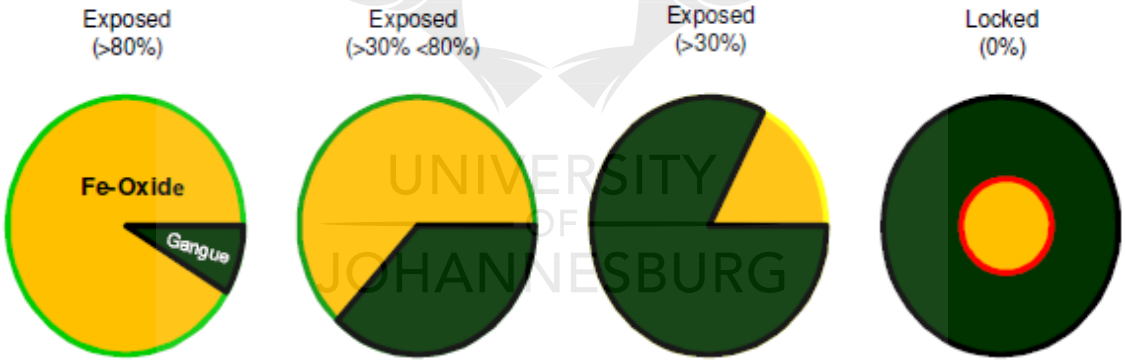

Figure A2: Explanation of exposure classes

Table A 5: Exposure and mineral association characteristics of Fe-oxides

Class	**Area of Fe-oxides %**
Exposed (≥80%)	80.61
Exposed (≥10%<80)	18.41
Exposed <10%	0.48
Total	**99.50**
Locked in silicates	0.27
Locked in fluorites	0.06
Locked in sulphides	0.00
Locked in oxides	0.00
Locked in phosphates and carbonates	0.01
Locked in fluorite/silicates	0.12
Locked in sulphides/silicates/fluorite	0.00
Locked on poly-mineral boundary	0.04
Total locked	**0.5**
Total	**100**

- *Liberation characteristic explanation*

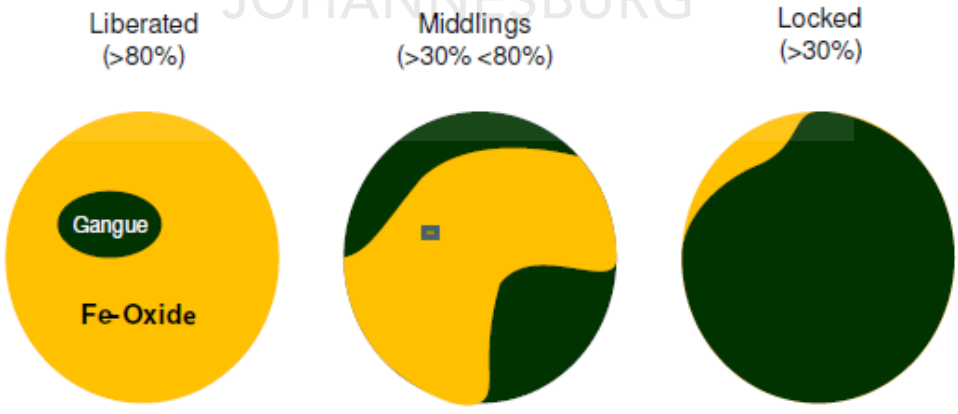

Figure A3: Explanation of liberation characteristic analysis

7.3 Flotation of fluorspar tails

7.3.1 Mass Balance calculation

The mass balance around the flotation cell was conducted, based on the following diagram:

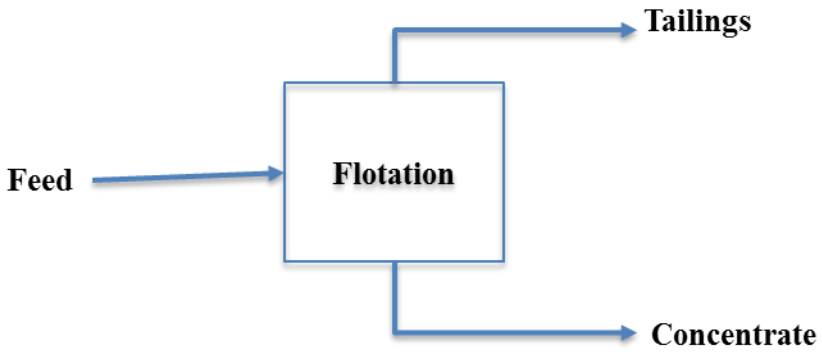

Figure A4: Overall flotation diagram

Mass balance calculation are important as they tell how much of the feed reported in the floats and how much in the sinks. The tailing refers to the waste mineral stream and concentrates refers to the valuable mineral stream. Mass balance also identifies the material losses in the system, which could be due to spillages etc. The mass balance was calculated as following:

$$F = T + C \quad \text{.....eqn (i)}$$

Where F is feed, T is tailings which is the floats in this study, C is the concentrate which is the sinks in this study. The mass split was calculated as follows:

$$\%mass\ in\ sinks = \frac{C}{F} \times 100 \quad \text{.....eqn (ii)}$$

$$\%mass\ in\ floats = \frac{T}{F} \times 100 \quad \text{.....eqn (iii)}$$

7.3.2 Metal recovery calculation

The recovery would show the weighted percentage iron that reported in the sinks during flotation. Though all iron in the feed should ideally report in the sinks, however, this is not likely as some of the iron could be carried to the froth section via entrainment and entrapment. Presence of locked or poorly liberated iron can also cause iron losses to froth resulting in reduced recovery. Recovery and metal loss calculation were shown in page 41, equation 12 and 13, of this report.

7.3.3 Calculations example: DDA and Betachcem 30D system

- *Mass balance calculation*

1000g feed was prepared to slurry using 2litre domestic water at atmospheric temperature. Flotation experiment was conducted at operating conditions reflected in Table A6.

Table A 6: Flotation operating conditions

Parameter	Level
pH	10-10.5
DDA dosage	500g/t
Betachem 30D dosage	500g/t
Conditioning time	15min
Air rate	Valve ¾ open
Agitation	1300rpm
Solids	50%

After flotation the concentrate and tails stream were dried and weighed whereby the concentrates weighed 542.61g and tailings 416.97g. Since the mass balance is as follows;

$$F = C + T = 1000g$$
$$Since, C + T = 542.16 + 416.97 = 959.58g$$
$$It\ was\ observed\ that\ F \neq C + T$$

The discrepancy when comparing input with output could be due to material loss due to spillages, during equipment washing and material left in the filter papers. This loss was calculated as following:

$$Material\ loss = \frac{F - C - T}{F} \times 100$$
$$= \frac{1000 - 542.61 - 416.97}{1000} \times 1000$$
$$= 4.04\%$$

Generally material loss of up to 10% is acceptable during flotation, hence 4.04% loss was deemed to be within acceptable limits.

- *Mass split calculation*

The percentage mass was calculated to determine the mass pull,

$$\%\text{mass in sinks} = \frac{C}{F} \times 100$$
$$= \frac{542.61}{1000} \times 100$$
$$= 54.3\%$$

$$mass\ in\ floats = \frac{T}{F} \times 100$$
$$= \frac{416.97}{1000} \times 100$$
$$= 41.7\%$$

7.3.4 Recovery calculation

Chemical composition of the feed, tailings and concentrate stream was conducted to determine iron grade and recovery. The iron assay in concentrate stream was measured 63.79% and 48.9% Fe in feed. Metal recovery was then calculated according to equation 2.12;

$$\text{Recover, R} = \frac{Cc}{Ff} \times 100$$
$$= \frac{542.61 \times 0.6379}{1000 \times 0.489} \times 100$$
$$= 70.78\%$$

7.3.5 Taguchi DOE for flotation using soluble starch- DDA

The parameters investigated for this system was soluble starch dosage, DDA dosage, pH, solids content and conditioning time. L25 orthogonal matrix was used for arranging experimental settings. Minitab 17 was used for computing of data and its analysis thereof. An example of the resulting data spreadsheet in Table A7.

Table A 7: Taguchi data spreadsheet

Starch (g/t)	DDA (g/t)	pH	Solids (%	C/time (min)	Grade	SNRA1	MEAN1	CV1	SNRA2	MEAN2	CV2	SNRA3	MEAN3	CV3	SNRA4	MEAN4	CV4
750	200	4	35	3	45,97	5,5054	33,4289	0,53056	28,593	33,4289	0,53056	28,593	33,4289	0,53056	28,593	33,4289	0,53056
750	300	6	40	6	46,12	35,3027	46,687	0,01717	33,382	46,687	0,01717	33,382	46,687	0,01717	33,382	46,687	0,01717
750	400	8	45	10	47,21	28,641	48,4776	0,03698	33,7019	48,4776	0,03698	33,7019	48,4776	0,03698	33,7019	48,4776	0,03698
750	500	10	50	15	55,04	11,3427	68,0835	0,27094	36,1795	68,0835	0,27094	36,1795	68,0835	0,27094	36,1795	68,0835	0,27094
750	600	12	55	20	51,98	9,2363	68,7709	0,34529	35,9628	68,7709	0,34529	35,9628	68,7709	0,34529	35,9628	68,7709	0,34529
1000	200	6	45	15	52,73	10,7794	66,2783	0,28909	35,8789	66,2783	0,28909	35,8789	66,2783	0,28909	35,8789	66,2783	0,28909
1000	300	8	50	20	55,37	14,9371	63,4001	0,17912	35,8322	63,4001	0,17912	35,8322	63,4001	0,17912	35,8322	63,4001	0,17912
1000	400	10	55	3	55,81	10,899	69,9041	0,28513	36,3565	69,9041	0,28513	36,3565	69,9041	0,28513	36,3565	69,9041	0,28513
1000	500	12	35	6	53,77	8,8692	72,1453	0,3602	36,3086	72,1453	0,3602	36,3086	72,1453	0,3602	36,3086	72,1453	0,3602
1000	600	4	40	10	42,4	0,2226	25,1004	0,9747	20,7085	25,1004	0,9747	20,7085	25,1004	0,9747	20,7085	25,1004	0,9747
1300	200	8	55	6	54,28	10,9332	67,9203	0,28401	36,1107	67,9203	0,28401	36,1107	67,9203	0,28401	36,1107	67,9203	0,28401
1300	300	10	35	10	54,92	9,6487	71,5883	0,32928	36,3834	71,5883	0,32928	36,3834	71,5883	0,32928	36,3834	71,5883	0,32928
1300	400	12	40	15	53,45	9,0876	71,1124	0,35125	36,2259	71,1124	0,35125	36,2259	71,1124	0,35125	36,2259	71,1124	0,35125
1300	500	4	45	20	50,36	3,3924	34,0619	0,67668	27,4917	34,0619	0,67668	27,4917	34,0619	0,67668	27,4917	34,0619	0,67668
1300	600	6	50	3	56,01	11,4174	47,0696	0,26862	32,9817	47,0696	0,26862	32,9817	47,0696	0,26862	32,9817	47,0696	0,26862
1500	200	10	40	20	57,04	11,2433	70,7503	0,27405	36,502	70,7503	0,27405	36,502	70,7503	0,27405	36,502	70,7503	0,27405
1500	300	12	45	3	50,94	7,3218	73,228	0,43044	36,0644	73,228	0,43044	36,0644	73,228	0,43044	36,0644	73,228	0,43044
1500	400	4	50	6	53,64	14,4145	47,2802	0,19023	33,2571	47,2802	0,19023	33,2571	47,2802	0,19023	33,2571	47,2802	0,19023
1500	500	6	55	10	56,8	19,4523	52,8218	0,10651	34,3823	52,8218	0,10651	34,3823	52,8218	0,10651	34,3823	52,8218	0,10651
1500	600	8	35	15	56,12	-0,8995	31,4529	1,10911	19,5792	31,4529	1,10911	19,5792	31,4529	1,10911	19,5792	31,4529	1,10911
2000	200	12	50	10	53,64	8,6162	72,7051	0,37084	36,3237	72,7051	0,37084	36,3237	72,7051	0,37084	36,3237	72,7051	0,37084
2000	300	4	55	15	53,91	15,5098	61,1624	0,16769	35,5461	61,1624	0,16769	35,5461	61,1624	0,16769	35,5461	61,1624	0,16769
2000	400	6	35	20	52,41	9,5277	42,3994	0,3339	31,8134	42,3994	0,3339	31,8134	42,3994	0,3339	31,8134	42,3994	0,3339
2000	500	8	40	3	59,44	29,6013	60,8649	0,03311	35,6802	60,8649	0,03311	35,6802	60,8649	0,03311	35,6802	60,8649	0,03311
2000	600	10	45	6	58,96	53,8928	59,0443	0,00202	35,4235	59,0443	0,00202	35,4235	59,0443	0,00202	35,4235	59,0443	0,00202

7.3.6 Confirmation test for SS-DDA system

An experiment was conducted using the optimum condition predicted by Taguchi and the following concentrate and tails quality was found.

Table A 8: Confirmation test results for SS-DDA concentrate stream

	Composition
F	2.9853
Na_2O	0.0820
MgO	0.0418
Al_2O_3	0.5680
SiO_2	5.3104
P_2O_5	0.3441
SO_3	0.2506
K_2O	0.0282
CaO	7.7281
TiO_2	0.0433
MnO	0.3821
Fe_2O_3	81.2976
Co_2O_3	0.0652
CuO	0.0868
ZnO	0.0123
As_2O_3	0.0792
Y_2O_3	0.2807
MoO_3	0.0301
SnO_2	0.0756
La_2O_3	0.0957
CeO_2	0.2131
Performance	
Fe assay	56.87%
Recovery	78%
Mass split	62.32%

7.3.7 Betachem 30D- DDA system

Since the highest SN ratio for dextrin dosage was at 300g/t and a large gap purposely existed between this level and the next (1000g/t), a decision was made to investigate other dosages in between (500 and 750g/t). The detailed results tabulated in Table A9.

Table A 9: Impact of varied depressant concentration on concentrate quality

	300g/t	**500g/t**	**750g/t**
F	2.6819	1.3700	2.0743
Na_2O	0.0483	0.0676	0.0913
MgO	0.0332	0.0412	0.0712
Al_2O_3	0.5676	0.6394	0.8369
SiO_2	5.6834	6.1561	4.4730
P_2O_5	0.3681	0.3456	0.3644
SO_3	0.2203	0.2488	0.3082
Cl	0.0099	0.0183	0.0289
K_2O	0.0238	0.0265	0.0228
CaO	5.9548	3.3421	4.4742
TiO_2	0.0574	0.0762	0.0599
Cr_2O_3	ND	ND	0.0224
MnO	0.3762	0.4237	0.3877
Fe_2O_3	83.4602	86.3567	85.9146
Co_2O_3	ND	0.0936	ND
CuO	0.0930	0.0182	0.1087
As_2O_3	0.0830	0.0826	0.0917
Y_2O_3	0.2746	0.2581	0.2458
MoO_3	0.0322	0.0326	0.0310
SnO_2	0.0627	0.0627	0.0505
La_2O_3	0.0684	0.0632	0.0954
CeO_2	0.2160	0.1890	0.2473
Nd_2O_3	ND	0.0879	ND
Performance			
%Fe assay	58.38%	60.41%	60.09%

Table A9 continued:			
	300g/t	**500g/t**	**750g/t**
Recovery, %	68.62%	74.73%	74.45%
Mass split, %	52.68%	55.67%	56.19%

7.3.8 Soluble starch – DDA system final confirmation test

This test considered additional parameters such as agitation speed, air rate which were not considered in Table A8. The detailed experiment results are shown in Table A10.

Table A 10: Detailed results for final SS-DDA system

	Sinks	**Floats**
F	2.3332	9.7874
Na_2O	0.0718	0.0602
MgO	0.0280	0.0307
Al_2O_3	0.6712	0.5431
SiO_2	3.6006	12.8309
P_2O_5	0.3645	0.3417
SO_3	0.3685	0.5467
Cl	0.0208	0.0199
K_2O	0.0174	0.0386
CaO	3.6966	15.5449
TiO_2	0.0557	0.0532
Cr_2O_3	0.0231	0.0276
MnO	0.3474	0.4424
Fe_2O_3	87.5095	58.7738
CuO	0.0855	0.0813
ZnO	0.0125	0.0104
As_2O_3	0.0738	0.0622
Y_2O_3	0.2268	0.2855
MoO_3	0.0270	0.0225
SnO_2	0.0585	0.0605
La_2O_3	0.1000	0.1083

Table A10 continued:		
	Sinks	**Floats**
CeO_2	0.2267	0.2264
Nd_2O_3	0.0807	0.1018
PbO	ND	ND
Performance		
Fe grade in sinks	61.21%	
Recovery	67.90%	
Mass split	55.79%	

7.3.9 Flotation kinetics of soluble starch and Betachem 30D

Flotation kinetics was conducted, using the detected optimum conditions, in order to investigate iron depression ability of soluble starch and the dextrin. DDA was used as the collector. Table A11 shown the detailed chemical analysis results.

Table A 11: Flotation kinetics for BET30D-DDA systems

	30 seconds	**60 seconds**	**120 seconds**	**180 seconds**
F	11.1283	10.7006	8.7516	9.6434
MgO	ND	0.0386	0.0292	0.0208
Al_2O_3	0.5609	0.4920	0.5356	0.4591
SiO_2	21.7970	13.3499	9.3115	6.3386
P_2O_5	0.3058	0.3266	0.3624	0.3853
SO_3	1.2670	0.6001	0.4734	0.3771
Cl	0.0264	0.0237	0.0284	0.0275
K_2O	0.0576	0.0412	0.0384	0.0274
CaO	19.9126	19.3491	17.3882	17.8599
TiO_2	0.0670	0.0500	0.0761	0.0701
Cr_2O_3	0.0415	0.0345	0.0467	0.0473
MnO	0.2641	0.2986	0.3349	0.2898
Fe_2O_3	43.5769	53.6900	61.4107	63.1142
NiO	ND	ND	ND	0.1087

Table A11 continued:				
	30 seconds	**60 seconds**	**120 seconds**	**180 seconds**
CuO	0.0914	0.0966	0.1003	0.1008
As_2O_3	0.0655	0.0662	0.0722	0.0788
Y_2O_3	0.2776	0.3196	0.3374	0.3419
MoO_3	0.0231	0.0258	0.0276	0.0290 p
SnO_2	0.0689	0.0652	0.0684	0.0643
La_2O_3	0.1153	0.1261	0.1220	0.1240
CeO_2	0.2258	0.3056	0.3289	0.3426
Nd_2O_3	0.0860	ND	0.1235	0.1495
Na_2O	0.0413	ND	0.0325	ND

Table A 12: Flotation kinetics of soluble starch – DDA system

	30 seconds	**60 seconds**	**120 seconds**	**180 seconds**
F	10.7372	12.8326	11.2930	9.7905
Na_2O	0.0381	0.0533	0.0495	0.0497
MgO	0.0497	0.0434	0.0747	0.0774
Al_2O_3	0.5942	0.5270	0.6243	0.6421
SiO_2	26.8179	18.6673	16.1353	13.2862
P_2O_5	0.3007	0.3225	0.3311	0.3355
SO_3	0.8370	0.6208	0.4799	0.4797
Cl	0.0114	0.0106	ND	0.0108
K_2O	0.0620	0.0491	0.0588	0.0564
CaO	19.8299	22.3933	21.1525	19.2251
TiO_2	0.0572	0.0703	0.1034	0.0882
Cr_2O_3	0.0629	0.0496	0.1041	0.1022
MnO	0.4561	0.4440	0.2973	0.2877
Fe_2O_3	39.1819	42.8846	48.2680	54.5185
ZnO	0.0116	0.0093	ND	0.0107
CuO	0.0895	0.0755	0.0729	0.0705
As_2O_3	0.0438	0.0552	0.0442	0.0534

Table A12 continued:				
	30 seconds	**60 seconds**	**120 seconds**	**180 seconds**
Y_2O_3	0.2737	0.0188	0.2998	0.2966
MoO_3	0.0160	0.0542	0.0199	0.0204
SnO_2	0.0540	0.1008	0.0574	0.0613
La_2O_3	0.0887	0.2797	0.1141	0.1140
CeO_2	0.2328	0.1063	0.2744	0.2876
Nd_2O_3	0.1071	0.0201	0.1097	0.1139
SrO	0.0036	0.0032	0.0042	0.0036
ZrO_2	0.0034	0.0039	0.0065	0.0051
PbO	0.0138	0.0111	0.0157	0.0129
Yb_2O_3	0.0258	0.0242	ND	ND

7.4 Further optimization experiments

7.4.1 Effect of feed de-sliming

De-sliming of feed was conducted with objective of reducing iron loss due to slime coating of quartz particles. Table A13 shows the chemical composition changes in feed due to de-sliming and iron losses in slimes.

Table A 13: Quantification of metal loss due to feed de-sliming

	De-slimed feed	**-20µm (slimes)**
F	5.5938	4.0495
Na_2O	0.0945	0.0603
MgO	0.6048	0.0399
Al_2O_3	0.5451	0.6384
SiO_2	15.4706	6.3521
P_2O_5	0.3362	0.3259
SO_3	0.5179	0.2476
Cl	0.0274	ND
K_2O	0.0300	0.0253
CaO	9.4425	9.8225

Table A13 continued:		
	De-slimed feed	**-20µm (slimes)**
TiO_2	0.0806	0.0675
Cr_2O_3	0.0247	ND
MnO	0.3115	0.3579
Fe_2O_3	68.7639	76.55
CuO	0.0871	0.0856
ZnO	0.0154	ND
As_2O_3	0.0741	0.0789
Y_2O_3	0.2535	0.2782
MoO_3	0.0276	0.0291
SnO_2	0.0585	0.0791
La_2O_3	0.1017	0.1348
CeO_2	0.2377	0.2053
Nd_2O_3	0.1009	ND

7.4.2 Effect of DDA concentration variation

An expectation of reduced reagent consumption was made; collector dosage was varied when de-slimed feed was used. This resulted in conduction flotation of de-slimed feed at various collector dosage, as shown in Table A14.

Table A 14: Effect of DDA dosage variation using de-slimed feed

	Sinks			**Floats**		
	300	**400**	**500**	**300**	**400**	**500**
F	0.9272	0.9780	1.0193	14.3351	12.6984	11.5759
Na_2O	ND	0.0496	ND	0.0385	0.0570	0.0262
MgO	0.0414	0.0352	ND	0.0434	0.0375	0.0352
Al_2O_3	0.6292	0.7686	0.6349	0.4788	0.5593	0.4944
SiO_2	4.3807	4.1787	2.9696	19.4198	18.8194	17.1940
P_2O_5	0.3800	0.3758	0.3702	0.2864	0.3039	0.3230
SO_3	0.2600	0.3520	0.2435	0.7819	0.7677	0.6955
Cl	0.0180	0.0287	0.0180	0.0171	0.0288	0.0179

Table A14 continued						
	Sinks			**Floats**		
	300	**400**	**500**	**300**	**400**	**500**
K_2O	0.0200	0.0228	0.0193	0.0463	0.0449	0.0428
CaO	2.4060	1.9580	1.9682	23.2881	20.3038	18.7088
TiO_2	0.0778	0.0674	0.0910	0.0664	0.0586	0.0661
Cr_2O_3	ND	0.0227	0.3813	0.0259	0.0182	ND
MnO	0.3535	0.3696	0.1095	0.3349	0.2436	0.2639
Fe_2O_3	89.5299	89.8675	91.2749	39.9819	45.0415	49.5587
CuO	0.1053	0.1085	0.0162	0.0730	0.0797	0.0695
ZnO	ND	0.0169	0.0892	ND	ND	ND
As_2O_3	0.0878	0.0855	0.2376	0.0485	0.0563	0.0570
Y_2O_3	0.2605	0.2466	0.0259	0.2799	0.2806	0.2874
MoO_3	0.0339	0.0346	0.0715	0.0071	0.0206	0.0226
SnO_2	0.0572	0.0683	ND	0.0183	0.0698	0.0621
La_2O_3	0.1077	0.0624	0.1128	0.0586	0.0936	0.1017
CeO_2	0.2278	0.2234	0.2426	0.2559	0.2887	0.2895
Nd_2O_3	0.0961	0.0794	0.1047	0.1142	0.1282	0.1077
Performance						
%Fe	62.62%	62.86%	63.84%			
Recovery, %	69.14%	73.45%	75.16%			
Mass split	52.78%	60.25%	58.25%			

7.4.3 Effect of increased conditioning time

A decision was made to conduct the Betachem 30D – DDA system at pre-determined conditioning time, as per Taguchi, of 15minutes. A comparison between 6 minutes and 15 minutes conditioning time is given in details in Table A15.

Table A 15: Effect of increased conditioning time on concentrate quality

	Conditioning time - 6 min		**Conditioning time – 15min**	
	Sinks	**Floats**	**Sinks**	**Floats**
F	1.3700	8.1099	0.6544	7.8858
Na_2O	0.0676	0.0426	0.0735	0.0518
MgO	0.0412	0.0406	0.0540	0.0337
Al_2O_3	0.6394	0.5809	0.8692	0.5482
SiO_2	6.1561	14.3256	3.7589	15.2725
P_2O_5	0.3456	0.3234	0.3661	0.3586
SO_3	0.2488	0.5353	0.4270	1.1245
Cl	0.0183	0.0173	0.0275	0.0353
K_2O	0.0265	0.0407	0.0341	0.0481
CaO	3.3421	18.4977	1.0098	15.3652
TiO_2	0.0762	0.0572	0.0704	0.0714
Cr2O3	ND	0.0303	ND	0.0208
MnO	0.4237	0.5078	0.4556	0.2514
Fe_2O_3	86.3567	55.7907	91.2363	57.7931
CuO	0.0182	0.0834	0.1192	0.0944
Co2O3	0.0936	ND	ND	ND
As_2O_3	0.0826	ND	0.1095	0.0804
Y_2O_3	0.2581	0.3082	0.2153	0.2933
Nb2O5	ND	ND	0.0380	ND
MoO_3	0.0326	0.0232	0.0367	0.0329
SnO_2	0.0627	ND	0.0624	0.0797
La_2O_3	0.0632	0.0996	0.0835	0.1500
CeO_2	0.1890	0.2646	0.2113	0.3138
Nd_2O_3	0.0879	0.0935	0.0653	0.0951
PbO	ND	0.0149	0.0222	Not detected

7.4.4 Comparing results of increased conditioning time and de-slimed feed

Table A 16: Comparison between concentrate of de-slimed feed and that of increased conditioning time

	Extended conditioning time 15 minutes		**De-slimed feed**	
	Sinks	**Floats**	**Sinks**	**Floats**
F	0.6544	7.8858	1.0193	11.5759
Na_2O	0.0735	0.0518	ND	0.0262
MgO	0.0540	0.0337	ND	0.0352
Al_2O_3	0.8692	0.5482	0.6349	0.4944
SiO_2	3.7589	15.2725	2.9696	17.1940
P_2O_5	0.3661	0.3586	0.3702	0.3230
SO_3	0.4270	1.1245	0.2435	0.6955
Cl	0.0275	0.0353	0.0180	0.0179
K_2O	0.0341	0.0481	0.0193	0.0428
CaO	1.0098	15.3652	1.9682	18.7088
TiO_2	0.0704	0.0714	0.0910	0.0661
MnO	0.4556	0.2514	0.3813	0.2639
Fe_2O_3	91.2363	57.7931	91.2749	49.5587
CuO	0.1192	0.0944	0.1095	0.0695
As_2O_3	0.1095	0.0804	0.0162	0.0570
Y_2O_3	0.2153	0.2933	0.0892	0.2874
Nb_2O_5	0.0380	ND	0.2376	0.0226
MoO_3	0.0367	0.0329	0.0259	0.0259
SnO_2	0.0624	0.0797	0.0715	ND
La_2O_3	0.0835	0.1500	0.1128	0.0621
CeO_2	0.2113	0.3138	0.2426	0.2895
Nd_2O_3	0.0653	0.0951	0.1047	0.1077
PbO	0.0222	ND	ND	0.1017
Cr_2O_3	ND	0.0208	ND	ND

Table A16 continued				
	Extended conditioning time 15 minutes (Sinks)		**De-slimed feed (Sinks)**	
Performance				
Fe grade	63.79%		63.84%	
Recovery	72.44%		75.16%	
Mass split	54.26%		58.25%	

7.4.5 Betachem 30D - Betacol 373 system

Table A 17: Impact of collector changes on flotation

	3328g/t		**5548g/t**		**7770g/t**	
	Sink	**Float**	**Sinks**	**Floats**	**Sinks**	**Floats**
F	1.5662	7.8480	0.8566	7.3116	1.6301	7.2320
Na_2O	0.0545	0.0247	0.0444	0.0363	0.0422	0.0328
MgO	0.0341		0.0512	0.0841	0.0311	0.0164
Al_2O_3	0.6040	0.5021	0.7425	0.6904	0.6090	0.4206
SiO_2	3.3911	17.2593	5.0477	15.6610	6.9465	16.3548
P_2O_5	0.3573	0.3102	0.3622	0.2997	0.3621	0.2632
SO_3	0.4476	0.7287	0.4157	0.2972	0.3888	0.2820
Cl	ND	0.0216	0.1258	0.0944	0.1111	0.0808
K_2O	0.0279	0.0402	0.0279	0.0295	0.0297	0.0253
CaO	3.1022	14.6373	1.8380	13.3820	3.2552	13.3976
TiO_2	0.1092	0.1113	0.0620	0.0457	0.0524	0.0401
Cr_2O_3	0.0180	ND	0.0308	0.0253	ND	0.0373
MnO	0.6256	0.2569	0.4108	0.1853	0.3427	0.2204
Fe_2O_3	88.7525	57.2926	89.0369	61.0301	85.3032	60.9265
CuO	0.1184	0.0837	0.0877	0.0558	0.0774	0.0518
As_2O_3	0.1065	0.0608	0.0849	0.0464	0.0834	0.0518
Y_2O_3	0.2322	0.2567	0.2423	0.2506	0.2576	0.2312
MoO_3	0.0387	0.0267	0.0316	0.0181	0.0324	0.0210
SnO_2	0.0532	0.0597	0.0515	0.0577	0.0744	0.0489
La_2O_3	0.0835	0.0852	0.1059	0.0811	0.0948	ND

Table A17 continued						
	3328g/t		**5548g/t**		**7770g/t**	
	Sink	**Float**	**Sinks**	**Floats**	**Sinks**	**Floats**
CeO_2	0.2011	0.2530	0.1961	0.2086	0.2756	0.2001
Nd_2O_3	0.1161	0.1113	0.0914	0.1090	ND	0.0654
ZnO	ND	ND	0.0138	ND	ND	ND
Nb_2O_5	ND	ND	0.0425	ND	ND	ND
Performance						
Fe grade	62.08%		62.28%		59.66%	
Recovery	69.07%		61.18%		66.08%	
Mass split	53.15%		46.93%		52.91%	

7.4.6. Comparison between Betacol 373 and DDA

Table A18 shows detailed chemical analysis results for Betacol 373 and DDA collectors

Table A 18: Comparison between Betacol 373 and DDA

	Final Betacol 373		**Final DDA**	
	Sink	**Float**	**Sinks**	**Floats**
F	1.5662	7.8480	0.6544	7.8858
Na_2O	0.0545	0.0247	0.0735	0.0518
MgO	0.0341		0.0540	0.0337
Al_2O_3	0.6040	0.5021	0.8692	0.5482
SiO_2	3.3911	17.2593	3.7589	15.2725
P_2O_5	0.3573	0.3102	0.3661	0.3586
SO_3	0.4476	0.7287	0.4270	1.1245
Cl	ND	0.0216	0.0275	0.0353
K_2O	0.0279	0.0402	0.0341	0.0481
CaO	3.1022	14.6373	1.0098	15.3652
TiO_2	0.1092	0.1113	0.0704	0.0714
Cr_2O_3	0.0180	ND	ND	0.2514
MnO	0.6256	0.2569	0.4556	57.7931
Fe_2O_3	88.7525	57.2926	91.2363	0.0944
CuO	0.1184	0.0837	0.1192	0.0804

Table A18 continued				
	Final Betacol 373		**Final DDA**	
	Sink	**Float**	**Sinks**	**Floats**
As_2O_3	0.1065	0.0608	0.1095	0.2933
Y_2O_3	0.2322	0.2567	0.2153	0.0329
SnO_2	0.0532	0.0597	0.0624	0.1500
La_2O_3	0.0835	0.0852	0.0835	0.3138
CeO_2	0.2011	0.2530	0.2113	0.0951
Nd_2O_3	0.1161	0.1113	0.0653	0.0222
Performance				
Fe grade	62.08%		63.79%	
Recovery	69.07%		72.44%	
Mass split	53.15%		54.26%	